AN UPDATED UNDERSTANDING OF THE ACTIVITIES AND SPECIFICITIES OF THE GLYCOSYLTRANSFERASE FAMILY 37 OF *ARABIDOPSIS THALIANA*

by

MARIA J. SOTO

(Under the Direction of Michael G. Hahn)

ABSTRACT

A. thaliana has thirteen FUTs, ten of which are classified as members of glycosyltransferase family 37 (GT37) according to the Carbohydrate-Active enZYmes (CAZy) database, and all of them are predicted to be Golgi-localized type-II transmembrane proteins (Lombard et al., 2014; Sarria et al., 2001). Thus far, three out of the ten GT37 FUTs from *A. thaliana* have been functionally characterized: *At*FUT1, *At*FUT4, and *At*FUT6. *At*FUT1 has been extensively studied biologically, biochemically, and structurally, has been demonstrated to be xyloglucan-specific, and has been established as the sole FUT carrying out this function *in planta*. *At*FUT4 and *At*FUT6 have been less extensively studied but have been previously suggested to be partially or non-redundant, arabinogalactan protein (AGP) specific FUTs. Further and more detailed study of fusion-protein versions of *At*FUT4 and *At*FUT6 produced by transient transfection in mammalian HEK293 cell line, has confirmed the AGP specificity of *At*FUT4 and *At*FUT6 and further led to novel discoveries on their activities and specificities. Numerous and varied *in vitro* assays have

demonstrated that *At*FUT4 and *At*FUT6 are in fact identical in their recognition and ability to fucosylate various arabinogalactan (AG) and non-AG-like oligosaccharides, leading us to propose that they are in fact functionally redundant. Additionally, their ability to recognize and fucosylate various non-AG oligosaccharides further confirms the fucosylation site as residing on an arabinose residue but extends the breadth of oligo- and polysaccharides that these enzymes can recognize and successfully fucosylate. *In planta* studies on the *ATFUT4* and *ATFUT6* genes utilizing Promoter: β-glucuronidase expression and localization has demonstrated that in the *A. thaliana* root, the only tissue in which both *ATFUT4* and *ATFUT6* co-localize, *ATFUT4* sub-localizes to the elongation zone, while *ATFUT6* sub-localizes to the meristematic zone. These differences in sub-localization, serve as a possible explanation as to why both *ATFUT4* and *ATFUT6* are functional in the root, despite carrying out similar enzymatic functions. Additionally, here we report the first study on the activities of some of the remaining members of the GT37 family, demonstrating that some exhibit FUT-specific activity towards the hydrolysis of GDP-Fuc.

INDEX WORDS: *Arabidopsis thaliana*, *At*FUT4, *At*FUT6, arabinogalactan proteins,

arabinogalactan, xyloglucan, fucosyltransferase, fucosylation

AN UPDATED UNDERSTANDING OF THE ACTIVITIES AND SPECIFICITIES OF THE GLYCOSYLTRANSFERASE FAMILY 37 OF *ARABIDOPSIS THALIANA*

By

MARIA J. SOTO

B.S. University of Houston, USA, 2014

A Dissertation Submitted to the Graduate Faculty of The University of Georgia in Partial Fulfillment of the Requirements for the Degree

DOCTOR OF PHILOSOPHY

ATHENS, GEORGIA

2019

AN UPDATED UNDERSTANDING AT THE ACTIVITIES AND SPECIFICITIES OF THE GLYCOSYLTRANSFERASE 37 FAMILY OF *ARABIDOPSIS THALIANA*

by

MARIA J. SOTO

Major Professor:	Michael Hahn
Committee:	Alan Darvill
	Breeanna Urbanowicz
	Kelley Moremen
	James Leebens-Mack

Electronic Version Approved:

Ron Walcott
Interim Dean of the Graduate School
The University of Georgia
December 2019

DEDICATION

I dedicate this work to my family, for their continuous support, love, and constant encouragement, and to Alex for keeping me laughing, motivated and well-fed throughout the duration of my studies.

ACKNOWLEDGEMENTS

I would first like to thank my major professor, Dr. Michael G. Hahn for his guidance and encouragement that he has provided to me throughout my graduate studies. I would also like to express my gratitude to my committee members Dr. Alan Darvill, Dr. Will York, Dr. Kelley Moremen, Dr. Jim Leebens-Mack, and Dr. Breeanna Urbanowicz for their support and collaborations to my research. I would also like to thank the people who generously provided me with assistance and materials conducting my research especially Dr. Fabian Pfrengle. I would particularly like to thank the members of Dr. Debra Mohnen's Lab and Dr. Will York's labs for their constant help and collaboration.

Lastly, I immensely appreciate the love and support of my boyfriend, parents, siblings, and friends over the years.

TABLE OF CONTENTS

Page

CHAPTER 1

INTRODUCTION

The plant cell wall is a glycopolymer-rich network that surrounds the plant cell, ensuring its proper growth and development. The plant cell wall is a composite of the primary and secondary cell wall which have significant differences in their structure and function. As their names suggest, the primary cell wall is the first to be deposited around the plant cell and is synthesized during active growth and expansion. The secondary cell wall, on the other hand, is deposited in a subset of specialized cell-types when growth has ceased (Liepman *et al.*, 2010). Ninety-percent of the primary cell wall is constituted of glycopolymers, including; cellulose, hemicelluloses such as xylan and xyloglucan (XyG), and pectic polysaccharides such as homogalacturonan (HG) rhamnogalacturonan I (RG-I) and rhamnogalacturonan II (RG-II). The remaining ten-percent of the primary cell is made up of glycoproteins such as the arabinogalactan proteins (AGPs), which are members of the hydroxyproline-rich glycoproteins (HRGP) family (Cosgrove, 2014). Secondary cell walls are also composed of cellulose and hemicellulose, but have reduced levels of pectins and proteins. Secondary cell walls, instead, have significant amounts of lignin, adding to both their strength and recalcitrance (Meents *et al.*, 2018). Except for lignin, which is synthesized through oxidative coupling of 4-hydroxyphenylpropanoids (Ralph *et al.*, 2004), the glycopolymers and glycoproteins of the primary and secondary cell wall are synthesized, and modified through the action of carbohydrate-active enzymes that are largely categorized as glycosyltransferases (GTs) and glycoside hydrolases (GHs) (Cantarel *et al.*, 2009; Lombard *et al.*, 2014). As their names

suggest, GTs form glycosidic bonds while GHs hydrolyze and/or rearrange existing glycosidic bonds. In the model plant species *Arabidopsis thaliana* (*A. thaliana*), it is estimated that 10% of the genome, about 2,500 genes and gene products, are related to the biosynthesis and remodeling of the plant cell wall (Yong *et al.*, 2005). The vast array of GTs and GHs that are encoded in a typical plant genome are necessary due to the structural diversity and complexity of the glycoproteins and glycopolymers that make up plant cell walls.

Cell wall glycoproteins and glycopolymers are comprised of numerous monosaccharide building blocks, such as glucose (Glu), galactose (Gal), arabinose (Ara), galacturonic acid (GalA), xylose (Xyl), rhamnose (Rha), and fucose (Fuc), among others. GTs specific for the transfer of these individual sugar building blocks synthesize plant cell wall glycans in an array of linkage combinations, conformations, and degrees of polymerization. One specific class of GTs, fucosyltransferases (FUTs), catalyze the transfer of Fuc. In plants, Fuc is a component of the pectic plant cell wall polysaccharides, RG-I and RG-II in an α-(1,2) and α-(1,4)-linkage (Atmodjo *et al.*, 2013), the hemicellulose, XyG, in an α-(1,2)-linkage (Pauly and Keegstra, 2016), and on the glycoprotein, AGP, in an α-(1,2)-linkage (Tan *et al.*, 2012). RG-I consists of a backbone of repeating disaccharide units of $[\alpha\text{-}(1,4)\text{-D-GalA-}\alpha\text{-}(1,2)\text{-L-Rha}]_n$ with sidechains composed of Ara and Gal residues, with Fuc and glucuronic acid (GlcA) present to a lesser extent (Ridley *et al.*, 2001; Willats *et al.*, 2001a; Mohnen, 2008). RG-II is the most structurally complex of the pectins and consists of a homogalacturonan (HG) backbone of α-(1,4)-linked GalA that is further substituted by side branches (denoted A-F) consisting of 12 different monosaccharides, including Fuc (Ndeh *et al.*, 2017b). XyG is composed of a β-(1,4) linked Glc backbone with side-chains initiated by α-(1,6) linked Xyl residues, and is often further decorated with Gal and Fuc residues (Pauly and Keegstra, 2016). Finally, AGPs are members of the HRGP superfamily and consist of

a protein backbone rich in hydroxyproline (Hyp), Ala, Ser, and Thr residues, that are *O*-glycosylated on non-contiguous Hyp residues with polysaccharide chains of β-(1,3) linked Gal and β-(1,6) linked Gal side-chains modified with α-linked Ara residues, as well as α-(1,2) linked Fuc, α-linked rhamnose Rha, α-linked GlcA, and other sugars to a lesser extent (Showalter and Basu, 2016).

In *A. thaliana*, the FUTs that catalyze the transfer of Fuc in an α-(1,2)-linkage are classified in GT37 according to the Carbohydrate-Active enZYmes Database (CAZy, www.cazy.org). The CAZy database classifies putative GTs into families based on sequence similarity and predicted function. *A. thaliana* has 10 GT37 FUTs, with known and unknown functions. *A. thaliana* fucosytransferase 1 (AtFUT1), *A. thaliana* fucosytransferase 4 (*At*FUT4), and *A. thaliana* fucosytransferase 6 (*At*FUT6) have been characterized to varying extents, while the remaining family members have been minimally investigated (Sarria *et al.*, 2001). *At*FUT1 has been thoroughly studied, and has been demonstrated to catalyze the regiospecific transfer of a fucosyl residue onto the Gal of the L-side chain closest to the reducing end of XyG oligosaccharide repeats in a terminal α-1,2 linkage. Structural characterization of *At*FUT1 by X-ray crystallography combined with investigations using molecular dynamic and quantum computations, suggests that *At*FUT1 fucosylates XyG using a water mediated mechanism (Perrin *et al.*, 1999; Faik *et al.*, 2000; Sarria *et al.*, 2001; Rocha *et al.*, 2016; Urbanowicz *et al.*, 2017). *At*FUT4 and *At*FUT6 have been less extensively studied, and have been postulated to be non-redundant or partially redundant FUTs specific for the synthesis of AGPs (Sarria *et al.*, 2001; Wu *et al.*, 2010; Tryfona *et al.*, 2012, 2014; Liang *et al.*, 2013). The overall goal of this dissertation was to conclusively characterize the activities of *At*FUT4 and *At*FUT6 in order to expand our understanding of the activities and specificities of the characterized GT37 FUTs.

In addition to α-(1,2)-FUTs, there are also α-(1,3) FUT, α-(1,4) FUT, α-(1,6) FUT, protein *O*–fucosyltransferase family 1 (POFUT1) and protein *O*–fucosyltransferase family 2 (POFUT2) (Martinez-Duncker *et al.*, 2003) FUTs. Chapter 2 reviews the plant FUTs that have been biochemically characterized and investigated for associated phenotypes. Additionally, Chapter 2 includes a phylogenetic analysis of 206 plant FUTs, demonstrating the peculiar species-specific relationship that plant FUTs exhibit as opposed to mammalian and invertebrate FUTs which associate by predicted functions.

Chapter 3 describes the cloning, expression, and characterization of fusion-protein versions of *At*FUT4 and *At*FUT6 produced by transient transfection of mammalian human embryonic kidney (HEK293) cells. Biochemical analyses of these enzymes using techniques including, MALDI-TOF MS, GDP-Glo, and microarray data show that the *At*FUT4 and *At*FUT6 fusion-protein have identical specificities towards several arabinogalactan (AG) -like and non-AG-like oligosaccharides, and maintain their AG specificity as they do not fucosylate a mixture of XyG oligosaccharides. NMR and linkage analyses of unreacted oligosaccharides as compared to those incubated with *At*FUT4 conclusively show that *At*FUT4 and *At*FUT6, like *At*FUT1, are α-(1,2)-FUTs. Finally, GUS-promoter localization studies of the *AtFUT4* and *AtFUT6* genes demonstrate that *AtFUT4* and *AtFUT6* sub-localize to different cell-types of the developing *A. thaliana* root *in planta.*

Chapter 4 describes preliminary data on the successful cloning and expression of a subset of the remaining GT37 *A. thaliana* FUTs in HEK293 mammalian cells. The remaining FUT proteins that were successfully cloned, expressed, and purified were assayed for their propensity to hydrolyze GDP-Fuc. Additionally, large-scale expression and purification of both *At*FUT4 and

*At*FUT6 were completed for preliminary crystallography trials. Chapter 5 is a conclusion chapter including possible future studies.

CHAPTER 2

Plant Fucosyltransferases and the Emerging Biological Importance of Fucosylated Plant Structures

Soto, M.J., Urbanowicz, B.R., and Hahn, M.G. 2019. Plant Fucosyltransferases and the Emerging Biological Importance of Fucosylated Plant Structures. *CRC. Crit. Rev. Plant Sci*. **38**: 327 – 338. Reprinted here with permission of publisher 11/1/2019.

ABSTRACT

Plants frequently incorporate the monosaccharide L-fucose (Fuc; 6-deoxy-L-galactose) into glycans and glycopolymers located in diverse cellular locations. The incorporation of Fuc onto these varied glycans is carried out by fucosyltransferases (FUTs), that make up a protein superfamily with equally varied and diverse functions. The structures wherein Fuc is found have numerous proposed and validated functions, ranging from plant growth and development, cell expansion, adhesion and signaling, to energy metabolism, among others. FUTs from several different plant species have been identified and described; however, very few of them have been extensively characterized biochemically and biologically. In this review, we summarize plant FUTs that have been biochemically characterized and biologically investigated for associated phenotypes, offering greater insight and understanding into the physiological importance of Fuc in plants and in plant cell wall structures, glycans, and proteins.

K**eywords**: Fucosyltransferase, xyloglucan, arabinogalactan proteins, rhamnogalacturonan, *N*-glycan, *O*-fucosylation

INTRODUCTION

Fucose (Fuc; 6-deoxy-L-galactose) is a deoxyhexose sugar that is found in the glycans of diverse macromolecules in numerous species of plants, bacteria, fungi, mammals, and invertebrates. Fuc and other sugars are incorporated into macromolecules via the action of glycosyltransferases (GTs), which are enzymes that catalyze the transfer of a sugar from an activated sugar donor containing a phosphate leaving group. The incorporation of Fuc into these varied structures is carried out by specific enzymes, fucosyltransferases (FUTs), which are Leloir glycosyltransferases that catalyze the transfer of Fuc from guanidine 5'-diphosphate-β-L-Fucose (GDP-Fuc) to a suitable acceptor substrate, often an *N*-glycan, polysaccharide, or protein. FUTs belong to an enzyme superfamily that is sub-categorized based on the linkage in which Fuc is added onto the acceptor substrate, as follows: α-(1,2) FUT, α-(1,3) FUT, α-(1,4) FUT, α-(1,6) FUT, protein *O*–fucosyltransferase family 1 (POFUT1) and protein *O*–fucosyltransferase family 2 (POFUT2) (Martinez-Duncker, et al., 2003). Furthermore, these enzymes are classified into GT families, including; GT10, GT11, GT23, GT37, GT41, GT65, and GT68 in the Carbohydrate-Active enZYmes Database (CAZy, www.cazy.org); however, only GT10, GT37, and GT41 FUTs have been found in plants thus far (Coutinho *et al.*, 2003; Cantarel *et al.*, 2009; Both *et al.*, 2011; Lombard *et al.*, 2014).

In plants, Fuc has been found in the hemicellulosic polysaccharide, xyloglucan (XyG) in an α-(1,2)-linkage (Pauly and Keegstra, 2016); in the pectic polysaccharides, rhamnogalacturonan I (RG-I) in an α-(1,2)-linkage, and rhamnogalacturonan II (RG-II) in both α-(1,2) and α-(1,4) linkages (Atmodjo *et al.*, 2013); and on the extracellular, arabinogalactan proteins (AGPs) in an α-(1,2)-linkage (Tan *et al.*, 2012), all of which are cell wall glycans. In addition, Fuc can also be present attached to proteins, either on *N*-glycans in an α-1,3 linkage to the proximal *N*-acetyl

glucosamine (GlcNAc) of the core, in an α-1,4 linkage to the terminal GlcNAc residue of complex-type *N*-glycans (Staudacher *et al.*, 1999); or directly attached to serine/threonine residues of proteins, in an *O*-linkage (Hallgren *et al.*, 1975; Figure 2.1).

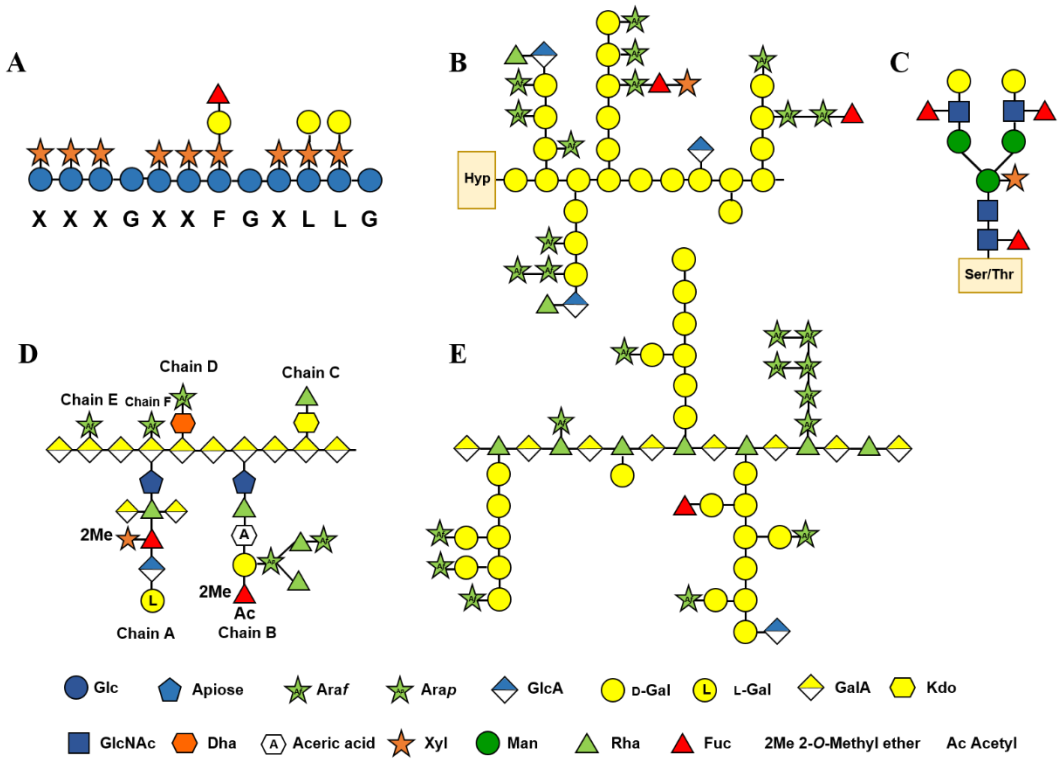

Figure 2.1. Representative structures of fucosylated cell wall poly- and oligosaccharides. (A) Xyloglucan, (B) Arabinogalactan proteins, (C) *N*-Glycans, (D) Rhamnogalacturonan II, and (E) Rhamnogalacturonan I. Glc, glucose; Ara*f*, arabinofuranose; Ara*p*, arabinopyranose; GlcA, glucuronic acid; Gal, galactose; GalA, galacturonic acid; Kdo, 3-deoxy-D-*manno*-2-octulosonic acid; GlcNAc, *N*-acetylglucosamine; Dha, 3-deoxy-D-*lyxo*-2-heptulosonic acid; Xyl, xylose; Man, mannose; Rha, rhamnose; Fuc, fucose; Hyp, hydryxoproline; Ser, serine; Thr, threonine.

A common feature of FUTs is that they all use the activated sugar nucleotide, GDP-Fuc as a donor. GDP-Fuc is synthesized from GDP-Mannose (GDP-Man), in a pathway consisting of three steps: 4,6-dehydration, 3,5-epimerization, and 4-reduction (Reiter and Vanzin, 2001). In the model

plant species, *Arabidopsis thaliana* (*A. thaliana*) these three reactions are carried out by two separate types of enzymes. The first are GDP-D-Man-4,6-dehydratases encoded by isoforms *GMD1* and *GMD2*. *GMD2* was first identified in a mutagenesis screen as *AtMUR1*, taken from the Latin word, *murus*, or wall (Reiter *et al.*, 1993, 1997). The second enzyme is a GDP-4-keto-6-deoxy-D-Man (GDP-KDM) 3,5-epimerase-4-reductase, encoded by *GER1* (Bonin et al. 1997; Bonin and Reiter 2000). Interestingly, the *GMD2* (*AtMUR1*) gene product contributes to the *de novo* biosynthesis of GDP-Fuc in most tissues, while *GMD1* contributes to its synthesis in a limited number of cell types (Bonin *et al.*, 2003). GDP-Fuc can also be synthesized from a salvage pathway that involves the direct phosphorylation of free Fuc followed by the attachment of guanosine monophosphate (GMP) (Feingold and Avigad, 1980).

In this review, we will offer an overview of plant FUTs that have been biochemically and biologically investigated and characterized. Although the number of plant FUTs that have been extensively characterized are few, the FUTs responsible for the addition of Fuc to many known fucosylated plant cell wall polysaccharides and other glycan structures have been identified, with the exception of the FUTs specific for RG-I and RG-II. Though relatively few in number, the plant FUTs included in this review offer valuable insight into the wide diversity of activities and specificities of these plant enzymes.

Xyloglucan-specific FUTs

XyGs are a family of hemicellulosic polysaccharides that have a β-(1,4)-linked-Glucose (Glc) backbone with sidechains that are initiated at the *O*-6 position with α-D-xylose (Xyl) (Pauly and Keegstra, 2016). XyGs are thought to contribute to cell wall strengthening in dicots and non-graminaceous monocots by binding to the hydrophobic surfaces of cellulose fibrils (Darvill *et al.*, 1985a; Cosgrove, 2014). To date, 19 different XyG sidechains have been identified from various

plant species, and are described using an accepted single-letter nomenclature (Fry *et al.*, 2006; Tuomivaara *et al.*, 2015; Figure 2.1A). For example, an unsubstituted Glc is denoted by the letter **G**, a backbone residue appended with α-D-Xyl is termed **X**, and when this xylosyl residue is further substituted by β-D-Gal it is called **L**. The **F** sidechain, characteristic of fucogalactoxyloglucan, consists of a backbone Glc residue that is substituted with α-L-Fuc-(1,2)-β-D-Gal-(1,2)-α-D-Xyl (Fry *et al.*, 1993; Tuomivaara *et al.*, 2015).

Three XyG-specific FUTs have been identified and characterized in plants, all of which are classified in the plant-specific GT37 family. The first XyG-specific FUT to be identified was isolated and purified from microsomal fractions of etiolated pea, *Pisum sativum*, stems (Farkas and Maclachlan, 1988). The enzyme, called *Ps*FUT1, was demonstrated to catalyze the *in vitro* transfer of radiolabeled Fuc from GDP-Fuc onto a Gal residue of exogenously available XyG acceptors. *Ps*FUT1 was shown to prefer tamarind XyG, where almost all Gal residues are not fucosylated, over XyG isolated from wildtype (WT) pea cell walls, where most Gal residues are already fucosylated. In the process of characterizing *Ps*FUT1 and its corresponding gene in pea, *AtFUT1* in *A. thaliana* was identified, based on sequence similarity to the pea gene. The corresponding gene in *A. thaliana* is also listed as *MUR2*, and was initially identified by screening chemically mutagenized *A. thaliana* plants for changes in neutral monosaccharide content of their walls (Reiter *et al.*, 1997). The mutation responsible for the *mur2* chemotype was eventually shown to be in the gene *AtFUT1* (Faïk *et al.*, 1997; Perrin *et al.*, 1999). Heterologous expression of *AtFUT1* in a mammalian COS cell line yielded 41 times higher fucosyltransferase activity for tamarind XyG relative to a control COS cell line expressing an empty vector, confirming that *At*FUT1, like *Ps*FUT1, is a XyG-specific FUT (Perrin *et al.*, 1999). Interestingly, *in planta At*FUT1 has also been shown to fucosylate galacturonic acid (GalA) in certain types of XyGs,

demonstrating that *At*FUT1 is capable of recognizing at least two XyG acceptor residues, Gal and GalA (Peña *et al.*, 2012).

In *A. thaliana*, XyG is produced by a Golgi-localized multi-protein complex that consists, at a minimum, of three xylosyltransferases (XXTs), XXT1, XXT2, and XXT5 as well as one β-(1,4)-glucan synthase, Cellulose Synthase-Like C4 (CSLC4) in the trans-Golgi network (TGN) (Chou *et al.*, 2012). *At*FUT1 can simultaneously form homo-complexes through disulfide bonds or heterocomplexes via two interaction surfaces on the protein. Two separate heterocomplexes formed by *At*FUT1 have been documented, one with the galactosyltransferases (MUR3 and XLT2), another with XXT2 and XXT5 (Chou *et al.*, 2015; Lund *et al.*, 2015). Together these results suggest that *At*FUT1 along with the galactosyltransferases MUR3 and XLT2 also form part of the multi-protein complex involved in XyG biosynthesis (Chou *et al.*, 2012, 2015; Lund *et al.*, 2015).

In addition to the biochemical research done to determine the activity and specificity of *At*FUT1, structural studies have led to its successful crystallization (Rocha *et al.*, 2016; Urbanowicz *et al.*, 2017) and detailed analysis of its mechanism of activity (Urbanowicz *et al.*, 2017). Subsequent analyses of the enzyme structure determined that it adopts the glycosyltransferase B (GT-B) fold and is metallo-independent, like all other FUT proteins that have been structurally characterized to date. A third XyG-specific FUT was identified in rice, *Oryza sativa*, by phylogenetic and coexpression analyses, and was subsequently named *Os*MUR2. Although the *Os*MUR2 protein has yet to be biochemically or biologically characterized in rice, the XyG Fuc deficiency in the *mur2 A. thaliana* mutant was successfully rescued when this mutant line was transformed with *OsMUR2*, indicating that *At*FUT1 and *Os*MUR2 are functionally equivalent *in planta* (Vanzin *et al.*, 2002; Liu *et al.*, 2015).

In addition to being implicated in cell wall strengthening, fucosylated XyG has long been postulated to be involved in several plant growth responses (Pauly and Keegstra, 2016). To characterize the function of *Ps*FUT1 *in planta*, pea hairy root lines expressing full-length *PsFUT1* antisense mRNA were constructed (Wen et al., 2008). Hairy root lines expressing the *PsFUT1* antisense mRNA had 40-50% of the WT levels of *Ps*FUT1 mRNA. Emerging root tips appeared WT in morphology; however, elongating cells developed bulges that progressed into undifferentiated calluses within 2-4 weeks (Wen et al., 2008). Additionally, antisense hairy root tips surface labeled with the CCRC-M1 monoclonal antibody, that specifically recognizes α-L-fucosylated XyG (Puhlmann *et al.*, 1994), displayed labeling patterns that differed from those observed in WT hairy root cells. This was due to cells being collapsed and wrinkled, which inhibited recognition and binding by CCRC-M1, as was discovered upon visualization with scanning electron microscopy (SEM) (Wen et al., 2008).

Similar disruptions to morphology have been reported for the trichomes of *mur*2 *A. thaliana* mutants, which have less than 2% of WT levels of fucosylated XyG (Vanzin *et al.*, 2002). Accordingly, *mur2* mutants lack fucosylated XyG in all major plant organs, indicating that *At*FUT1 is solely responsible for the fucosylation of XyG. Despite the severe reduction of fucosylated XyG throughout the entire plant, *mur2* mutant plants grow indistinguishably from WT plants when grown under normal conditions, as well as under cold, heat, and salt stress, with the only detectable phenotype being the previously mentioned disruptions to trichomes (Vanzin *et al.*, 2002).

AGP-Specific FUTs

AGPs are an abundant and diverse family of cell wall glycoproteins, with numerous and varied functions in plants, including cellular growth and stress responses. AGPs contain abundant amounts of hydroxyproline (Hyp), Ala, Ser, and Thr residues, and are extensively glycosylated on

non-contiguous Hyp residues. Polysaccharide chains on the glycan portions of AGPs consist of β-(1,3) linked galactose (Gal) backbones decorated with β-(1,6) linked Gal side-chains that are further modified with α-linked arabinose (Ara) residues, as well as α-(1,2) linked Fuc, α-linked rhamnose (Rha), α-linked glucuronic acid (GlcA), and other sugars to a lesser extent (Showalter and Basu, 2016).

One AGP-specific FUT, α-L-FTase, from radish (*Raphanus sativus* L.), and two AGP-specific FUTs from *A. thaliana*, *At*FUT4 and *At*FUT6, have been identified and studied (Misawa *et al.*, 1996; Wu *et al.*, 2010; Tryfona *et al.*, 2012, 2014; Liang *et al.*, 2013). α-L-FTase was identified in microsomal preparations from roots of 6-day old radish seedlings. Enzyme activity for α-L-FTase was measured fluorimetrically, and it was found that the enzyme successfully fucosylated a pyridylaminated (PA) trisaccharide consisting of L-Ara*f*-α-(1,3)-D-Gal*p*-β-(1,6)-D-Gal*p* (AraGalGal-PA). Subsequent chemical and enzymatic analyses of the fucosylated reaction product, (FucAraGalGal-PA), confirmed that fucosylation occurred on the *O*-2 of L-Ara*f* attached to β-(1,6)-linked D-Gal (Misawa *et al.*, 1996). *At*FUT4 and *At*FUT6 are members of the plant-specific GT37 family and were initially postulated to be putative FUTs based on their sequence similarity to *At*FUT1 (Sarria *et al.*, 2001). Early studies conducted on *At*FUT4 and *At*FUT6 were done using tobacco Bright Yellow-2 (BY-2) suspension-cultured cells that make non-fucosylated AGPs. Transient overexpression of *At*FUT4 and *At*FUT6 in BY-2 cells resulted in the production of AGPs with a Fuc moiety appended to *O*-2 of L-Ara*f* (Wu *et al.*, 2010). However, *At*FUT4 and *At*FUT6 were unable to add Fuc to other glycopolymers such as RG-I and XyG *in vitro*, demonstrating the specificity of these two FUTs for AGPs. While *At*FUT4 and *At*FUT6 appear to have similar activities *in vitro*, their expression patterns *in planta* differ. *AtFUT6* is only expressed in the root, while *AtFUT4* is expressed in both the leaf and root (Sarria *et al.*, 2001). Due to

differences in their expression patterns, studies have demonstrated that *At*FUT4 is solely responsible for the fucosylation of leaf AGPs, while *At*FUT4 and *At*FUT6 are both required for the fucosylation of root AGPs (Liang et al., 2013; Tryfona et al., 2012, 2014).

Characterization of *fut4*, *fut6*, and *fut4/fut6* single and double mutants in *A. thaliana* revealed that the loss of these genes does not seriously impact plant growth. More specifically, when grown under normal physiological conditions *fut4*, *fut6*, and *fut4/fut6* grew comparably to WT plants when evaluated for phenotypes such as rosette size, height, branch number, dry weight, and flowering time (Tryfona *et al.*, 2014). Interestingly, the *fut4/fut6* double mutant displayed an observable phenotype that was detected when mutant plants were subjected to stressful growth conditions, particularly salt stress. Under salt-stress conditions, ranging from 100-150 mM NaCl, *fut4/fut6* double mutants had significantly shorter roots relative to WT control plants also grown under salt stress (Liang *et al.*, 2013; Tryfona *et al.*, 2014). This observation supports the hypothesis that fucosylated AGPs are involved in some aspect of cell expansion in elongating root cells. Furthermore, these results suggest that the presence or absence of Fuc on AGP glycan structures may be a key determinant for proper cell growth under osmotic, or potentially other extracellular/environmental stresses.

This finding is in support of previous studies on *mur1* mutants of *A. thaliana*, which are impaired in Fuc biosynthesis. Accordingly, the AGPs isolated from *mur1* mutants are not substituted with Fuc in leaves and roots. Furthermore, these mutants also exhibited decreased root growth resulting from concurrent regions of normal and abnormal cell elongation. Despite phenotypic similarities, *mur1* mutants lack Fuc in all analyzed fucosylated glycopolymers, including AGPs, XyG, *N*-glycans, RG-I, and RG-II. Thus, the root growth phenotype of *mur1* plants cannot be solely ascribed to the lack of fucosylated AGPs, but rather an overall reduction

of Fuc in plant structures (Bonin *et al.*, 1997). Regardless, the decreased root growth of *fut4/fut6* and *mur1* mutants appear to be related to the under-fucosylation of AGPs and, possibly other structures, suggesting the importance of Fuc attached on oligosaccharides and/or glycoproteins for proper cell expansion and elongation in plants.

More recent findings on the *At*FUT4 and *At*FUT6 proteins suggest that they are functionally equivalent *in vitro*, as both are able to fucosylate various arabinogalactan (AG)-related oligosaccharide structures (unpublished results of the authors). Furthermore, the differences in expression patterns of the *AtFUT4* and *AtFUT6* genes at the cellular level, suggest that *At*FUT4 is responsible for the majority of AGP fucosylation throughout the plant body, while both *AtFUT4* and *AtFUT6* work concurrently in the root, albeit in different locations. *AtFUT4* expression localizes only to the basal regions of the tap root and emerging lateral roots, while *AtFUT6* is expressed only in the tips of the tap root and emerging lateral roots (unpublished results of the authors).

Pectic Polysaccharides

In addition to XyG and AGPs, RG-I and RG-II are two other major classes of cell wall polysaccharides that contain Fuc. The pectic polysaccharides RG-I and RG-II are among the most structurally complex cell wall polysaccharides in plants. RG-I has a backbone of repeating [α-(1,4)-D-GalA-α-(1,2)-L-Rha]$_n$ units, with sidechain modifications of variously linked arabinose and galactose residues that also contain Fuc and GlcA to a lesser extent (Ridley *et al.*, 2001). RG-II consists of an α-(1,4)-linked galacturonic acid (GalA) backbone, modified with sidechains A-F that consist of 12 different monosaccharides, including Fuc and 2-*O*-methyl-L-Fuc (MeFuc) present in sidechains A and B, respectively (Ndeh *et al.*, 2017a). RG-I and RG-II are implicated

in various plant functions, ranging from cellular growth and expansion to wall porosity (Darvill *et al.*, 1985a; Ridley *et al.*, 2001; Willats *et al.*, 2001b; Mohnen, 2008).

While Fuc has long been known to be present on RG-I and RG-II, the FUTs specific for adding Fuc to these polysaccharides remain unidentified. The Fuc found on RG-I is α-(1,2)-linked, and as such, the FUT responsible for this fucosylation is potentially one of the 7 uncharacterized members of GT37, which are predicted to be α-(1,2) FUTs in *A. thaliana* (Sarria *et al.*, 2001). RG-II also has two well characterized L-Fuc residues and a terminal L-Gal, which only differs from L-Fuc by having a hydroxymethyl group at C-6. There is a terminal non-reducing 2-*O*-Me-α-L-Fuc residue that is α-(1,2)-linked to D-Gal in sidechain B that is often acetylated. The Fuc-Gal disaccharide structure in sidechain B of RG-II is identical to that found in XyG; therefore, we hypothesize that the FUT responsible for catalyzing the transfer of Fuc to this Gal is related to the XyG-specific *At*FUT1 and also is a member of GT37. The second Fuc in RG-II is a 1,4-linked α-L-Fuc residue in the core oligosaccharide structure of sidechain A. This Fuc is more likely added by a FUT from an entirely different GT family, possibly a member of the GT10 family that include α-(1,3)- and α-(1,4)-specific FUTs (Martinez-Duncker *et al.*, 2003). However, three FUTs from this family, one in *A. thaliana* (Wilson *et al.*, 2001), one in mung bean (*Vigna radiata*) (Leiter *et al.*, 1999), and one from tomato (*Solanum lycopersicum*) (Wilson, 2001), have been characterized, and all three are involved in *N*-glycosylation. Interestingly, there is also a terminal L-Gal present in sidechain A that is α-(1,2)-linked to D-GalA. Prior work on the *mur1* mutant of *A. thaliana*, which encodes GMD2, results in plants that lack L-Fuc and substitute L-Fuc with L-Gal (O'Neill *et al.*, 2001; Reuhs *et al.*, 2004), indicating that the FUTs catalyzing the synthesis of these glycans can also utilize GDP-L-Gal as a donor. Taken together, we hypothesize that the enzyme responsible for catalyzing the addition of the non-reducing terminal L-Gal on side chain A is also a member of

GT37. The identification and detailed characterization of these additional FUTs would provide a more complete view on the fucosylation of cell wall polysaccharides, providing additional comparative insight into the specific activities of the GT37 FUTs, as well as the possible GT10 FUT involved in the synthesis of RG-II sidechain A.

_N_-glycan Specific FUTs

N-glycosylation is a highly conserved modification in plants and animals and is one of the most important post-translational modifications of proteins. *N*-glycosylation involves the attachment of oligosaccharides to asparagine residues with an Asn-X-Ser/Thr consensus sequence, termed a sequon, with X being any amino acid other than proline (Staudacher et al., 1999). Unlike, mammalian *N*-glycans, that have an α-(1,6)-linked Fuc onto the proximal *N*-acetylglucosamine (Glc*NAc*) of the core oligosaccharide attached to the protein, plants often incorporate an α-(1,3)-linked Fuc rather than α-(1,6)-linked Fuc in this same position (Strasser *et al.*, 2004). This fucosyl residue is the key element that makes plant *N*-glycans antigenic to mammals, and has hindered the use of plants for the production of recombinant glycoproteins for medical applications (Bardor *et al.*, 2003; Harmoko *et al.*, 2016). The α-(1,3) and α-(1,4) FUTs required for *N*-linked glycan biosynthesis are more closely related to each other than to the α-(1,2) FUTs of GT37, such as those responsible for the fucosylation of XyGs and AGPs, and are therefore separately classified in GT10 in the CAZy database (Martinez-Dunker *et al.*, 2003). The first FUT with *N*-glycan core α-(1,3)-fucosyltransferase activity was identified and purified from mung bean (*Vigna radiate)* seedlings (Leiter et al., 1999; Staudacher et al., 1995). The enzyme was demonstrated to transfer Fuc from GDP-Fuc onto the Asn-linked Glc*NAc* core residue of *N*-glycans, as well as onto *N*-glycopeptides and oligosaccharides with the Glc*NAc*$_2$Man$_3$Glc*NAc*$_2$ glycan structure. The enzyme was unable to transfer onto *N*-glycans without terminal Glc*NAc* residues or onto *N*-acetyllactosamine, lacto-*N*-

biose and *N*-acetylchito-oligosaccharides (Leiter et al., 1999; Staudacher et al., 1995). Following the characterization of the α-(1,3) FUT from mung bean, three genes related to the mung bean gene sequence were identified in *A. thaliana*; *AtFucTA* (*AtFUT11*), *AtFucTB* (*AtFUT12*), and *AtFucTC* (*AtFUT13*) (Wilson *et al.*, 2001). Of the three, only *AtFucTA* (*AtFUT11*) was successfully expressed in *Pichia pastoris*, and was demonstrated to catalyze the same reaction as the FUT from mung bean (Wilson *et al.*, 2001). Finally, an α-(1,4) FUT from tomato, expressed in *Pichia pastoris*, was demonstrated to have Lewis-a activity on the *N*-glycans of tomato, catalyzing the transfer of Fuc from GDP-Fuc to lacto-*N*-tetraose as well as β-(1,3) and β-(1,4)-galactosylated *N*-glycans (Wilson, 2001). Although *N*-glycan specific FUTs have been identified and biochemically studied in other plant species (Table 2.1), no follow up studies have been conducted for phenotypes associated with their mutations in those plant species, and as such, they will not be discussed in the scope of this review.

FUT Type	Plant Species	Citation
α-(1,3) FUT	*Zea mays*	Bondili et al., 2006
α-(1,4) FUT	*Silene alba*	Léonard *et al.*, 2005
α-(1,4) FUT	*Vaccinium myrtillus L.*	Palma et al., 2001
α-(1,4) FUT	*Mangifera indica L.*	Okada et al., 2017
Undetermined	*Ricinus communis*	Roberts, Mellor and Lord, 1980

Table 2.1. Plant FUTs from additional plant species. These FUTs have been biochemically characterized to varying extents, but no mutational studies have been conducted for associated phenotypes.

Few studies have been carried out to understand what, if any, impact the loss of α-(1,3) and α-(1,4) FUTs would have in plants. The *A. thaliana fucTA, fucTB,* and *fucTC* mutants have yet to be characterized. However, *A. thaliana* mutants that are otherwise impaired in the plant *N*-glycosylation pathway are generally embryo lethal or developmentally impaired and are, therefore, unable to be bred (Boisson et al., 2001; Lukowitz et al., 2000; von Schaewen, et al., 1993). Studies to elucidate the physiological significance of α-(1,3) and α-(1,4) *N*-glycan fucosylation have been successfully carried out in other model plant species, like rice and tobacco (Harmoko et al., 2016; Joly et al., 2002; Sim et al., 2018). Two independent studies conducted on T-DNA insertion lines for an α-(1,3)-fucosyltransferase gene in rice, *Os*08g36840, found that mutants are impaired in a number of features, including shoot growth, root elongation, flowering time, and plant height. Furthermore, these plants are also impaired in their ability to respond to stresses such as high salinity, and the rice pathogen *Magnaporthe oryzae* (Harmoko et al., 2016; Sim et al., 2018). Mutants were also found to have lower levels of auxin-related transcription factors relative to their progenitor lines, and were accordingly determined to be impaired in polar auxin transport, the primary mechanism for the transport of auxin in the vascular meristem (Harmoko et al., 2016; Helen & Goldsmith, 1977). Studies on an α-(1,4) FUT protein in tobacco flowers showed that a constant, but relatively low level of expression (~20 pmol Fuc h^{-1} mg^{-1} protein) could be detected in different parts of the tobacco flower, and a 3-fold increase in activity was detected in both the stamen during anthesis and in pollinated pistils, with the highest levels of activity (~120 pmol Fuc h^{-1} mg^{-1} protein) being measured in mature pollen grains. The basal FUT activity detected in tobacco flowers suggest that α-1,4 fucosylation of *N*-glycans is a basic requirement during tobacco flower maturation, while the peaks in activity during pollen maturation could be ascribed to

microgametogenesis and pollen tube elongation; no analyses on mutations in tobacco FUT proteins or genes have been conducted (Čapková *et al.*, 1997; Joly *et al.*, 2002).

POFUTs

As with *N*-glycan fucosylation, protein *O*-fucosylation is conserved between plants and other organisms, and entails the transfer of Fuc from GDP-Fuc directly onto a serine/threonine residue of proteins, an activity that was first identified in human urine (Hallgren *et al.*, 1975). Protein *O*-fucosylation in mammals and invertebrates is found on folded Epidermal Growth Factor-like (EGF) repeats and Thrombospondin Type 1 repeats (TSRs) and occurs in the endoplasmic reticulum (ER), where it is catalyzed with strict specificity by POFUT1 (GT65) and POFUT2 (GT68), respectively (Wang *et al.*, 2001; Luo *et al.*, 2006). About 100 potential human proteins have EGF repeats that POFUT1 could target, with the Notch receptor family being the most prevalent protein family to contain this motif (Okajima and Irvine, 2002; Shi and Stanley, 2003). The Notch signaling pathway is widely conserved evolutionarily and has been implicated in neurogenesis and embryonic development (Imayoshi and Kageyama, 2011). About 49 proteins in humans contain the TSR sequence targeted by POFUT2, most of which are secreted factors destined for the extracellular matrix, or are cell surface proteins that are involved with modulating cell signaling (Schneider *et al.*, 2017).

The putative POFUTs in plants are unrelated to the POFUT1 and POFUT2 families found in other organisms. The plant POFUTs instead, were classified by the presence of a domain of unknown function (DUF) 246 (PF03138/IPR024709). Plants with this DUF246 domain are sometimes termed plant GT65R proteins (Hansen *et al.*, 2012). They appear to be prevalent in plant genomes, with *A. thaliana* having 39 predicted POFUT-like genes (Hansen *et al.*, 2012; Smith *et al.*, 2018a) and are involved in growth and reproduction (Smith *et al.*, 2018b). Despite

their predicted prevalence, this family of GTs is by far the most understudied, with studies on members of this family having only been published within the last decade. Those that have been identified, though, have not been biochemically characterized until recently, as described below.

Plants carrying mutations in proteins with a DUF246 domain have been investigated due to the variety of interesting phenotypes exhibited by plants when these genes are lost or disrupted, including the effects on diverse cell wall polymers. A Golgi-localized DUF246 containing protein, FRIABLE1 (FRB1), was found to affect cell adhesion and organ fusion in *A. thaliana*, and was the first member of this family to be identified in plants (Neumetzler *et al.*, 2012). Loss of the *FRB1* gene product resulted in pleiotropic effects on cell wall architecture, particularly cell adhesion. This was due to alterations in both extensins and pectins that resulted in changes to the structure of the cell wall and middle lamella and consequently affected cell adhesion (Neumetzler *et al.*, 2012). Interestingly another member of this family, ESMERALDA1 (ESMD1) did not exhibit any associated phenotype when the *esmd1* single mutant plant were generated. However, *frb1-2/esmd1-1* double mutants showed a rescue of the cell adhesion defect associated with *frb1* (Verger *et al.*, 2016). In another suppressor screen, *quasimodo* mutants, defective in the putative pectin methyltranferase gene *QUASIMODO2* (*TSD2*, *OSU1*) similarly show a cell-detachment phenotype (Verger *et al.*, 2016) that was rescued in the *qua2-1/esmd1-1* double mutant. Furthermore, a *qua2-1/frb1-2/esmd1-1* triple mutant also showed rescue of the cell-detachment phenotype, indicating that knocking out *ESMD1* rescues the cell adhesion defects caused by single mutations in *QUA2* and *FRB1*(Verger *et al.*, 2016). Recently, four members of the DUF246 family were biochemically characterized for the first time and shown to be UDP-β-L-Rha dependent 4-α-rhamnosyltransferases (RRTs) involved in the synthesis of the repeating disaccharide unit [2)-α-L-Rha-(1 ,4)-α-D-GalA-(1] of the RG-I backbone (Takenaka *et al.*, 2018). This family is now

classified as a new plant-specific GT family, GT106. The functional characterization of these enzymes calls into question the original bioinformatics predictions that this family is involved in protein fucosylation; however, more members will need to be biochemically characterized to elucidate the role of this protein family in plants (Takenaka *et al.*, 2018).

The putative POFUT, SPINDLY (SPY) is classified as a GT41 enzyme and was recently shown to *O*-fucosylate DELLA proteins. DELLA proteins are negative transcriptional regulators of gibberellin (GA) signaling (Zentella *et al.*, 2017). In *A. thaliana*, *O*-fucosylation activates DELLA proteins, so that they are then able to interact with other transcription factors involved in, for example, brassinosteroid and light signaling pathways (Zentella *et al.*, 2017). Finally, the most recently studied putative plant POFUT, is *A. thaliana O*-FUCOSYLTRANSFERASE1 (*At*OFUT1). Mutant analyses showed that this protein is involved in pollen-pistil interactions, where a pollen tube physically penetrates specialized tissues during fertilization and germination (Smith *et al.*, 2018a). Phylogenetic analysis indicated that *At*OFUT1 is more similar to metazoan POFUT1s, which are GDP-Fuc dependent FUTs that fucosylate specific Ser or Thr residues in CXXXX(S/T)C consensus sequences within EGF repeat or TSR domains (Smith et al., 2018). In contrast to other putative or known plant POFUTs, *At*OFUT1 is categorized as a non-classified glycosyltransferase (GTnc) in the CAZy database. *Atoft*1 mutants were significantly impaired in the ability of their pollen tubes to penetrate the stigma-style interface, resulting in an almost 2,000-fold decrease in pollen transmission efficiency, and consequently displayed 5 to 10-fold decreased seed set (Smith et al., 2018). However, more data will be needed to confirm the biochemical function of *At*OFUT1.

Plant FUT phylogeny

Although the activities that plant FUTs catalyze are broad and diverse due to the innate complexities of plant cell wall polysaccharides, proteins and associated glycans, the plant FUTs are also distinguishable in how they relate phylogenetically to each other and to FUTs from the other kingdoms of life. Unlike vertebrate FUTs that form clades based on predicted specificity and function (Martinez-Duncker *et al.*, 2003), the few and limited trees that have been published on plant FUTs exhibit an unusual relationship, with clades largely forming by species rather than predicted function (Sarria et al., 2001; Liu, Paulitz and Pauly, 2015).

A much larger phylogenetic analysis, generated for this review, of 206 plant FUTs sequences from 33 species corroborates this unique phylogenetic relationship among plant FUTs, with terminal clades generally comprising single-, or closely related species (Figure 2.2). This unique phylogenetic relationship, overall, suggests that sequence homology alone cannot be used to deduce functional homology of FUTs from one plant species to another. This is exemplified by the case of the rice XyG FUT, *Os*MUR2, that is phylogenetically distinct from its functional homolog in *A. thaliana*, *At*FUT1 (Liu *et al.*, 2015) (Figure 2.2).

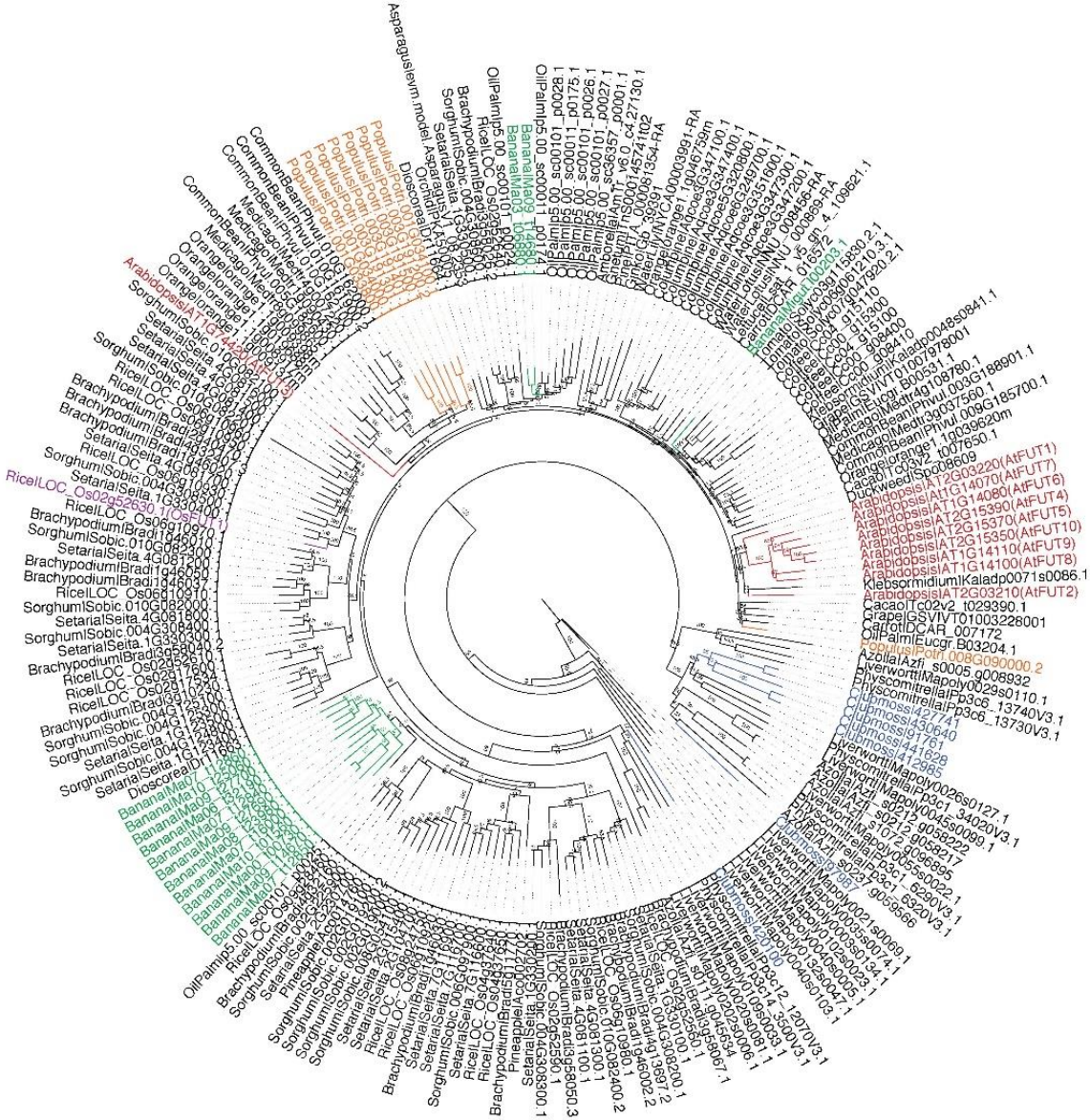

Figure 2.2. Phylogenetic tree of 206 plant FUTs from 33 species. A multiple sequence alignment of the amino acid sequences of these genes was truncated from position 1-340 and from positions 1,156-1,178 to omit large, poorly resolved gaps in the alignment. The truncated alignment was then used to make a phylogenetic tree by Neighbor-Joining with 200 bootstraps and rooted with a *Physcomitrella* clade consisting of the genes Physcomitrella|Pp3c6_13740V3.1 and Physcomitrella|Pp3c6_13730V3.1; both the alignment and tree were made in Geneious. Highlighted in red are the ten *A. thaliana* genes, nine of which form a terminal clade. The phylogenetically distinct, yet functional homolog to *At*FUT1 in rice, *Os*MUR2, is highlighted in purple. Finally, three more species are highlighted: banana in green, in which 12 out of 15 genes form a terminal clade; clubmoss in blue, in which five out of seven genes form a terminal clade; and *Populus* in orange, in which seven out of eight genes form terminal clades. These three additional clades are highlighted as further examples of the unusual, species-specific phylogenetic grouping of the plant FUTs.

It is interesting to note that while the FUTs from monocot grasses cluster within one sector of the phylogenetic tree distinct from other plant FUTs (Figure 2.2), the FUTs from any single monocot grass species are dispersed among the various terminal clades within the monocot grass domain of the tree. This pattern suggests that there might be functional orthologies among FUTs from different grass species, but this awaits experimental verification. It is also interesting that monocot grasses have large FUT families (>10) in spite of the fact that two commonly fucosylated cell wall glycans, XyGs and rhamnogalacturonans, are significantly less abundant in monocot grass walls than in walls from dicots and monocots outside of the Poales.

The unusual phylogenetic tree structure for plant FUTs also suggests that these proteins have very species-specific functions, perhaps even down to the cellular level. The three GT37 FUTs biochemically characterized thus far in *A. thaliana*, *At*FUT1, *At*FUT4, and *At*FUT6, exemplify this, as *At*FUT1 is XyG-specific, while *At*FUT4 and *At*FUT6 are both AGP-specific, but sub-localize to two distinct regions of the developing root (Sarria *et al.*, 2001; unpublished results of

the authors). As we have alluded to throughout this review, a greater number of plant FUTs need to be functionally characterized to see if this hypothesis is valid. Unfortunately, the unusual phylogenetic relationship exhibited by known and putative plant FUTs will complicate the functional characterization of additional FUTs in diverse plant species.

CONCLUSIONS

The carbohydrate-active enzymes involved in the biosynthesis of the plant cell wall are varied and unique in their activities and functions, and are typically encoded by large gene families, with the various known and putative FUTs being no exception to this pattern. While the activities of plant FUTs and the fucosylation of diverse glycans and proteins have been studied readily across many organisms, the biological importance of fucosylation *in planta* is just starting to be understood. With suggested and proven functions ranging from cellular communication and growth to cellular adhesion, the presence or absence of Fuc on various plant structures appears to have serious implications for proper plant development and response to diverse stimuli and stress. The FUTs specific for XyG fucosylation are by far the most thoroughly studied and well-understood. However, recent progress on the activities of the AGP-specific FUTs has offered additional insights into the activities and specificities of the plant-specific GT37 family. *N*-glycan fucosylation and the recent identification of the downstream targets of POFUTs, offer insight into the involvement of Fuc modifications in structures beyond the cell wall, as well as into the differences between conserved pathways in plants and vertebrates.

Characterization of FUTs in plant species other than *A. thaliana* has proven difficult, but not impossible. The continued research into the identification and characterization of functional homologs from additional plant species, as well as the identification of the FUTs specific for RG-I and RG-II fucosylation promise to extend our understanding of the physiological role and

importance of Fuc in plant cell wall polysaccharides. In addition, the characterization of more FUTs from other plant species would aid in understanding the unique evolutionary diversification pattern exhibited by this important family of biosynthetic enzymes in plants.

ACKNOWLEDGEMENTS

Work on fucosyltransferases in the authors' laboratories has been supported by the National Science Foundation Plant Genome Program (IOS-0923992) and the Center for Bioenergy Innovation (Oak Ridge National Laboratory), a US Department of Energy (DOE) Bioenergy Research Center supported by the Office of Biological and Environmental Research in the DOE Office of Science. The authors also acknowledge the Division of Chemical Sciences, Geosciences, and Biosciences, Office of Basic Energy Sciences of the US Department of Energy through grant DE-SC0008472 for funding studies of cell-type specific pectins in plant cell walls. The authors are grateful to Alan Darvill for a critical reading of the manuscript and to Jim Leebens-Mack for providing the dataset used for generation of the phylogenetic tree.

AUTHOR CONTRIBUTIONS:

M.J.S, B.R.U., and M.G.H. wrote the manuscript.

COMPETING INTERESTS:

The authors declare no competing interests.

DATA AND MATERIALS AVAILABILITY:

The data that support the findings of this study are present in the paper and any data are available from M.G.H. and B.R.U. upon reasonable request.

CHAPTER 3

*At*FUT4 and *At*FUT6: Enzymatically Redundant Arabinogalactan Protein-Specific Fucosyltransferases

Maria J. Soto, Digantkumar Gopaldas, Pradeep Kumar Prabahkar, Colin Ruprecht, Maria J. Peña, Ian Black, Fabian Pfrengle, Kelley W. Moremen, Breeanna R. Urbanowicz, and Michael G. Hahn.

To be submitted to *Frontiers in Plant Biology*.

ABSTRACT

Studies on plant glycosyltransferases (GTs) have often been hampered due to the innate difficulties and challenges faced in successfully expressing functional recombinant plant proteins in sufficient quantities for detailed characterization. The expression of plant GTs in mammalian cell culture lines can circumvent this issue, facilitating the large-scale production of active enzymes. In this way, two *Arabidopsis thaliana* (*A. thaliana*) fucosyltransferases (FUTs), *At*FUT4 and *At*FUT6, were expressed and purified for further study. *At*FUT4 and *At*FUT6 are members of the plant-specific glycosyltransferase family 37 (GT37) and transfer fucose (Fuc) from GDP-Fuc onto arabinose (Ara) residues of arabinogalactan proteins (AGPs). Based on previous studies, *At*FUT4 and *At*FUT6 have been postulated to be AGP-specific FUTs. Here, we report an updated understanding on the activities and specificities of *At*FUT4 and *At*FUT6. Our multiple findings using protein expression and *in vitro* analyses such as MALDI-TOF MS, and NMR suggest that the enzymatic activities and specificities of *At*FUT4 and *At*FUT6 are identical towards various arabinogalactan (AG)-like and non-AG-like oligosaccharide acceptors. We also report with GUS promoter-reporter gene studies that the *AtFUT4* and *AtFUT6* genes sub-localize to different parts of the developing plant root *in planta.* As such, we conclude that the *At*FUT4 and *At*FUT6 proteins are biochemically, but not physiologically redundant.

Keywords: Fucosyltransferase, arabinogalactan proteins, xyloglucan, *At*FUT1, *At*FUT4, *At*FUT6, GT37

INTRODUCTION

The plant cell wall is a complex polymeric network composed of diverse polysaccharides, proteins, polyphenolics, and hydroxyproline-rich glycoproteins (HRGPs). The polysaccharide and glycoprotein components of the cell wall confer a range of important functions, from structural integrity to cell-cell communication (Darvill et al., 1985). These complex glycopolymers are comprised of numerous monosaccharide building blocks, such as glucose (Glc), galactose (Gal), arabinose (Ara), galacturonic acid (GalA), xylose (Xyl), rhamnose (Rha), and fucose (Fuc), among others. The diversity of plant cell wall glycans can be attributed to the various linkage combinations, conformations, and degrees of polymerization in which these monosaccharides can be organized.

Fuc is a deoxyhexose sugar that is commonly found on the side-chains and core regions of glycans in plants, animals, bacteria, fungi, and invertebrates. In the cell walls of plants, Fuc is a common modification, and can be found on, rhamnogalacturonan I and rhamnogalacturonan II (RG-I and RG-II) (Atmodjo et al., 2013), xyloglucan (XyG) (Pauly and Keegstra, 2016), and arabinogalactan proteins (AGPs) (Tan et al., 2012). RG-I and RG-II are pectic polysaccharides, RG-I consists of a backbone of repeating disaccharide units of GalA and Rha with Ara and Gal sidechains that can be further modified with Fuc and glucuronic acid (GlcA) present to a lesser extent (Mohnen, 2008; Ridley et al., 2001; Willats et al., 2001). RG-II is structurally complex, consisting of a homogalacturonan (HG) backbone of α-(1,4)-linked GalA, that is modified by 6 sidechains (denoted A-F) consisting of 12 different monosaccharides, including Fuc (Ndeh et al., 2017). XyG is a hemicellulosic polysaccharide composed of a β-(1,4) linked Glc backbone with side-chains initiated by α-(1,6) linked Xyl residues; these are often further decorated with Gal and Fuc residues (Pauly and Keegstra, 2016). Together, primary cell wall polysaccharides, including

pectins and hemicelluloses, are heavily implicated to be involved in plant growth, cell expansion, wall porosity, and several other functions (Mohnen, 2008; Ridley et al., 2001; Willats et al., 2001, Pauly and Keegstra, 2016).

AGPs are extracellular glycoproteins of the HRGP superfamily, and have been postulated to have roles in a variety of plant growth and developmental responses, including cell expansion and division, hormone signaling, and abiotic stress responses (Seifert and Roberts, 2007; Tan et al., 2012) . AGPs are extensively *O*-glycosylated and consist of a core protein backbone rich in proline (Pro), alanine (Ala), serine (Ser), and threonine (Thr), and carbohydrate moieties account for 90-98% of the total weight of a typical AGP (Tan et al., 2012). To allow for *O*-glycosylation, Pro residues of the protein backbone are post-translationally modified by prolyl hydroxylation, converting Pro to hydroxyproline (Hyp) (Seifert and Roberts, 2007). AGPs are then *O*-glycosylated on non-contiguous Hyp residues with arabinogalactan (AG) groups composed mainly of a β-(1,3) linked Gal backbone substituted with β-(1,6) linked Gal side-chains that are further modified with α-(1,3) or α-(1,5) linked Ara residues. Further, in some species and plant tissues, additional side chain modifications, including Fuc and Rha, have been identified (Knoch et al., 2014; Seifert and Roberts, 2007).

The addition of Fuc onto plant polysaccharides and proteoglycans is carried out by fucosyltransferases (FUTs). FUTs are glycosyltransferases (GTs) that catalyze the transfer of Fuc from guanidine 5'-diphosphate-β-L-fucose (GDP-Fuc) onto a suitable acceptor substrate, typically a glycan or protein. Although largely understudied in plants, known and putative FUTs are highly prevalent in many plant genomes (Soto et al., 2019). Interestingly, unlike the FUTs found in vertebrates and invertebrates that form clades based on predicted function (Martinez-Duncker et al., 2003), the FUTs in plants form terminal clades largely composed of single or closely related

species (Soto et al., 2019). The model plant species *Arabidopsis thaliana* (*A. thaliana*) has by far the most thoroughly studied plant FUTs. *A. thaliana* has ten FUTs that are classified as members of glycosyltransferase family 37 (GT37) according to the Carbohydrate-Active enZYmes (CAZy) database, all of which are predicted to be Golgi-localized type-II transmembrane proteins (Lombard et al., 2014; Sarria et al., 2001). Thus far, three out of the ten GT37 FUTs from *A. thaliana* have been functionally characterized: *At*FUT1, *At*FUT4, and *At*FUT6 (Figure 3.1A, B).

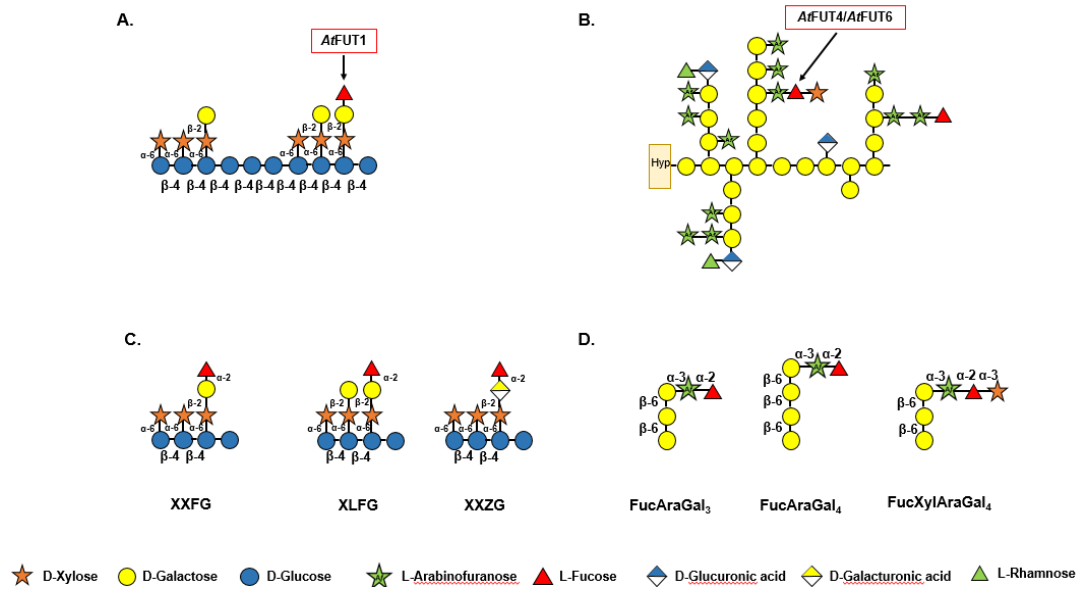

Figure 3.1. Cell wall structures that *At*FUT1, *At*FUT4, and *At*FUT6 are specific for, and fucosylated oligosaccharides from XyG and AGPs that have been structurally characterized. (A.) Proposed structure of XyG from *A. thaliana*, and the activity of *At*FUT1. (B.) Composite structure for the structure of AGPs several plant species, and the putative activities of *At*FUT4 and *At*FUT6. (C.) Fucosylated XyG oligosaccharides derived from *A. thaliana* XyG (Peña et *al.*, 2012; Tuomivaara et *al.*, 2015). (D.) Fucosylated AGP side chains derived from *A. thaliana* AGPs (Tryfona et *al.*, 2012; 2014.)

*At*FUT1 is the most well-characterized member of the GT37 family. It catalyzes the regiospecific transfer of a fucosyl residues onto Gal of the L-side chain closest to the reducing end of XyG oligosaccharide repeats in a terminal α-1,2 linkage, to form the triglycosyl side-chain α-L-Fuc*p*-(1,2)-β-D-Gal*p*-(1,2)-α-D-Xyl*p*, also known as the F-side chain according to the accepted XyG nomenclature (Fry et al., 1993; Tuomivaara et al., 2015; Figure 3.1A, C). Structural characterization of *At*FUT1 by X-ray crystallography (Rocha et al., 2016; Urbanowicz et al., 2017), combined with investigations using molecular dynamic and quantum computations, suggests that *At*FUT1 fucosylates XyG using a water mediated mechanism (Urbanowicz et al., 2017). The unusual phylogenetic relationship that plant FUTs exhibit has made identifying functionally homologous FUTs in other species difficult. For example, the functional homolog to *At*FUT1 in rice, *Os*MUR2, is phylogenetically distinct from *At*FUT1 and was identified through co-expression analyses based on the homologous genes in *A. thaliana* that had been shown to be involved in XyG biosynthesis (Liu et al., 2015). *At*FUT4 and *At*FUT6 have been less extensively studied, and were first identified based on their sequence similarity to *At*FUT1 (Sarria et al., 2001). Initial studies on *At*FUT4 and *At*FUT6 relied on the expression of these enzymes in Bright Yellow-2 (BY-2) tobacco suspension-cultured cells by transient transfection. Digitonin-solubilized extracts from microsomal membranes prepared from transgenic tobacco BY2 cells overexpressing either *At*FUT4 or *At*FUT6 were demonstrated to incorporate [^{14}C]Fuc from GDP-[^{14}C]Fuc differentially onto AGP acceptors, suggesting that these enzymes were AGP-specific FUTs (Wu et al., 2010). In this initial study, the *At*FUT4 protein enriched from BY-2 tobacco suspension cells was unable to fucosylate AGP extracts from BY-2 tobacco suspension cell lines expressing the *At*FUT6 protein. The same inverse relationship was also reported for *At*FUT6, whereby the *At*FUT6 protein enriched from BY-2 tobacco suspension cells was unable to fucosylate AGP

extracts from lines expressing the *At*FUT4 protein. These apparent differences in activity led to the conclusion that *At*FUT4 and *At*FUT6 are both AGP-specific, but non-redundant, potentially transferring Fuc onto different acceptor sites of AGPs (Wu et al., 2010). This notion was further supported by the differing gene expression patterns exhibited by these two genes, with *AtFUT4* being expressed in both the root and leaf, while *AtFUT6* is solely expressed in roots (Liang et al., 2013; Sarria et al., 2001; Tryfona et al., 2014). Interestingly, similar expression patterns have been shown for the ArabinoGalactan Methyltransferases (AGMs) AGM1 and AGM2, which are required for 4-*O*–methylation of terminal GlcA of AGPs (Smith et al., 2019; Temple et al., 2019).

Enzymatic derivitization and subsequent structural characterization of root and leaf AGPs from WT *A. thaliana*, as well as from *fut4*, *fut6*, and *fut4/fut6* single and double mutant plants, led to the identification of three identical fucosylated oligosaccharides from both tissues; $FucAraGal_3$, $FucAraGal_4$, and $FucXylAraGal_3$ (Tryfona et al., 2012; 2014; Figure 3.1D). Detailed analysis of the AGPs produced by the *fut4*, *fut6* and *fut4/fut6* mutants suggests that these gene products are non-redundantly involved in the transfer of terminal 1,2-fucosyl residues to *β*-(1,6)-linked galactan side chains of (AG), forming an α-L-Fuc*p*-(1,2)-α-L-Ara*f*-(1,3)-β-Gal*p*-(1,6)-β-Gal*p*-(1,6)-Gal*p* sidechain, which can be further modified by the addition of Xyl (Tryfona et al., 2012, 2014; Figure 3.1D). Further, structural analyses of the AGPs of these mutants demonstrated that *AtFUT4* is solely responsible for the production of these fucosylated oligosaccharides in leaves, while both *AtFUT4* and *AtFUT6* are required in roots (Liang et al., 2013; Tryfona et al., 2012, 2014). The inconsistencies between these two previous studies led to the updated conclusion that *At*FUT4 and *At*FUT6 are both AGP-specific, but partially-redundant in their activities on AGPs. In this report we demonstrate through multiple analyses that *At*FUT4 and *At*FUT6 are fully-redundant in their apparent substrate specificity towards various AG-like and surprisingly, non-AG-like

oligosaccharides. We also report that the requirement for both *At*FUT4 and *At*FUT6 for root AGP fucosylation may be explained by the differential sub-localization expression patterns of the *AtFUT4* and *AtFUT6* genes. We show here that *AtFUT6* localizes primarily to the root cap and meristematic zones, while *AtFUT4* localizes to the maturation and elongation zones.

MATERIALS AND METHODS

Production of Constructs for Heterologous Expression in HEK293 Mammalian Cell Lines

Full length cDNA clones obtained from The Arabidopsis Information Resource (TAIR) were used as templates to amplify truncated coding region sequences, excluding the predicted transmembrane domain, for the *At*FUT4 and *At*FUT6 proteins. *At*FUT4 was truncated at amino acid residue 54, while *At*FUT6 was truncated at amino acid residue 42. To generate Gateway entry clones, *attB*-PCR products were created using two-step adapter PCR, as explained in the Gateway Technology Manual (ThermoFisher Scientific). Primer sequences can be found in Table 3.1.

Table 3.1. Sequence of primers used to amplify truncated *At*FUT4 and *At*FUT6, and for the amplification of the native *AtFUT4* and *AtFUT6* promoter regions for subsequent GUS transformation. The underlined regions in the primers sequences for *At*FUT4 and *At*FUT6 specify the partial *attB* adapter sequences used in the first round of PCR amplification. Expression and secretion of the GFP-*At*FUT4 and GFP-*At*FUT6 fusion-proteins was determined by measuring the fluorescence of the recombinant protein into the media used to transiently transfect the HEK293 cells.

Enzyme/Gene	Amino Acid Truncation	Forward Primer Sequence 5' - 3'	Reverse Primer Sequence 5' - 3'	GFP Fluorescence
*At*FUT4	Δ 54	*AACTTGTACTTTCAAGGC*AACGACGAATCCGAAACA	*ACAAGAAAGCTGGGTCCTA*TAACTCATCAAAAAGCT	1423
*At*FUT6	Δ 42	*AACTTGTACTTTCAAGGC*AACGACTTCAACAACCAAC	*ACAAGAAAGCTGGGTCCTA*TAACTCATCAAATAGCTTA	1028
AtFUT4::GUS	Not Applicable	AAGCTTTTGTGCTCGCTTGAATCAGAAG	GGATCCGTTGACTTTTAGTTTGTGAAGATGATT	N/A
AtFUT6::GUS	Not Applicable	GGATCCCTTCAAACCAAAAGCTCTG	AAGCTTATTTTACAAATCGAAACAG	N/A

Following the first round of PCR amplification, the universal primers attB_AdapterF, 5'GGGGACAAGTTTGTACAAAAAAGCAGGCTCTGAAAACTTGTACTTTCAAGGC-3', and attB_Adapter-R, 5'-GGGGACCACTTTGTACAAGAAAGCTGGGTC-3', were used to complete the *attB* recombination sites and to introduce a tobacco etch virus (TEV) protease cleavage site, for subsequent protein purification steps. The *attB*-PCR products were then cloned into a plasmid cloning vector, pDONR221, using the Gateway BP Clonase II Enzyme Mix (ThermoFisher Scientific) again, according to the manufacturer's instructions. To ensure that amplification and integration of the DNA sequence had occurred correctly, the resulting plasmids were sequence verified using M13 universal primers. Expression clones were then created by recombining the entry clones into the pGEn2-DEST destination vector (Moremen et al., 2018) using the Gateway LR Clonase II Enzyme Mix (ThermoFisher Scientific), according to the manufacturer's instructions. Proteins produced in the pGEn2-DEST vector encode a fusion protein consisting of; an *N*-terminal NH_2-signal sequence, an 8xHis tag, an Avi Tag recognition site, superfolder GFP (SGFP), and the seven amino acids comprising the TEV protease recognition site, followed by the truncated coding regions of *At*FUT4 or *At*FUT6.

Protein Expression and Purification

The expression of the *At*FUT4 and *At*FUT6 recombinant enzymes was carried out by transiently transfecting HEK293 human embryonic kidney cells (Freestyle 293-F cells, ThermoFisher Scientific), as previously described (Moremen et al., 2018; Urbanowicz et al., 2017). Chromatography experiments were performed on an AKTA FPLC System (GE Healthcare, https://www.gehealthcare.com). Prior to loading the Nickel-column, the media was adjusted to contain HEPES (25 mM, pH 7.2), sodium chloride (400 mM), and imidazole (20 mM). Small-scale purification of secreted 8xHis-GFP recombinant enzymes from HEK293 cells was carried

out with HisTrap HP columns (GE Healthcare) following the manufacturer's instructions. Protein cross-contamination was avoided by purifying each enzyme, GFP-*At*FUT4 or GFP-*At*FUT6, on individual 1-ml HisTrap columns that were washed before use to remove weakly bound Ni^{2+} ions. Protein purification procedures were performed as described (Urbanowicz et al., 2017; Amos et al., 2018). GFP-*At*FUT1, was similarly prepared (Urbanowicz et al., 2017), and was included in this study as a positive control.

Oligosaccharides Tested as Possible Acceptor Substrates

In order to assay the activities of GFP-*At*FUT1, GFP-*At*FUT4, and GFP-*At*FUT6, a series of chemically synthesized and commercially available oligosaccharides were tested as potential acceptor substrates. Four chemically synthesized oligosaccharides were synthesized through automated glycan assembly, and are indicated in this paper by numbers as 65, 68, 69, 70 according to the nomenclature utilized in the papers reporting their synthesis (Bartetzko and Pfrengle, 2019; Ruprecht et al., 2017; Figure 3.2A). These oligosaccharides were selected due to their structural similarities to the previously identified fucosylated sidechains of WT AGPs, $FucAraGal_3$, $FucAraGal_4$, and $FucXylAraGal_3$ (Tryfona et al., 2012, 2014; Figure 3.1D). A XyG oligosaccharide mixture consisting of XXXG, XXLG, and XLLG, prepared as described (Tuomivaara et al., 2015; Figure 3.2B), was from laboratory stocks prepared at the Complex Carbohydrate Research Center. Additionally, three α-(1,5)-linked arabinan oligosaccharides (Megazyme, https://www.megazyme.com/), arabinobiose, arabinotriose, and arabinotetraose, were tested as potential acceptor substrates (Figure 3.2C). Finally, two galactan oligosaccharides, a β-(1,3)-linked galactobiose and β-(1,6)-linked galactobiose (Megazyme, https://www.megazyme.com/) were also evaluated herein (Figure 3.2D).

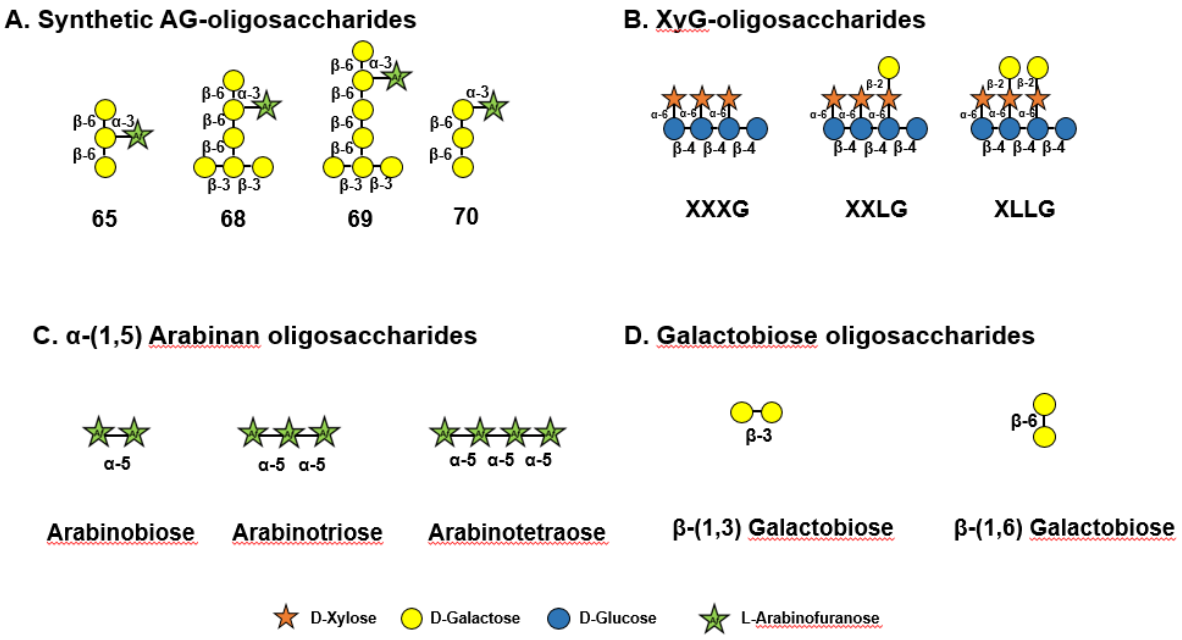

Figure 3.2. Structures of acceptor substrates tested in this study. (A.) Acceptors 65, and 68-70 are chemically synthesized oligosaccharides from the lab of Fabian Pfregle (Bartetzko, et al., 2015; Ruprecht et al., 2017). Acceptors 65 and 70 are composed of only a β-(1,6)-linked galactan side chain and an α-(1,3)-linked arabinose on the second galactose unit for 65, and on the third galactose unit for unit 70. Acceptors 68 and 69 have a β-(1,3)-linked galactan backbone, and a β-(1,6)-linked galactan side chain of 3 galactan units for acceptor 68 and 4 galactan units for acceptor 69, with an α-(1,3)-linked arabinose on the second galactose for acceptor 68 and an α-(1,3)-linked arabinose on the third galactose for acceptor 69. (B.) Acceptors XXXG, XXLG, and XLLG are composed of a β-(1,4)-linked glucan backbone, substituted with α-(1,6)-linked xylose residues, which in the case of XXLG and XLLG, are further modified with β-(1,2)-linked galactose residues. (C.) α-(1,5)-linked arabinobiose, arabinotriose, and arabinotetraose. (D.) β-(1,3)-linked galactobiose and β-(1,6)-linked galactobiose.

Matrix-Assisted Laser Desorption/Ionization-Time of Flight Mass Spectrometry

Product formation was detected with matrix-assisted laser desorption/ionization-time of flight mass spectrometry (MALDI-TOF MS) using a Microflex LT spectrometer (Bruker). Standard reactions were carried out overnight for at least 16 hours at 24°C in 25 mM HEPES, pH 7.2, and

consisted of 100 ng of enzyme, 100 μM of GDP-Fuc (Promega), and 250 μM of acceptor substrate for the AG oligosaccharides (65, and 68-70). For the α-(1,5)-linked arabinan oligosaccharides and the β-(1,3)-linked and β-(1,6)-linked galactiobiose oligosaccharides (Megazyme, https://www.megazyme.com/), 1 mM of GDP-Fuc and 2 mM of each acceptor was used. After overnight incubation, 5 μl aliquots of the reactions were incubated with 1 μl of Dowex-50 cation exchange resin (Bio-rad) for 1 hour, followed by centrifugation. 1 μl aliquots of the supernatants were then mixed with 1 μl of matrix solution (20 mg/ml of 2,5-dihydroxbenzoic acid (DHB) in 50% (v/v) methanol) and spotted and crystallized on the target plate. A minimum of 200 laser shots were summated in order to generate the positive-ion spectra that were recorded.

Protein Activity and Kinetic Analyses with GDP-Glo™ Glycosyltransferase Assay Kit

Transferase activity was also measured using the GDP-Glo™ Glycosyltransferase Assay Kit (Promega). The GDP-Glo™ Kit measures activity depending on the amount of GDP produced as a by-product of FUT activity, and was used according to the manufacturer's instructions. Standard 5 μl reactions were carried out using this kit and were prepared in 25 mM HEPES, pH 7.2. Reactions consisted of 100 μM GDP-Fuc as the donor, 250 μM of the synthetic AG oligosaccharides (65, and 68-70) or the XyG mixture, and 100 ng of enzyme. Assays were initiated with the addition of enzyme and were carried out for a period of 20 minutes at 24°C.

To measure the amount of GDP produced, 5 μl reactions were incubated for an hour at room temperature with equal volumes of GDP-Glo Detection Reagent in a 384-well white, polystyrene, low volume plate (Corning Inc., https://corning.com). Luminescence values were obtained by reading the assay plate with a microplate reader (GloMax® Microplate Reader, Promega https://www.promega.com). To quantify the amount of GDP produced, a standard curve was prepared according to the manufacturer's instructions.

Nuclear Magnetic Resonance Experiments and Linkage Analysis

NMR experiments were carried out to determine where on the arabinan acceptor substrates Fuc was being transferred. Experiments were recorded at 25°C with a Varian Inova NMR spectrometer at 600 MHz using a 5 mm cold probe. Reactions consisted of 50 mM sodium phosphate buffer pH 7.2, with 1 mM of GDP-Fucose, 2 mM of the arabinan acceptor substrates and 500 ng of enzyme. Reactions were left to incubate at 37°C for at least 2 days to ensure ample product formation for structural analyses. Following the multi-day incubation period, samples were lyophilized. 200 μl of D_2O were then added and samples were re-frozen and re-lyophilized twice. Samples were dissolved in D_2O a third and final time and placed in a 3 mm NMR tube. The two-dimensional spectra (gCOSY, and NOESY) were recorded using standard Varian pulse programs. Chemical shifts are given in ppm relative to an internal dimethyl sulfoxide standard (δ^1H 2.721). All of the NMR spectra were processed using MestReNova software (Mestrelab Research S.L., Santiago de Compostela, Spain).

Linkage analyses were performed on the reaction products of *At*FUT4 with arabinobiose, arabinotriose, and arabinotetraose. For glycosyl linkage analysis, the samples were permethylated, depolymerized, reduced, and acetylated; and the resultant partially methylated alditol acetates (PMAAs) analyzed by gas chromatography-mass spectrometry (GC-MS). The procedure is a slight modification of the one described by Heiss et al. (2009). For the analysis, the samples were transferred to borosilicate test tubes with Teflon lined screw caps. Initially, the samples were suspended in 200ul of dimethyl sulfoxide. The samples were then left to stir overnight. The samples were permethylated using NaOH and MeI. Following sample workup, the permethylated material was hydrolyzed using 2 M trifluoroacetic acid (2 h in sealed tube at 121 °C), reduced with $NaBD_4$, and acetylated using acetic anhydride/TFA. The resulting PMAAs were analyzed on an

Agilent 7890A GC interfaced to a 5975C MSD (mass selective detector, electron impact ionization mode); separation was performed on Supelco 2331 fused silica capillary column (30m × 0.25 mm ID).

Generation of *AtFUT4*::GUS and *AtFUT6*::GUS Transgenic Plants and GUS Staining

To study the expression pattern and localization of *AtFUT4 in planta*, an *AtFUT4*::GUS fusion-reporter gene was constructed and transformed into WT *A. thaliana* plants for subsequent GUS staining and visualization (Jefferson et al., 1987). To construct the *AtFUT4*::GUS fusion reporter, primers including restriction sites for *Bam*HI and *Hind*III were used to PCR amplify a ~2500-base pair fragment upstream of the *AtFUT4* open reading frame using WT (Col-0) Arabidopsis genomic DNA as a template (Primer sequences listed in Table 3.1). The amplified region, presumably containing the *AtFUT4* native promoter, was then cloned into the pBI101 plant transformation vector in-frame with the GUS reporter gene (Jefferson et al., 1987). The resulting vector was sequence verified to ensure the inclusion of the *AtFUT4* promoter and 5' UTR, after which it was used to transform GV3101:PM90 *Agrobacterium tumefaciens* through electroporation (Jefferson et al., 1987). Positively transformed *Agrobacterium* colonies were selected on Luria Broth (LB) plates with rifampicin, gentamycin, and kanamycin and were verified by colony PCR, using a combination of primers that anneal to the *AtFUT4* promoter region as well as the GUS gene (Table 3.1). Once transformed and verified, the *Agrobacterium* cells containing the *AtFUT4* promoter region were used to transform WT *A. thaliana* using the floral dip method (Clough and Bent, 1998). Successfully transformed *AtFUT4::GUS* plants were identified by growing seeds on Murashige and Skoog (MS) media supplemented with 2% (w/v) sucrose and 50 ug/ml kanamycin. An *AtFUT6*::GUS transgenic line had been produced previously in the lab following the same

method as was used for the production of *AtFUT4*::GUS plants. The primers used to amplify the promoter regions of both genes can be found in Table 3.1.

GUS transformed seedlings were stained with an X-Gluc staining solution consisting of 50 mM phosphate buffer pH 7.5, 0.5 mM ferricyanide, 0.5 mM ferrocyanide, 2 mM X-Gluc, 0.05% (v/v) Triton X, and 15% (v/v) methanol (Jefferson et al., 1987). When seedlings had reached the desired age for staining (12 days after sowing), they were submerged in X-Gluc staining solution and placed in a vacuum chamber for a minimum of 30 minutes, and then incubated at 37°C for 4-6 hours to obtain the desired level of staining. The X-Gluc staining solution was then removed, and the seedling were washed wish 70% (v/v) ethanol a minimum of 3 times to remove any excess stain and chlorophyll. Stained seedlings were imaged with an Olympus dissecting microscope at 40X magnification.

RESULTS AND DISCUSSION

*At*FUT4 and *At*FUT6 Recombinant Proteins Fucosylate Various AG-like and Non-AG-like Oligosaccharides *in vitro*

Production and expression of the globular catalytic domain of *At*FUT4 and *At*FUT6 was accomplished by transiently transfecting mammalian HEK293 suspension-cultured cells utilizing a fusion protein system that has been previously successful with mammalian and plant fucosyltransferases (Moremen et al., 2018; Urbanowicz et al., 2017).

To determine if the GFP-*At*FUT4 and GFP-*At*FUT6 fusion proteins maintained the same specificity as had been determined in previous studies, four structurally distinct AG-related oligosaccharides, synthesized through automated glycan assembly, were evaluated for their ability to serve as acceptor substrates (Bartetzko et al., 2015; Ruprecht et al., 2017; Figure 3.2A). Specifically, these acceptors were chosen due to their structural similarities to the previously

characterized fucosylated AGP side chains identified in *A. thaliana,* including; $FucAraGal_3$, $FucAraGal_4$, and $FucXylAraGal_4$ (Tryfona et al., 2012, 2014; Figure 3.1D). Additionally, the four AG oligosaccharides contain minor differences in structure, such as, the presence or absence of a β-(1,3) linked Gal backbone, the length of the β-(1,6) linked Gal side-chain, and/or the terminal or internal positioning of the α-(1,3) linked Ara on the Gal side-chain. These structural differences were selected in an attempt to determine whether GFP-*At*FUT4 and GFP-*At*FUT6 would have the same or differing specificity, and to determine if the presence or absence of the Gal backbone, the length of the Gal sidechain, and/or the positioning of the Ara residue would impart differences in the ability of *At*FUT4 and *At*FUT6 to fucosylate these oligosaccharides. The GFP-*At*FUT4 and GFP-*At*FUT6 fusion proteins were also tested against a XyG oligosaccharide mixture consisting of XXXG, XXLG, and XLLG, that were chemically and enzymatically derived from XyG isolated from suspension-cultured *mur1* mutant cells (which lack the terminal Fuc on the XyG side chains), and purified through size-exclusion chromatography (Wu et al., 2010; Pauly, Albersheim, & Darvill, 2001;Tuomivaara et al., 2015; Urbanowicz et al., 2017; Figure 3.2B). *At*FUT1, the XyG-specific member of the GT37 FUT family in *A. thaliana,* was similarly assayed against all AG and XyG oligosaccharides, and was included in this study as a control to probe acceptor substrate specificity of GT37 members.

Enzyme transferase activity for GFP-*At*FUT4, GFP-*At*FUT6, and GFP-*At*FUT1 was determined by incubation with the AG and XyG oligosaccharides for a period of at least 16 hours at 24°C. The resulting oligosaccharide reaction products, if present, were detected by MALDI-TOF MS. The reaction products were consistent with the transfer of a single Fuc residue onto the selected acceptors based on the observation of structures with a mass difference of 146 Da. Analysis of the reaction products showed that GFP-*At*FUT4 and GFP-*At*FUT6 added a single fucosyl residue to

each of the AG oligosaccharides (Figure 3.3A-D). In contrast, GFP-*At*FUT1 was not active on the AG oligosaccharides, but added Fuc to galactosylated XyG oligosaccharides, as expected from previous studies (Wu et al., 2010; Perrin et al., 1999; Urbanowicz et al., 2017; Figure 3.3E).

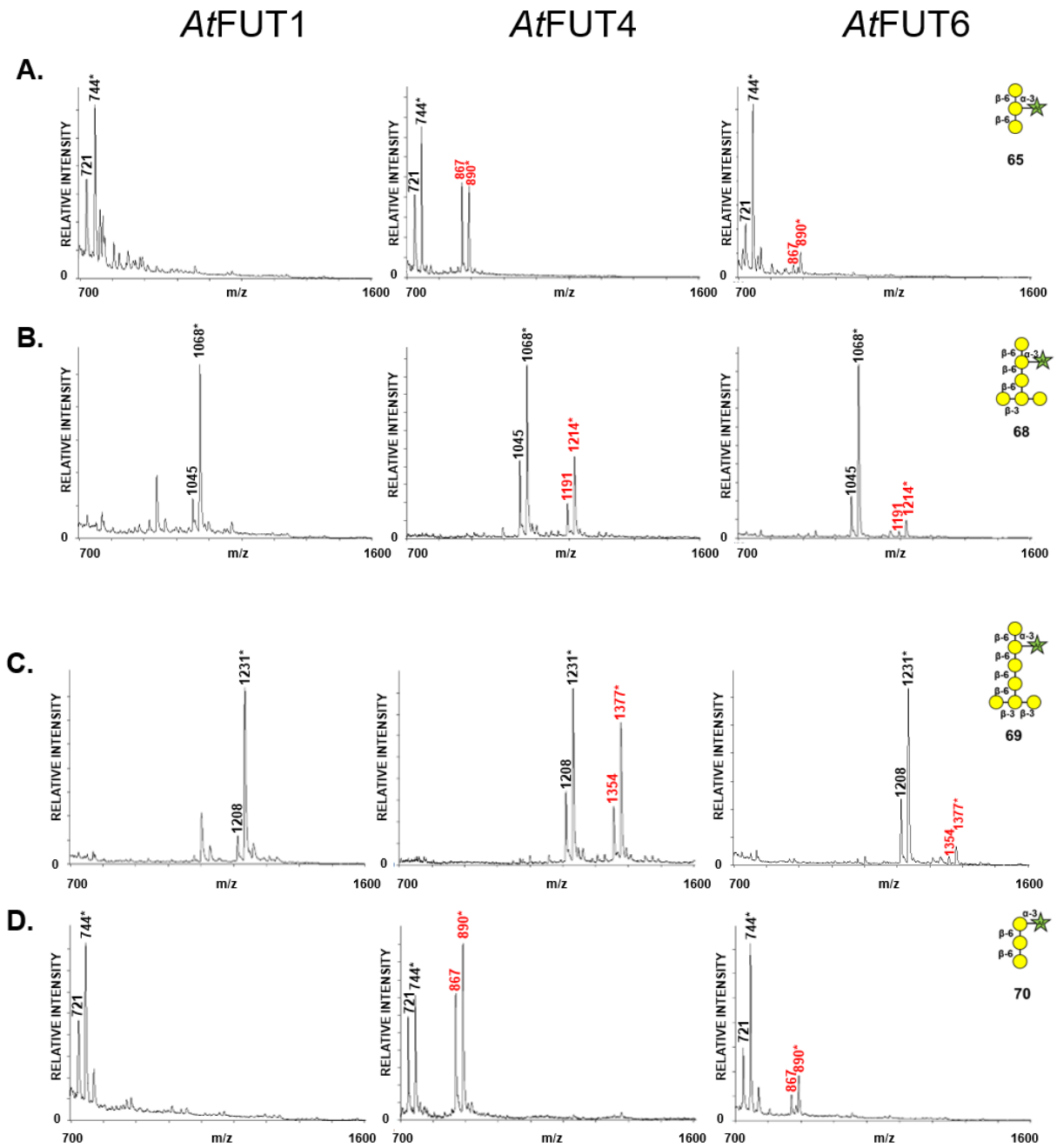

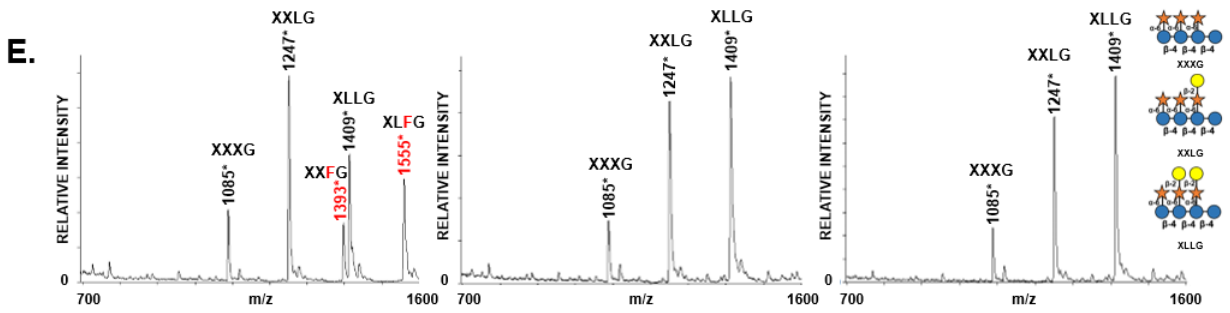

Figure 3.3. MALDI-TOF MS data for *At*FUT1, *At*FUT4, and *At*FUT6 with 65, 68-70, and XyG acceptor substrates demonstrates that the fusion-protein versions of these proteins maintain their previously proposed specificities. For all spectra (*) denotes [M + Na^+] adducts .(A.) *At*FUT1, *At*FUT4, and *At*FUT6 with acceptor 65 which has an unreacted mass of 721 or 744*; product formation at 867 and 890* indicating a mass increase of 146 Da corresponding to the transfer of a single fucose was only detected for *At*FUT4 and *At*FUT6. (B.) *At*FUT1, *At*FUT4, and *At*FUT6 with acceptor 68 which has an unreacted mass of 1045 or 1068*; product formation at 1119 and 1214* indicating a mass increase of 146 Da corresponding to the transfer of a single fucose was only detected for *At*FUT4 and *At*FUT6. (C.) *At*FUT1, *At*FUT4, and *At*FUT6 with acceptor 69 which has an unreacted mass of 1208 or 1231*; product formation at 1354 and 1377* indicating a mass increase of 146 Da corresponding to the transfer of a single fucose was only detected for *At*FUT4 and *At*FUT6. (D.) *At*FUT1, *At*FUT4, and *At*FUT6 with acceptor 70 which has an unreacted mass of 721 or 744*; product formation at 867 and 890* indicating a mass increase of 146 Da corresponding to the transfer of a single fucose was only detected for *At*FUT4 and *At*FUT6. (E.) *At*FUT1, *At*FUT4, and *At*FUT6 with XyG acceptors which have unreacted masses of 1085*, 1247*, and 1409*; product formation of XXFG adducts at 1393* and XLFG adducts at 1555* indicating a mass increase of 146 Da corresponding to the transfer of a single fucose were only detected for *At*FUT1.

Findings by Wu *et al.* (2010) suggested that the site of fucosylation for AGPs may lie on an Ara residue. In our study, the only structural commonality between all of the AG oligosaccharides tested as acceptors was the presence of a terminal Ara residue. Furthermore, the lack of selectivity by the enzymes for the four tested AG-related oligosaccharides, which differ from each other with

respect to the Gal sidechain and the Gal backbone, further suggests Ara as the site of fucosylation. The ability of GFP-*At*FUT4 and GFP-*At*FUT6 to fucosylate all of the AG oligosaccharides tested, regardless of their structural differences, also suggests that GFP-*At*FUT4 and GFP-*At*FUT6 are equally promiscuous in their ability to fucosylate various AG-like structures, but maintain their AG specificity as they did not fucosylate the XyG oligosaccharides. With all acceptors tested, GFP-*At*FUT4 had higher apparent activity than GFP-*At*FUT6, while in previous studies with microsomal *At*FUT4 and *At*FUT6, *At*FUT6 was reported as displaying more activity than *At*FUT4 (Wu et al., 2010). The differences in preparation methods from one study to the other may account for these observed differences in activity.

The transferase and hydrolase activities of GFP-*At*FUT4 and GFP-*At*FUT6 were also measured using Promega's GDP-Glo^{TM} kit. Glycosyltransferase reactions result in the production of two products: the glycosylated acceptor and the nucleotide. The Glo system measures transferase activity indirectly by converting the GDP that is released during transfer into ATP. An enzyme-linked luciferase/luciferin reaction then converts the ATP to luminescence, which can be correlated back to the GDP concentration with a GDP standard curve. Hydrolytic activity can also be measured since GTs have been demonstrated, in some cases, to hydrolyze their nucleotide-sugar donor when an acceptor is unavailable. This equates to the enzymatic transfer of the sugar in the nucleotide-sugar donor to a water molecule (Sheikh et al., 2017).

The GDP-Glo^{TM} data were consistent with the results of the MALDI-TOF MS analysis of the saccharide reaction products, with GFP-*At*FUT4 and GFP-*At*FUT6 having detectable activity for all four AG oligosaccharides, but not the XyG oligosaccharide mixture (Figure 3.4). Similarly, GFP-*At*FUT1 had detectable activity for the XyG oligosaccharides only (Figure 3.4). As with the MALDI-TOF MS data of the oligosaccharide reaction products, more transferase activity was

detected for GFP-*At*FUT4 than for GFP-*At*FUT6. Additionally, GFP-*At*FUT4 and GFP-*At*FUT6 both exhibited unexpectedly high hydrolytic activity towards GDP-Fuc in the absence of oligosaccharide acceptors (Figure 3.4). Unlike GFP-*At*FUT4 and GFP-*At*FUT6, GFP-*At*FUT1 had very low rates of GDP-Fuc hydrolysis in the absence of acceptor substrate, which is consistent with previous findings using the GDP-Glo^{TM} assay system to measure its activity (Urbanowicz et al., 2017). At this time, we do not have an explanation for the high observed rates of GDP-Fuc hydrolysis for GFP-*At*FUT4 and GFP-*At*FUT6, but hypothesize that the active sites of GFP-*At*FUT4 and GFP-*At*FUT6 may be more shallow than the active site of GFP-*At*FUT1, consistent with the ability of these enzymes to use multiple acceptor substrates. A shallower active site would presumably be more accessible to water, facilitating a higher rate of transfer from the nucleotide-sugar donor to a water molecule in the hydrolysis reaction.

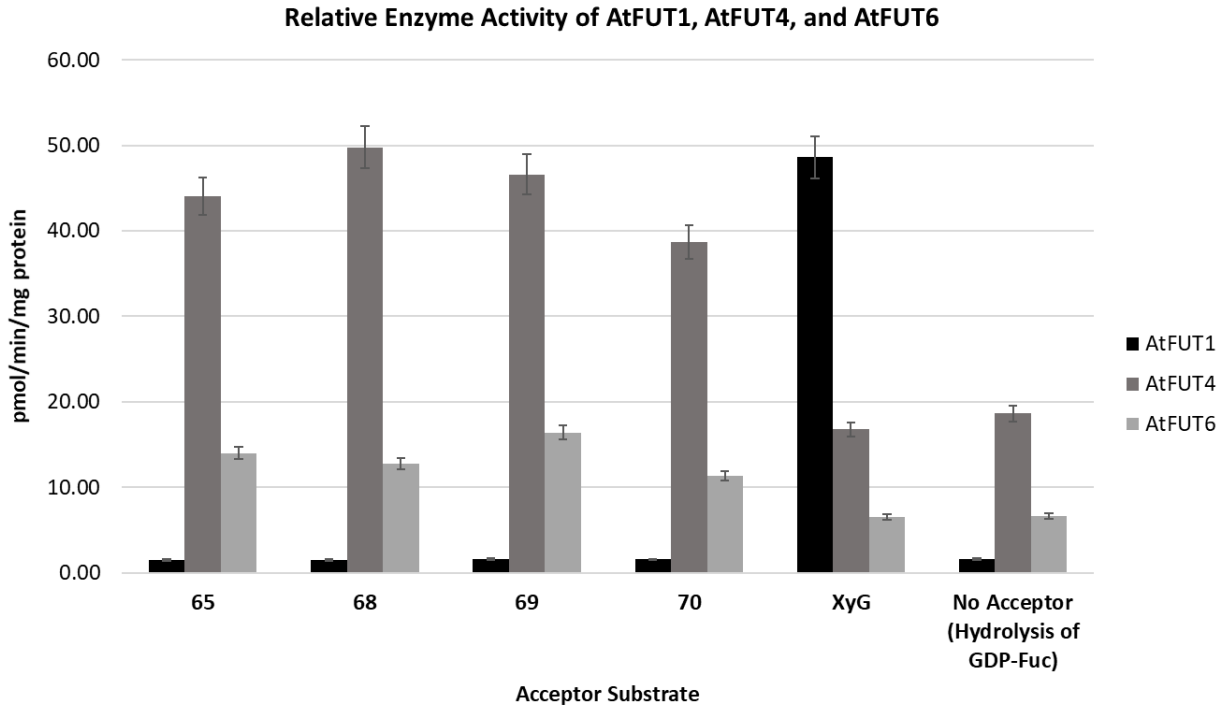

Figure 3.4. GDP-Glo Data for *At*FUT1, *At*FUT4, and *At*FUT6 with chemically synthesized AG oligosaccharide acceptors and XyG acceptors. Activity for *At*FUT1 was only detected with the XyG acceptors, and minimal activity was detected in the absence of an acceptor, equating to the hydrolysis of GDP-Fuc. Activity for *At*FUT4 and *At*FUT6 was only detected with the AG acceptors, but showed higher activities in the absence of acceptors, indicating the propensity of *At*FUT4 and *At*FUT6 to hydrolyze GDP-Fuc. Values represent the averages of 3 technical replicates per sample.

Finally, the activities of GFP-*At*FUT4 and GFP-*At*FUT6 were also tested in a high-throughput assay using a micro-array consisting of over 100 oligosaccharides synthesized through automated glycan assembly in collaboration with Fabian Pfrengle (Bartetzko and Pfrengle, 2019). GFP-*At*FUT4 and GFP-*At*FUT6 fucosylated the same AG oligosaccharides selected for this study, as well as a number of additional AG and non-AG oligosaccharides not included in this study (Figure 3.5). While the additional oligosaccharides that GFP-*At*FUT4 and GFP-*At*FUT6 were able to fucosylate vary in structure, linkage, and sugar composition, all possess a free α-(1,3) or an α-(1,5) linked single-Ara residue or arabinan chain, the presumed recognition site of fucosylation for *At*FUT4 and *At*FUT6. These results further refute previous findings suggesting that *At*FUT4 and *At*FUT6 are non- or only partially-redundant, and rather suggest that *At*FUT4 and *At*FUT6 are redundant *in vitro*, as both fucosylate exactly the same oligosaccharides among those tested, and further supports the notion that the recognition site for fucosylation lies on an Ara residue, irrespective of the larger side chain structure.

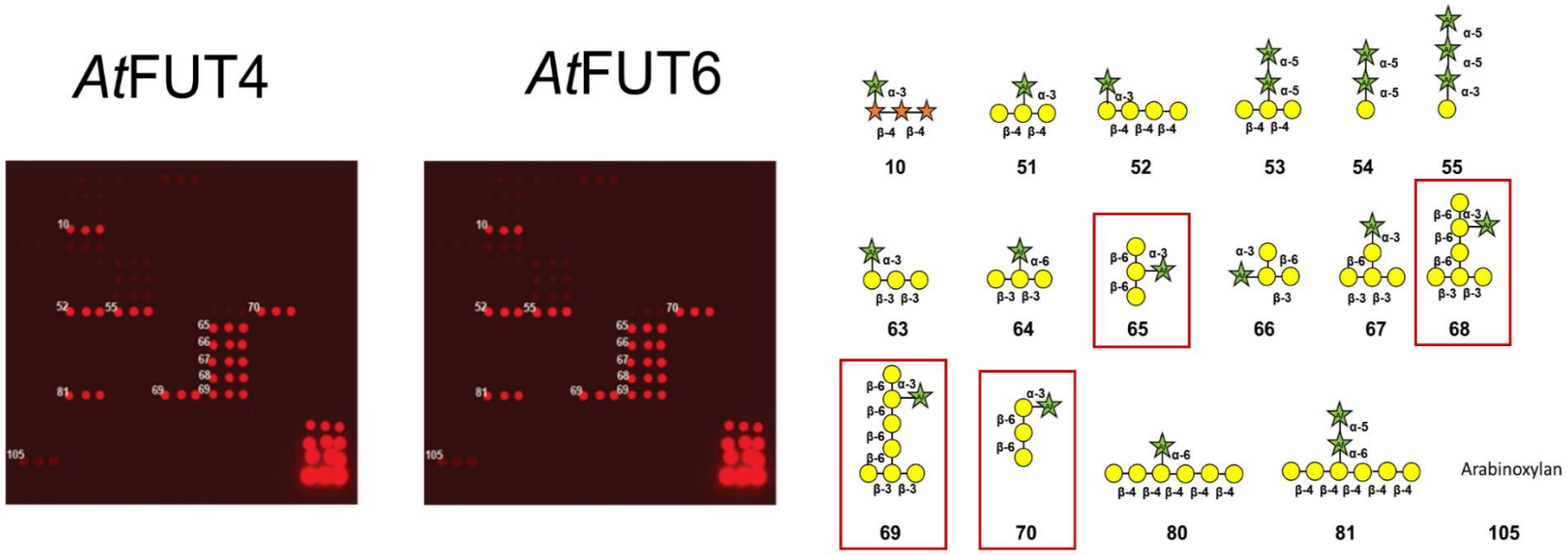

Figure 3.5. Microarray data for *At*FUT4 and *At*FUT6. Red spots on the microarray designate the structures for which transferase activity was detected. The structures corresponding to the numbers listed on the microarray are found to the left. The structures surrounded by red boxes are those that were assayed with *At*FUT4 and *At*FUT6 using MALDI-TOF and GDP-Glo™. As evidenced, *At*FUT4 and *At*FUT6 had identical activity towards structures with terminal α-(1,3) and/or α-(1,5)-linked Ara. Spots found at the bottom right of the microarray are loading controls.

Arabinan Oligosaccharides Are Suitable Acceptor Substrates and Support Ara Specificity of *At*FUT4 and *At*FUT6

Due to their method of synthesis, the AG oligosaccharides used in the first part of this study are limited in quantity and availability. As such, a more readily available acceptor substrate was sought to perform detailed biochemical analyses, if possible. From the AG-oligosaccharides tested in this study, the only structural commonality was the presence of a terminal Ara residue. The presence or absence of a β-(1,3) linked Gal backbone and the length of the β-(1,6) linked Gal side-chain on which the Ara residue is located, did not appear to impart any selectivity. Additionally, from a microarray assay, both α-(1,3)-linked Ara and α-(1,5)-linked Ara appear to serve as recognition sites for fucosylation by GFP-*At*FUT4 and GFP-*At*FUT6. Based on these findings, and to further investigate acceptor substrate specificity, a series of commercially available Ara and Gal oligosaccharides were tested as potentially suitable acceptor substrates. Due to the apparent sole selectivity of GFP-*At*FUT4 and GFP-*At*FUT6 for Ara in either an α-(1,3) or an α-(1,5) linkage, three, α-(1,5)-linked arabinan oligosaccharides, including: arabinobiose, arabinotriose, and arabinotetraose were selected as possible pseudo-acceptor substrates (Figure 3.2C). The three, α-(1,5) linked arabinan oligosaccharides are of varying lengths, and were chosen to determine the minimum length that would enable fucosylation, if GFP-*At*FUT4 and GFP-*At*FUT6 were able to utilize any of the molecules as acceptors. Furthermore, two galacto-oligosaccharides, including β-(1,3) galactobiose and β-(1,6) galactobiose, were also used to conclusively determine whether or not the site of fucosylation lies on an arabinose or a galactose residue (Figure 3.2D). No α-(1,3) linked arabino-oligosaccharides were commercially available at the time of this study.

Interestingly, all three α-(1,5)-linked arabinan oligosaccharides served as suitable acceptor substrates. MALTI-TOF MS analysis of the reaction products indicated that both GFP-*At*FUT4 and GFP-*At*FUT6 catalyze the transfer of a single Fuc to each of the arabino-oligosaccharides based on the observation of structures with a mass increase of 146 Da (Figure 3.6C-E). In contrast, analysis of the reactions containing β-(1,3) galactobiose or the β-(1,6) galactobiose as acceptor substrates showed no difference relative to control samples lacking enzyme. Taken together, these data suggest that Gal is not included in the acceptor site of fucosylation for GFP-*At*FUT4 and GFP-*At*FUT6, and additionally suggests that the galactan-based side chains of AGs may not be critical components for substrate specificity of these enzymes (Figure 3.6A-B). Taken together, these data suggest that a non-reducing terminal Ara is the acceptor site for fucosylation by *At*FUT4 and *At*FUT6.

In order to determine the position and the residue where the fucose was added on the arabinan pseudo-substrates, nuclear magnetic resonance (NMR) analyses were performed (Figure 3.7). Due to the lack of differences in the selectivity of GFP-*At*FUT4 and GFP-*At*FUT6 towards the arabinan oligosaccharides, NMR analyses was only performed with the reaction products of GFP-*At*FUT4. This was also done because GFP-*At*FUT4 has appreciably more activity that *At*FUT6. NMR analyses were only successfully performed on the reaction product of *At*FUT4 with the arabinotriose acceptor substrate. Analyses performed on the arabinobiose and arabinotetraose reaction products of *At*FUT4 yielded too many undecipherable overlapping signals (data not shown). NMR spectra of arabinotriose with GFP-*At*FUT4 as compared to unreacted arabinotriose, clearly contained two additional signals corresponding to terminally-linked Fuc, and Ara with Fuc attached at *O*2 (Figure 3.7).

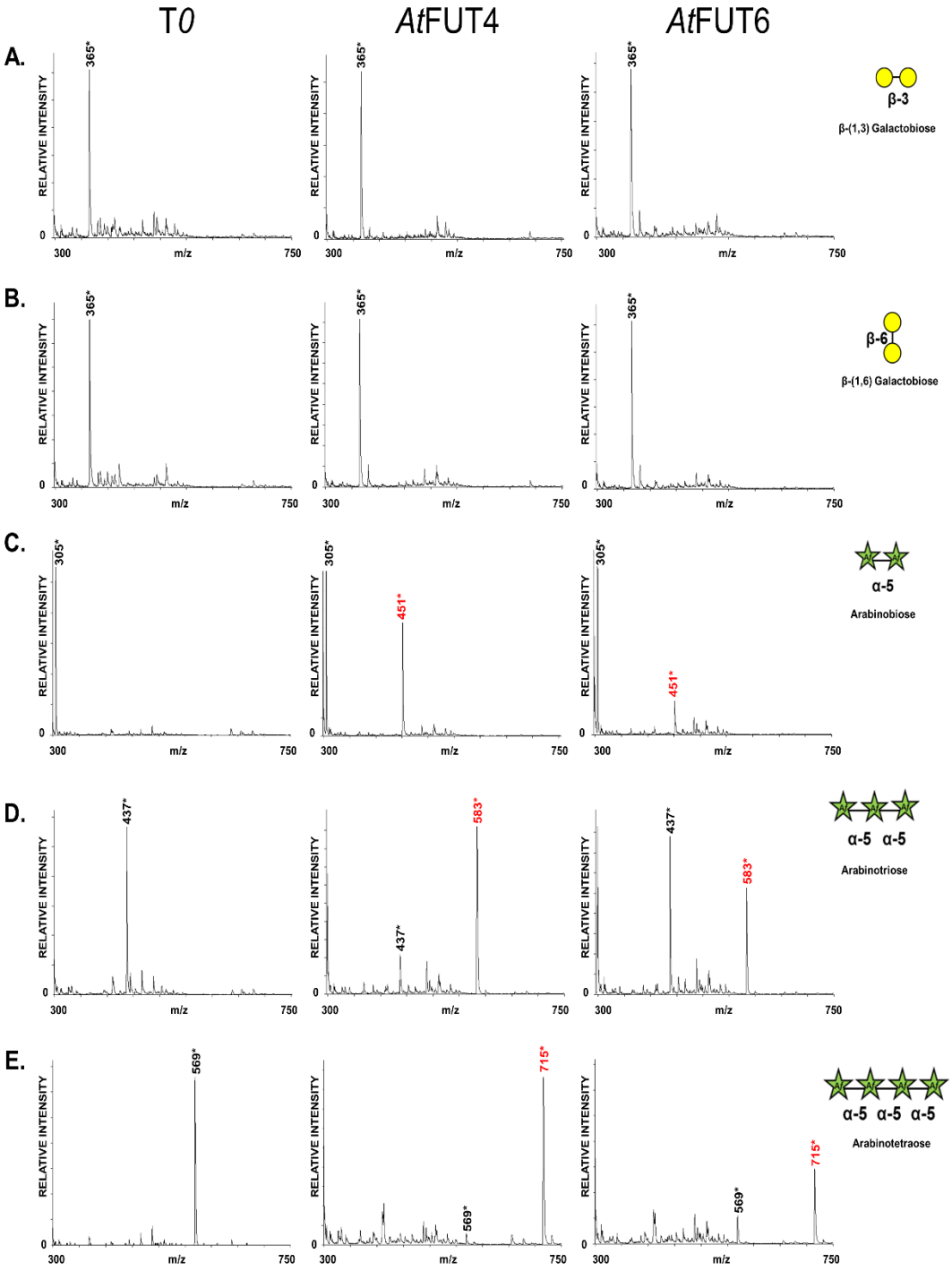
T0
AtFUT4
AtFUT6
A.
B.
C.
D.
E.
RELATIVE INTENSITY
m/z
300
750
365*
305*
437*
451*
569*
583*
715*
β-3
β-(1,3) Galactobiose
β-6
β-(1,6) Galactobiose
α-5
Arabinobiose
α-5 α-5
Arabinotriose
α-5 α-5 α-5
Arabinotetraose

Figure 3.6. MALDI-TOF MS data for *At*FUT4, and *At*FUT6 with arabinan and galactan acceptor substrates. For all spectra (*) denotes [M + Na^+] adducts. (A) *At*FUT4, and *At*FUT6 with β-(1,3)-linked Galactobiose acceptor which has an unreacted mass of 365*; product formation was not detected for either *At*FUT4, or *At*FUT6. (B) *At*FUT4, and *At*FUT6 with β-(1,6)-linked Galactobiose acceptor which has an unreacted mass of 365*; product formation was not detected for either *At*FUT4, or *At*FUT6. (C) *At*FUT4, and *At*FUT6 with α-(1,5)-linked arabinobiose acceptor which has an unreacted mass of 305*; product formation at 451* was detected for both *At*FUT4, and *At*FUT6. (D) *At*FUT4, and *At*FUT6 with α-(1,5)-linked, arabinotriose acceptor which has an unreacted mass of 437*; product formation at 583* was detected for both *At*FUT4, and *At*FUT6. (E) *At*FUT4, and *At*FUT6 with α-(1,5)-linked arabinotetraose acceptor which has an unreacted mass of 569*; product formation at 715* was detected for both *At*FUT4, and *At*FUT6.

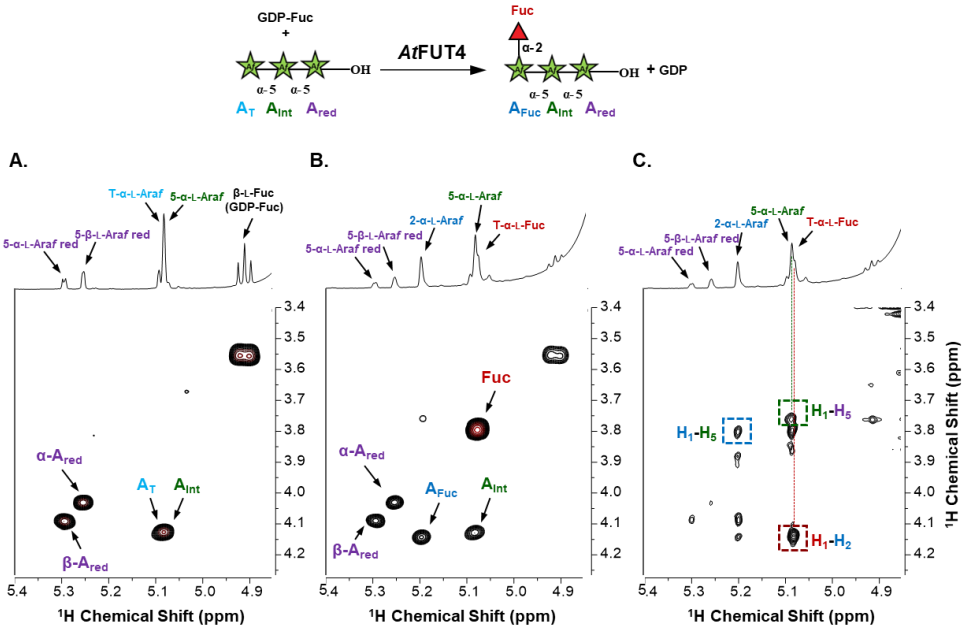

Figure 3.7. NMR analysis of the products formed when arabinotriose was incubated with *At*FUT4 and GDP-Fuc. The scheme of the reaction is showed in the top of the figure. The labeled crosspeaks in the two-dimensional gCOSY spectrum of the control (A.) correspond to the anomeric signals of the residues of the arabinotriose. After the reaction with *At*FUT4, the spectrum (B.) contained two additional signals, which were identified as terminal fucose and an arabinose with fucose attached at *O*2. The signals surrounded by squares in the NOESY spectrum of the *At*FUT4 reaction (C.) indicated the glycosidic linkages in the enzymatically generated oligosaccharide. For the complete list of assignments see Table 3.2.

These results conclusively demonstrate that *At*FUT4 is an α-(1,2) FUT, as is *At*FUT1, and that it catalyzes the transfer of a single Fuc onto Ara residues. To further confirm that Fuc was added onto a terminal Ara in an α-(1,2)-linkage in all of the arabinan oligosaccharides, linkage analyses were performed on the reaction products of *At*FUT4 incubated with arabinobiose, arabinotriose, and arabinotetraose. Linkage analysis confirmed the findings from the NMR analysis, and further proved that for arabinobiose and arabinotetraose, Fuc is also added onto the non-reducing terminal Ara of the oligosaccharides in an α-(1,2)-linkage (Figure 3.8). The presence of an 1,2-Ara*f* peak in the spectra for the reaction products of each oligosaccharide rather than 1,2,5-Ara*f* peaks demonstrate that Fuc is added onto the terminal Ara rather than the internal or reducing Ara residues.

Table 3.2. [1]H NMR signal assignments of arabinotriose incubated with GDP-Fuc and *At*FUT4 (A.) or without the enzyme (control) (B).

Residue	H1	H2	H3	H4	$H5_{a,b}$	H6
Chemical Shift (ppm)[1]						
A.			α-L-Ara*f*-(1,5)-α-L-Ara*f*-(1,5)-α-L-Ara*f*			
T-α-L-Ara*f*	5.090	4.13	3.95	4.09	3.83-3.72	
5-α-L-Ara*f*	5.084	4.13	4.22	3.89	3.80 7.7	
5-α-L-Ara*f*	5.258	4.03	4.03	4.23	3.86-3.76	
5-β-L-Ara*f*	5.294	4.09	4.00	4.23	3.86-3.76	
B.			α-L-Fuc*p*-(1,2)-α-L-Ara*f*-(1,5)-α-L-Ara*f*-(1,5)-α-L-Ara*f*			
T-α-L-Fuc*p*	5.076	3.79	3.89	3.8	4.08	1.24
2-α-L-Ara*f*	5.196	4.14	4.10	4.10	3.835-3.724	
5-α-L-Ara*f*	5.084	4.13	4.22	3.89	3.80 7.7	
5-α-L-Ara*f*	5.258	4.03	4.03	4.23	3.86-3.76	
5-β-L-Ara*f*	5.294	4.09	4.00	4.23	3.86-3.76	

[1]Chemical shifts are reported in ppm relative to internal dimethyl sulfoxide, δ_H 2.721.

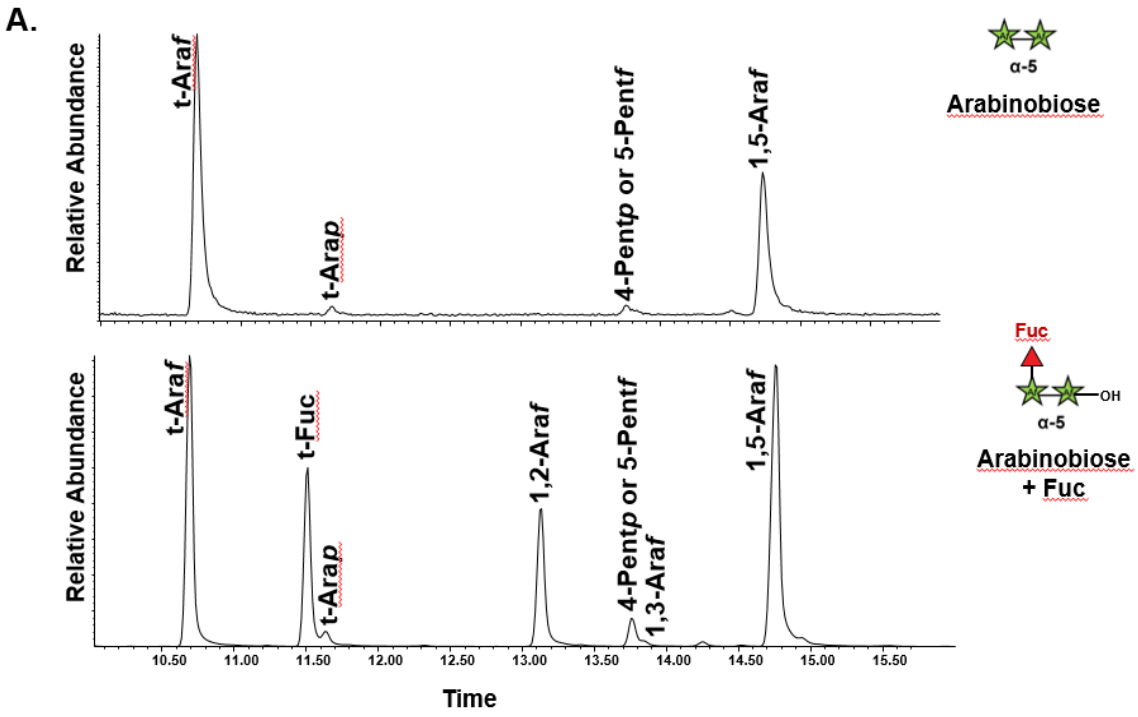
A.
Relative Abundance
t-Araf
t-Arap
4-Pentp or 5-Pentf
1,5-Araf
α-5
Arabinobiose
Relative Abundance
t-Araf
t-Fuc
t-Arap
1,2-Araf
4-Pentp or 5-Pentf
1,3-Araf
1,5-Araf
Fuc
OH
α-5
Arabinobiose
+ Fuc
10.50
11.00
11.50
12.00
12.50
13.00
13.50
14.00
14.50
15.00
15.50
Time

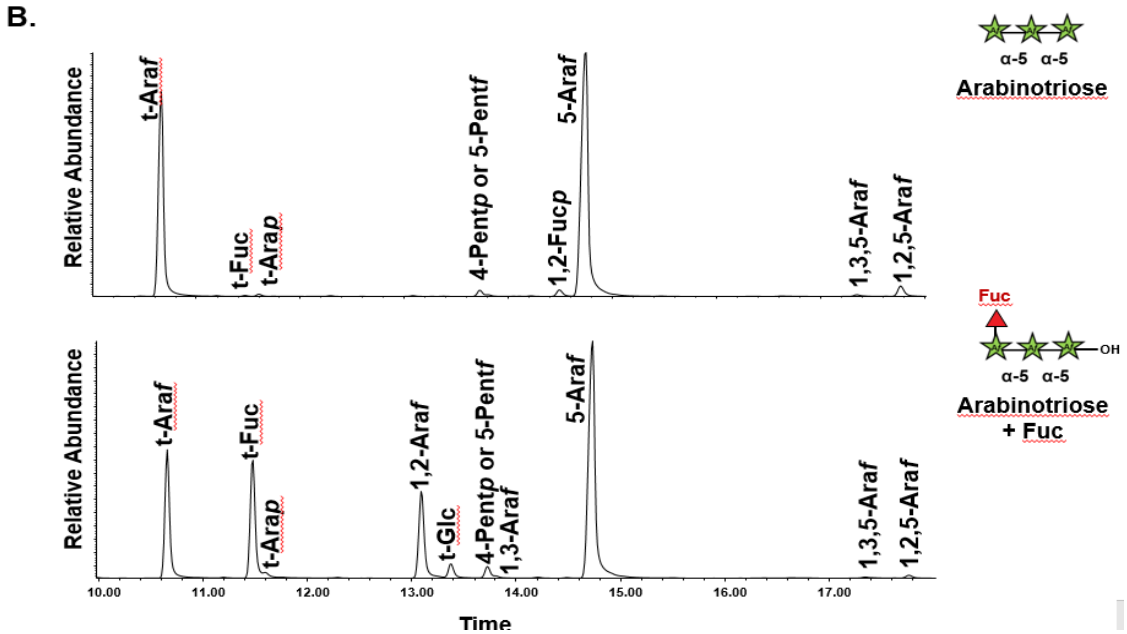
B.
Relative Abundance
t-Araf
t-Fuc
t-Arap
4-Pentp or 5-Pentf
1,2-Fucp
5-Araf
1,3,5-Araf
1,2,5-Araf
α-5 α-5
Arabinotriose
Relative Abundance
t-Araf
t-Fuc
t-Arap
1,2-Araf
t-Glc
4-Pentp or 5-Pentf
1,3-Araf
5-Araf
1,3,5-Araf
1,2,5-Araf
Fuc
OH
α-5 α-5
Arabinotriose
+ Fuc
10.00
11.00
12.00
13.00
14.00
15.00
16.00
17.00
Time

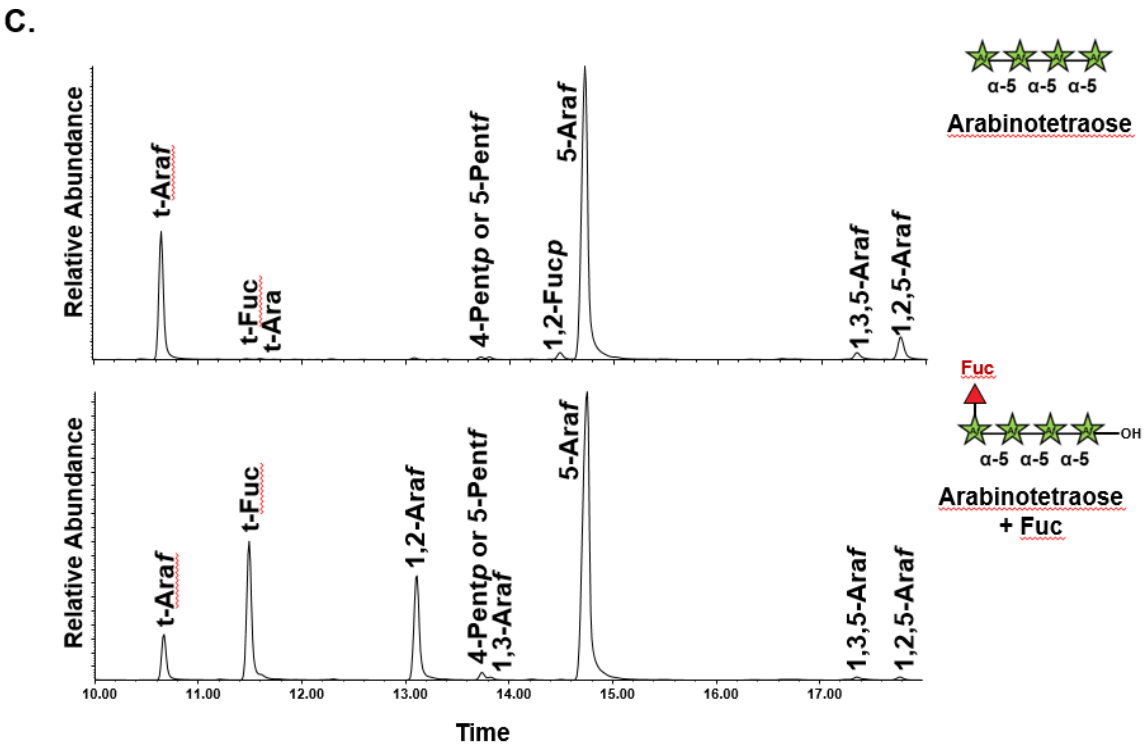

Figure 3.8. Linkage analysis of unreacted arabinan oligosaccharides as compared to the reaction products of the arabinan oligosaccharides incubated with *At*FUT4. (A.) Unreacted arabinobiose and arabinobiose incubated with *At*FUT4. (B.) Unreacted arabinotriose and arabinotriose incubated with *At*FUT4. (C.) Arabinotetraose and arabitetraose incubated with *At*FUT4. For all oligosacchrides, Fuc is added in an α-(1,2)-linkage onto the terminal non-reducing arabinose as evidenced by the 1,2-Ara*f* peak in the spectra for the reaction products of each oligosaccharide. As the 1,3,5-Araf and the 1,2,5-Ara*f* peaks appear in the unreacted and reacted spectra we do not ascribe this to transfer in those linkages.

GUS Promoter Studies Reveal that *At*FUT4 and *At*FUT6 Localize to Different Parts of the Developing Root

The expression patterns of *AtFUT4* and *AtFUT6* have been previously established at the whole organ level, with *AtFUT4* expression being shown to localize to both the leaf and

root, and *AtFUT6* expression localizing to only the root (Sarria et al., 2001). It was demonstrated that *AtFUT4* is solely responsible for the fucosylation of leaf AGPs, while both *AtFUT4* and *AtFUT6* function in the root to produce fucosylated AGPs (Liang et al., 2013; Tryfona et al., 2014). As both *AtFUT4* and *AtFUT6* are expressed and functional in the root, and produce the same fucosylated structures, we predicted that their co-expression in this tissue may be due to the proteins sub-localizing to different cell types. The expression pattern of two isoforms of GDP-D-mannose 4,6-dehydratase (*GMD1* and *GMD2*) in *A. thaliana* (Bonin et al., 1997; Bonin & Reiter, 2000; Bonin et al., 2003) provides a precedent for our prediction.

To investigate the cellular gene expression patterns of *AtFUT4* and *AtFUT6*, transgenic plants containing a β-glucuronidase (GUS) reporter gene under control of the native promoter and 5' UTR of *AtFUT4* and *AtFUT6* were generated. As expected, *AtFUT4::GUS* and *AtFUT6::GUS* exhibited differing, yet complementary, localization patterns. The first visible difference upon staining was at the tap root and lateral roots of the seedlings, with the root of *AtFUT4::GUS* seedlings staining everywhere expect for the elongation and meristematic zones (Figure 3.9A). The tap root of *AtFUT6::GUS* seedlings, on the other hand, stained most visibly in the elongation and meristematic zones (Figure 3.9B). This pattern was repeated in newly formed and emerging lateral roots. The lateral roots of *AtFUT4::GUS* seedlings show strong GUS activity at the base of the root but not at the tip, while the *AtFUT6::GUS* seedlings demonstrate the opposite pattern, exhibiting strong GUS activity only at the tip of the lateral root. The complementary GUS activity patterns detected for *AtFUT4::GUS* and *AtFUT6::GUS* suggests that *AtFUT4* and *AtFUT6* are cell-type specific in the root, and thus have differing physiological roles *in planta*.

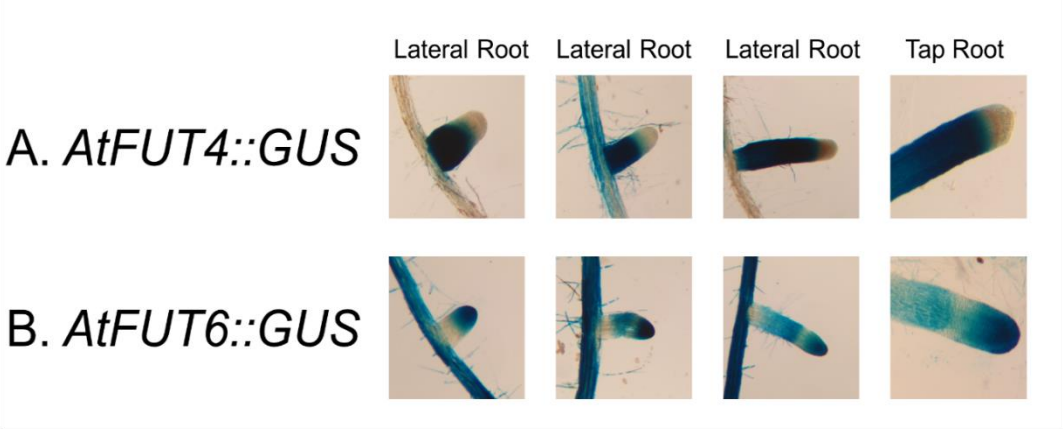

Figure 3.9. Imaging and staining of 12-day-old *AtFUT4::GUS* and *AtFUT6::GUS* seedlings. Seedlings were stained between 4 and 6 hours, and imaged at 40X magnification with an Olympus stereo microscope. The top panel shows the staining pattern for *AtFUT4::GUS*, for lateral roots of increasing lengths and of the tap root. Staining for *AtFUT4::GUS* appears to localize primarily to the maturation and elongation zones. The bottom panel shows the staining pattern for *AtFUT6::GUS*, for lateral roots of increasing lengths and of the tap root. Staining for *AtFUT6::GUS* appears to localize to the root cap and meristematic zone but not the maturation and elongation zones. This difference in apparent staining and localization pattern could serve as an explanation for the functional presence of both the *At*FUT4 and *At*FUT6 proteins in the root, despite their redundant biochemical activities.

CONCLUSIONS

The multiple lines of evidence presented here provide an updated view on the activities of the *At*FUT4 and *At*FUT6 proteins and on the expression localization patterns of the *AtFUT4* and *AtFUT6* genes. In contrast to previous findings, we show that *At*FUT4 and *At*FUT6 are enzymatically redundant and recognize equally various AG-like and non-AG-like oligosaccharides and polysaccharides as acceptor substrates. Additionally, we demonstrate that *At*FUT4 and *At*FUT6 recognize both α-(1,3) and α-(1,5) linked Ara residues on AG-like and non-AG-like oligosaccharides and polysaccharides, irrespective

of the β-(1,3)-linked Gal backbone or the β-(1,6)-linked Gal sidechains of their native targets, AGPs.

As exemplified in this study, *At*FUT4 and *At*FUT6 appear to have much broader and less stringent specificities than *At*FUT1. *At*FUT1 has been demonstrated to fucosylate only the β-(1,2)-linked Gal residues of tamarind XyG (Perrin et al., 1999) and *A. thaliana* XyG (Urbanowicz et al., 2017), and the β-(1,2)-linked galacturonic acid (GalA) residues of some XyGs (Peña et al., 2012; Figure 3.1C). While *At*FUT1 appears to recognize and fucosylate only one type of linkage, *At*FUT4 and *At*FUT6 recognize and fucosylate Ara in both α-(1,3) and α-(1,5) linkages on various AG-like and non-AG-like substrates. While *At*FUT4 and *At*FUT6 can recognize both α-(1,3) and α-(1,5) Ara, we show that *At*FUT4 and *At*FUT6, like *At*FUT1, are also α-(1,2)-specific FUTs. Furthermore, we show that the minimum requirement for fucosylation by *At*FUT4 and *At*FUT6 appears to be an Ara dimer, while *At*FUT1 minimally requires a much larger S1 subunit of XyG. Significant differences in the active sites of *At*FUT4 and *At*FUT6 as compared to the active site of *At*FUT1 may account for the broader diversity of reactions that *At*FUT4 and *At*FUT6 can catalyze. For example, the active sites of *At*FUT4 and *At*FUT6 may be more shallow than that of *At*FUT1, and as such may be able to accommodate a wider array of oligosaccharides and polysaccharides. A shallower catalytic site for *At*FUT4 and *At*FUT6 would also explain the higher observed propensity of *At*FUT4 and *At*FUT6 to hydrolyze GDP-Fuc than detected for *At*FUT1.

Despite the apparent similarities in the substrate specificities of the *At*FUT4 and *At*FUT6 proteins *in vitro*, promoter-reporter gene studies show that the *AtFUT4* and *AtFUT6* genes sub-localize to different areas of the root *in planta*. As with other proteins that have been

demonstrated to have cell-type specific expression patterns, for example *GMD1* and *GMD2* (Bonin et al., 2003), *AtFUT4* and *AtFUT6* are expressed in two distinct cellular regions of the plant root. As *AtFUT6* is only expressed in the root, this would suggest that *AtFUT4* is the major contributor to AGP fucosylation in this organ, while *AtFUT6* is functional in only a subset of cell types at the root tip. Studies on *fut4/fut6* double mutants, however, point to the requirement of both genes for proper AGP fucosylation in order to maintain cell expansion under salt-stress conditions (Tryfona et al., 2014).

The findings from this study provide an important update on the function and specificities of two GT37 FUTs, *At*FUT4 and *At*FUT6. This study also serves to further our understanding of the plant-specific GT37 family, and the differences in the activities and specificities of the characterized members of this family. Finally, the broader specificity of functions identified for these enzymes will aid in the creation of specific modification of plant cell wall structures and other, non-plant derived glycans.

FUNDING

Work on fucosyltransferases in the authors' laboratories has been supported by the National Science Foundation Plant Genome Program (IOS-0923992) and the Center for Bioenergy Innovation (Oak Ridge National Laboratory), US Department of Energy (DOE) Bioenergy Research Center supported by the Office of Biological and Environmental Research in the DOE Office of Science. The authors also acknowledge the Division of Chemical Sciences, Geosciences, and Biosciences, Office of Basic Energy Sciences of the United States Department of Energy through grant DE-SC0008472 for funding studies of cell-type specific pectins in plant cell walls. This work was supported by the Chemical

Sciences, Geosciences and Biosciences Division, Office of Basic Energy Sciences, U.S. Department of Energy grant (DE-SC0015662) to Parastoo Azadi at the Complex Carbohydrate Research Center and NIH grants P01GM107012, P41GM103390, U01GM120408, R01GM130915 for protein expression.

CHAPTER 4

PRELIMINARY DATA:

Cloning, Expression, and Preliminary Activity Data of FUT Gene Constructs and Preliminary Crystallography Data for *At*FUT4 and *At*FUT6

Maria J. Soto, Digantkumar Gopaldas, Pradeep Kumar Prabahkar, Colin Ruprecht, Fabian Pfrengle, Kelley W. Moremen, Breeanna R. Urbanowicz, and Michael G. Hahn. To be submitted to *Frontiers in Plant Biology*

ABSTRACT

Arabidopsis thaliana (*A. thaliana*) has a family of 10 fucosyltransferases (FUTs) that belong to the plant-specific glycosyltransferase family 37 (GT37). Previous studies on GT37 FUTs from *A. thaliana* have been conducted on *A. thaliana* fucosyltransferase 1 (*At*FUT1), *A. thaliana* fucosyltransferase 4 (*At*FUT4), and *A. thaliana* fucosyltransferase 6 (*At*FUT6). *At*FUT1 has been shown to be xyloglucan (XyG)-specific, while *At*FUT4 and *At*FUT6 have been demonstrated to both be arabinogalactan protein (AGP)-specific. The remaining members of GT37 from *A. thaliana*, however, have undetermined functions. In addition to XyG and AGPs, other plant cell wall structures such as rhamnogalacturonan I (RG-I) and rhamnogalacturonan II (RG-II) are also fucosylated. The FUTs responsible for the fucosylation of these structures remain unidentified. Cloning, expressing, and assaying the activities of the additional members of the GT37 FUTs from *A. thaliana* in a mammalian cell line expression system with proven efficacy for plant GTs shows that some of the uncharacterized members of this family are likely to have FUT-specific activity. Furthermore, the successful expression of *At*FUT4 and *At*FUT6 in the same expression system and the high protein titer yielded from their expression may lead to the successful crystallization of these proteins, as has been previously completed for *At*FUT1.

INTRODUCTION

Fucosyltransferases (FUTs), are inverting glycosyltransferase (GT) enzymes that catalyze the transfer of a fucosyl residue to glycans or proteins, and belong to a superfamily which can be subdivided based on the linkage in which fucose (Fuc) is added onto the acceptor substrate. Thus, FUTs are classified as: α-(1,2), α-(1,3), α-(1,4), α-(1,6), and protein O–fucosyltransferase family 1 (POFUT2) and protein O–fucosyltransferase family 2 (POFUT2) FUTs (Martinez-Duncker et al., 2003). The model plant species *Arabidopsis thaliana* (*A. thaliana*) has thirteen total FUT genes, ten of which are classified in the plant-specific, glycosyltransferase family 37 (GT37) in the carbohydrate-active enzyme database (CAZy; Sarria et al., 2001; Cantarel et al., 2009; Lombard et al., 2014). Of the 10 GT37 FUTs in *A. thaliana* three have annotated functions: *A. thaliana* FUT1 (*At*FUT1) which transfers fucose in an α-(1,2)-linkage onto a galactose (Gal) residue of XyG (Perrin et al., 1999; Pauly and Keegstra, 2016; Rocha et al., 2016; Urbanowicz et al., 2017), and *A. thaliana* FUT4 (*At*FUT4) and *A. thaliana* FUT6 (*At*FUT6) that are specific to the biosynthesis of AGPs, transferring fucose (Fuc) in an α-(1,2)-linkage onto an arabinose (Ara) residue (Wu et al., 2010; Tryfona et al., 2012, 2014; Liang et al., 2013; Soto et al., 2019 Chapter 2). For the remaining *A. thaliana* GT37 FUTs only the tissues in which they are expressed have been established (Sarria et al., 2001; Table 4.1).

In addition to XyG and AGPs, rhamnogalacturona I (RG-I) and rhamnogalacturonan II (RG-II) are also fucosylated cell wall polysaccharides. RG-I has an α-(1,2)-linked Fuc residue, while RG-II has both α-(1,2) and α-(1,4)-linked Fuc residues. Because the activities of *At*FUT1, *At*FUT4, and *At*FUT6 are highly specific, the fucosylation of RG-I and RG-II is likely completed by distinct enzymes. Additionally, since *At*FUT1, *At*FUT4,

and *At*FUT6 are all α-(1,2) FUTs, the FUTs catalyzing the transfer of the α-(1,2)-linked Fuc residue on RG-I, and the α-(1,2)-linked Fuc residue on RG-II are likely also members of GT37. FUTs catalyzing the transfer of Fuc in an α-(1,4)-linkage are separately categorized in GT10. As such, the FUT responsible for the α-(1,4)-linkage on RG-II is possibly a member of an entirely separate GT family.

Table 4.1. Known and unknown activities of GT37 *At*FUTs and gene localization from RT-PCR amplification. The activities and specificities of *At*FUT2, *At*FUT3, and *At*FUT7-*At*FUT10 remain unidentified. For genes *At*FUT2, *At*FUT5, *At*FUT7, *At*FUT8, *At*FUT9, and *At*FUT10 RT-PCR products from genomic DNA were visualized by Southern-Blot as no visible bands were detected on ethidium bromide-stained gels (Sarria et al., 2001).

A.thaliana FUT	Activity	Tissue Gene is Expressed In
*At*FUT1	Fucosylates galactose of (XyG) in an α-1,2 linkage (Perrin et al., 1999; Pauly and Keegstra, 2016; Urbanowicz et al., 2017)	Root, Stem, Leaf, Flower, Silique, Seedling
*At*FUT2	UNKNOWN	Root, Stem, Leaf, Flower, Silique, Seedling
*At*FUT3	UNKNOWN	Root, Stem, Leaf, Flower, Silique, Seedling
*At*FUT4	Fucosylate arabinose of AGPs in an α-(1,2) linkage (Wu et al., 2010; Tryfona et al., 2012, 2014; Liang et al., 2013; Soto et al., 2019)	Root, Stem, Leaf, Flower, Seedling
*At*FUT5	UNKNOWN	Root, Leaf, Flower, Silique, Seedling
*At*FUT6	Fucosylate arabinose of AGPs in an α-(1,2) linkage (Wu et al., 2010; Tryfona et al., 2012, 2014; Liang et al., 2013; Soto et al., 2019)	Root, Flower
*At*FUT7	UNKNOWN	Root, Stem, Leaf, Seedling
*At*FUT8	UNKNOWN	Stem, Leaf
*At*FUT9	UNKNOWN	Stem, Leaf
*At*FUT10	UNKNOWN	Root, Stem, Leaf, Seedling

In addition to the extensive biochemical research done to determine the activity and specificity of *At*FUT1, structural studies have led to its successful crystallization, with subsequent analyses of the structure determining that it adopts the glycosyltransferase B (GT-B) fold and is metallo-independent like all other structurally characterized FUT proteins so far. Solved FUT structures have been reported from the following species: *Mus*

muscus (Li et al., 2017), *Caenorhabditis elegans* (Lira-Navarrete et al., 2011; Valero-González et al., 2016), *Homo sapien* (Ihara et al., 2006; Chen et al., 2012; McMillan et al., 2017), *Heliobacter pylori* (Sun et al., 2007), *Bradyrhizomium* sp. strain WM9 (Brzezinski et al., 2007, 2012), and *A. thaliana* (Rocha et al., 2016; Urbanowicz et al., 2017). The activities of the crystallized FUT proteins can be found in Table 4.2.

Table 4.2. FUT structures that have been structurally solved grouped by organism.

Organism	Crystallized FUT Protein	CAZy Family	Activity
Mus muscus	POFUT1 (Li *et al.*, 2017)	GT65	*O*-fucosylation of EGF repeats
Homo sapien	FUT8 (Ihara *et al.*, 2007) POFUT1 (McMillan *et al.*, 2017) POFUT2 (Chen *et al.*, 2012)	GT23 GT65 GT68	α-(1,6)-FUT *O*-fucosylation of EGF repeats *O*-fucosylation TSR repeats
Caenorhabditis elegans	POFUT1 (Lira-Navarrete *et al.*, 2011) POFUT2 (Valero-Gonzales *et al.*, 2016)	GT65 GT68	*O*-fucosylation of EGF repeats *O*-fucosylation TSR repeats
Bradyrhizobium sp. WM9	NodZ (Brzezinski *et al.*, 2007, 2012)	GT23	α-(1,6)-FUT
Arabidopsis thaliana	*At*FUT1 (Rocha *et al.*, 2016; Urbanowicz *et al.*, 2017)	GT37	α-(1,2)-FUT
Heliobacter pylori	FucT (Sun *et al.*, 2007)	GT10	α-(1,3)-FUT

The crystal structure of *At*FUT1 is the only structure solved for an α-(1,2)-FUT, and the only one from a plant species. As discussed in Chapter 1, the phylogenetic relationships exhibited by plant FUTs is significantly different from those of vertebrate and invertebrate FUTs, such that sequence homology cannot be used to predict function of the plant FUTs. The differences plant FUTs exhibit phylogenetically may likewise be exhibited in their protein structures, making the structural characterization of additional FUTs from plants a worthwhile endeavor. The mechanisms that impart the differences in specificity for

*At*FUT1, and *At*FUT4 and *At*FUT6, remain largely unknown. Solving the structures of *At*FUT4 and *At*FUT6 would, therefore, serve multiple purposes: to elucidate the enzymatic structural differences that make possible the differential fucosylation of two important cell wall polysaccharides, XyG and AGPs; to expand the number of plant FUT structures solved; and to identify if structural variations in the GT-B fold adopted by plant FUTs may differ from mammalian and bacterial FUTs.

In this chapter we report preliminary studies on the remaining FUT constructs successfully expressed and purified in HEK293 cells, as well as preliminary crystallography trials for the GFP-*At*FUT4 and GFP-*At*FUT6 proteins. Here we show that the *At*FUT4 and *At*FUT6 fusion protein-constructs express highly in the HEK293 and HEK293S mammalian cell line expression systems and can be produced in quantities sufficient for crystallography studies. We also have prepared expression constructs for some of the remaining GT37 *A. thaliana* FUTs and have shown that these can be expressed successfully in the mammalian cell line expression system. Due to the fact that the reactions catalyzed by these remaining FUTs remain unknown, assays of their activities relied on the tendency of some GTs to hydrolyze their activated nucleotide-sugar donor in the absence of a suitable acceptor-substrate. This equates to the enzymatic transfer of the sugar in the nucleotide-sugar donor to a water molecule (Sheikh et al., 2017). Here we show, using the GDP-Glo™ and UDP-Glo™ assays systems from Promega, that some of the additional FUT proteins expressed have detectable activity for the enzymatic hydrolysis of GDP-Fuc, but not of other activated sugar nucleotide sugars such as UDP-xylose (Xyl) or UDP-galacturonic acid (GalA). The demonstration that some of the remaining GT37 FUTs have

a FUT-specific activity may narrow the search for the identification of the FUTs with specificities for RG-I and RG-II, respectively.

MATERIALS AND METHODS

Production of FUT Constructs and Expression in HEK293 Mammalian Cell Lines

Full length cDNA clones obtained from The Arabidopsis Information Resource (TAIR) were used as templates to amplify truncated coding region sequences for the *At*FUT2, *At*FUT3, *At*FUT4, *At*FUT6, *At*FUT7, *At*FUT8, and *At*FUT10 proteins. *At*FUT2 was unsuccessfully cloned from cDNA or genomic DNA. cDNA clones for *At*FUT5 and *At*FUT9 were unavailable from TAIR and attempts to clone these sequences from genomic DNA and mRNA derived cDNA were unsuccessful. As such, constructs were not produced for *At*FUT2, *At*FUT5, or *At*FUT9 in this manner, but future studies could aim to include these proteins as well through the use of gene synthesis. Some of the members of the GT37 FUT family have a predicted signal peptide according to ARAMEMNON, a plant membrane protein database (Schwacke et al., 2003). The presence of a signal peptide could interfere with the proper production and secretion of proteins made in the HEK293 mammalian cell line expression system, so two constructs were made for these genes. The constructs differed in the lengths of the truncations, to ensure the omission of the signal peptide. (Table 4.3).

Table 4.3. Primers and Fluorescence values for *At*FUT constructs. The underlined nucleotides in the primer sequences denote the *attB* adapter sequences used in the first round of PCR amplification for subsequent Gateway cloning. Fluorescence values are reported for 100 ml transfections in HEK293 cells. *Fluorescence values from 20 ml transfection in HEK293 cells. ǂFluorescence values from 1 L

*At*FUT Amino Acid Truncation	Forward Primer	Reverse Primer	Media GFP Fluorescence
*At*FUT3_Δ75	AACTTGTACTTTCAAGGCTCTAGAGTTCTTCAGAGCA	ACAAGAAAGCTGGGTCCTAATCTTTACAGCCATGGAAC	58
*At*FUT4_Δ54	AACTTGTACTTTCAAGGCAACGACGAATCCGAAACA	ACAAGAAAGCTGGGTCCTATAACTCATCAAAAAGCT	1423, 774ǂ
*At*FUT4*D*_Δ74	TTCGATGAAGGTTCTTGC	GCCTTGAAAGTACAAGTTTTC	82*
*At*FUT6_Δ42	AACTTGTACTTTCAAGGCAACGACTTCAACAACCAAC	ACAAGAAAGCTGGGTCCTATAACTCATCAAATAGCTTA	1028, 865ǂ
*At*FUT6*D*_Δ75	TTCGATGAAGGTTCTTGC	GCCTTGAAAGTACAAGTTTTC	103*
*At*FUT7_Δ30	AACTTGTACTTTCAAGGCCCGAGGGATAGACTGTTAG	ACAAGAAAGCTGGGTCCTATTTGGTATCATCAACTAG	853
*At*FUT8.1_Δ25	AACTTGTACTTTCAAGGCTTCAATTACCAGCTTCTGG	ACAAGAAAGCTGGGTCCTAATTTGAATCAACTAGCTTA	292
*At*FUT8.2_Δ35	AACTTGTACTTTCAAGGCAACGGTTCAAAGGATTCCA	ACAAGAAAGCTGGGTCCTAATTTGAATCAACTAGCTTA	122
*At*FUT10.1_Δ27	AACTTGTACTTTCAAGGCTACAAAGAAGCAACAGAGA	ACAAGAAAGCTGGGTCCTAGTCATCATATAGCTTAAGC	58
*At*FUT10.2_Δ96	AACTTGTACTTTCAAGGCTTTCCAGGTACTTCATGGT	ACAAGAAAGCTGGGTCCTAGTCATCATATAGCTTAAGC	238

To generate Gateway entry clones, attB-PCR products were created using two-step adapter PCR, as explained in the Gateway Technology Manual (ThermoFisher Scientific). Following the first round of PCR amplification, the universal primers attB_AdapterF, 5'GGGGACAAGTTTGTACAAAAAAGCAGGCTCTGAAAACTTGTACTTTCAAGG C-3', and attB_Adapter-R, 5'-GGGGACCACTTTGTACAAGAAAGCTGGGTC-3', were used to complete the attB recombination sites and to introduce a tobacco etch virus (TEV) protease cleavage site, for subsequent protein purification steps. The attB-PCR products were then cloned into a plasmid cloning vector, pDONR221, using the Gateway BP Clonase II Enzyme Mix (ThermoFisher Scientific) again, according to the manufacturer's instructions. To ensure that amplification and integration of the DNA sequence had occurred correctly, the resulting plasmids were sequence verified using M13 universal primers. Expression clones were then created by recombining the entry clones

into the pGEn2-DEST destination vector using the Gateway LR Clonase II Enzyme Mix (ThermoFisher Scientific), according to the manufacturer's instructions. Proteins produced in the pGEn2-DEST vector encode a fusion protein consisting of: an N-terminal NH2-signal sequence, an 8xHis tag, an Avi Tag recognition site, superfolder GFP and the seven amino acids comprising the TEV protease recognition site, followed by the truncated coding regions of the respective *At*FUT protein. The constructs that were successfully cloned, were expressed in initial 100 ml transfections of HEK293 cells (Figure 4.1).

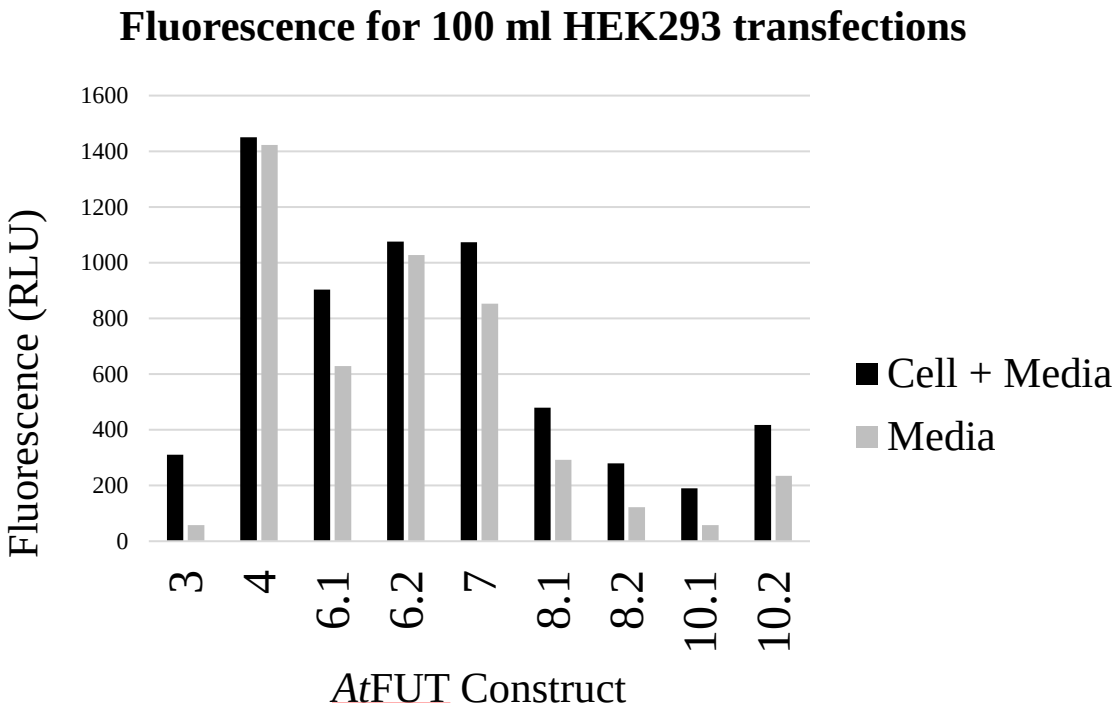

Figure 4.1. Fluorescence values for 100 ml transfection in HEK293 cells.

Additionally, deletion constructs of AtFUT4 and AtFUT6 were generated to omit a greater portion of the stem region preceding the globular catalytic domain. These deletion constructs were made to minimize the interference of the stem region and thereby possibly improve the quality of crystallization. Non-overlapping primers were designed for the pGEn2-DEST vectors of *At*FUT4 and *At*FUT6 using the NEBaseChanger software from

New England Biolabs (Table 3). Deletions were then carried out following the instructions of the Q5® Site-Directed Mutagenesis Kit, also from New England Biolabs. The resulting deletion constructs are denoted as *At*FUT4D_Δ74 and *At*FUT6D_Δ75. Primer sequences used to amplify the desired region of each respective *At*FUT protein, as well as for the deletion constructs, can be found in Table 4.3.

Protein Expression and Purification

The expression of the *At*FUT recombinant enzymes was carried out by transiently transfecting HEK293 or HEK293S human embryonic kidney cells (Freestyle 293-F cells, ThermoFisher Scientific), as previously described (Meng et al., 2013; Moremen et al., 2017; Urbanowicz et al., 2017; Amos et al., 2018). HEK293S cells have a mutation in the gene **N**-acetylglucosaminyltransferase I (GnT1) that inhibits the formation of complex *N*-glycans on the secreted proteins (Stanley, 2002). Fluorescence values, which relate to protein expression levels, for the various expression constructs can be found listed in Table 4.3.

Chromatography experiments for protein purification were performed on an AKTA FPLC System (GE Healthcare, https://www.gehealthcare.com). For purification of the fusion-proteins a Nickel-column was used, as Nickel binds to the His-tag of the fusion-proteins. Prior to loading the Nickel-column, the media was adjusted to contain HEPES (25 mM, pH 7.2), sodium chloride (400 mM), and imidazole (20 mM). Small-scale purification of secreted 8xHis-GFP recombinant enzymes from HEK293 cells was carried out with HisTrap HP Nickle-columns (GE Healthcare) following the manufacturer's instructions. Protein cross-contamination was avoided by purifying each enzyme, on individual 1-ml HisTrap columns, that were washed before use to remove weakly bound

Ni^{2+} ions. Purification of proteins was performed as described (Meng et al., 2013, Urbanowicz et al., 2017 and Amos et al., 2018).

For preliminary crystallography studies, GFP-*At*FUT4 and GFP-*At*FUT6 were prepared in 1 L cultures of the HEK293S cells, with media fluorescence readings of 774 and 865, respectively. The purified proteins were treated with GFP-tagged EndoF1 (Meng et al., 2013) and His-GFP-TEV protease (Wu et al., 2009) that were prepared from *E. coli*. EndoF1 cleaves N-glycans that can interfere with proper protein crystal formation, while TEV cleaves the N-terminal NH_2-signal sequence, 8xHis tag, Avi Tag, and superfolder GFP tags of the fusion-proteins, leaving only the tag-free globular catalytic domain. His-tagged version of EndoF1 and GFP-TEV were used as they would bind to the Nickel-column, effectively separating them from the tag-free *At*FUT4 and *At*FUT6 proteins. Purified GFP-*At*FUT4 and GFP-*At*FUT6 were treated with 1:10 ratios of His-GFP-TEV and GFP-EndoF1 and were left to incubate over a period of 2 days at 4°C. For large scale purification of GFP-*At*FUT4 and GFP-*At*FUT6 treated with His-GFP-TEV and His-EndoF1 the samples were passed through a second, separate HisPrep FF 16/10 column (GE Healthcare) to remove the cleaved N-terminal fusion tag, His-tagged GFP-TEV and His-tagged EndoF1. The eluted, tag-free *At*FUT4 and *At*FUT6 proteins were concentrated and sent to the National Renewable Energy Lab (NREL), at Golden, CO, USA for protein crystallography trials. About 500 µl of *At*FUT4 at ~36 mg/ml, and 1.1 ml of *At*FUT6 at about ~11.4 mg/ml were sent. The proteins sent to NREL had high concentrations of free GFP and were purified by size-exclusion upon arrival.

Small scale purification was done with the use of Nickel-resin. GFP-*At*FUT4 and GFP-*At*FUT6 treated with 1:10 ratios His-GFP-TEV and GFP-EndoF1 were incubated over a

period of 2 days at 4°C. Nickel-resin was then added to bind His-GFP-TEV and GFP-EndoF1 and the tags released from GFP-*At*FUT4 and GFP-*At*FUT6, allowing tag-free *At*FUT4 and *At*FUT6 to be collected separately. The Nickel-resin-purified proteins were repeatedly precipitated and washed, twice with Buffer A, followed by washes with 90% Buffer A +10% Buffer B, and finally 100% Buffer B for three washes. Fractions of all the washes were collected and run on an SDS-PAGE protein gel (Figure 4.3).

Protein Activity Assays with GDP-Glo™ and UDP-Glo™ Glycosyltransferase Assay Kit

Transferase activity was measured using the GDP-Glo™ and UDP-Glo™ Glycosyltransferase Assay Kits from Promega as described in Chapter 2. Assays to measure the hydrolytic activities of GFP-*At*FUT3, GFP-*At*FUT7, GFP-*At*FUT8.1, GFP-*At*FUT8.2, GFP-*At*FUT10.1 and GFP-*At*FUT10.2 were conducted with GDP-Fuc as well as two UDP-sugars, UDP-Xyl and UDP-GalA, and consisted of 100 ng of each enzyme and 250 µM of each nucleotide-sugar. Assays for *At*FUT1, *At*FUT4, and *At*FUT6 were only performed with GDP-Fuc. Hydrolysis assays with all three sugars were conducted simultaneously. Upon completion of the 1-hour hydrolysis reaction period, 5 µl aliquots were incubated for 1 hour with the corresponding UDP- or GDP-Glo Detection reagent.

RESULTS AND DISCUSSION

Constructs for *A. thaliana* GT37 FUTs can be Produced, and Expressed in Human Embryonic Kidney Cells to Result in the Secretion of Functional Recombinant Enzymes

Constructs for most of the remaining *At*FUT genes were successfully made, except for *At*FUT2, *At*FUT5, and *At*FUT9. Constructs for *At*FUT3, *At*FUT4, *At*FUT6, and *At*FUT7 were successfully generated, and in the cases of *At*FUT8 and *At*FUT10, two separate constructs with truncations of differing lengths were made to ensure the omission of a predicted signal peptide and/or additional transmembrane domain (Table 4.3). The constructs for *At*FUT4 and *At*FUT6 were the most highly expressed and extensively secreted into the media. *At*FUT7 was also highly expressed, but secreted to a lesser extent than *At*FUT6. The remaining constructs all expressed to lower but similar extents (Table 4.3).

The fluorescence values reported in Figure 4.1 indicate that the length of the truncation that is generated does have an impact on the production and secretion of the protein of interest. For example, in the case of FUT10, a larger truncation increases protein secretion while in the case of FUT8 a shorter truncation leads to more production and secretion of enzyme. This is also evidenced by the differences in secretion levels between the *At*FUT4 and *At*FUT6 proteins, and their deletion counter-parts which had larger truncations. While there is more evidence here to suggest that a larger truncation decreases proteins production and secretion, it is more likely that protein folding and the secondary structure of these resulting proteins is the determining factor in ensuring the proper production and secretion of these fusion-proteins. Future construct design, and the selection of truncation points should seek to ensure the proper inclusion of stabilizing features such as di-sulfide bonding to increase the likelihood of the production of high titers of functional protein.

In the absence of a suitable acceptor substrate, GTs have been demonstrated to hydrolyze their intended activated sugar-nucleotide donor, essentially transferring the

sugar to a water molecule (Sheikh et al., 2017). The *At*FUT3, *At*FUT7, *At*FUT8, and *At*FUT10 proteins are predicted to be FUTs based on sequence homology to other FUTs, but remain largely uncharacterized. In order to test if they had any detectable activity, they were assayed to determine if hydrolytic activity could be detected in the presence of GDP-Fuc as well as two UDP-sugars, UDP-Xyl and UDP-GalA, using the GDP-Glo and UDP-Glo assay systems from Promega. While GDP-Fuc hydrolysis is predicted to be the sole detectable activity for these putative FUTs, UDP-Xyl and UDP-GalA were included as negative controls.

The GFP-*At*FUT3, GFP-*At*FUT7, GFP-*At*FUT8.1, GFP-*At*FUT8.2, GFP-*At*FUT10.1, and GFP-*At*FUT10.2 proteins were assayed with GDP-Fuc, UDP-Xyl, and UDP-GalA for a period of 60 minutes. Hydrolytic activity is reported in luminescence output, and was only detected for GFP-*At*FUT7, GFP-*At*FUT8.1, GFP-*At*FUT8.2, GFP-*At*FUT10.1, and GFP-*At*FUT10.2 (Figure 4.2). No appreciable activity was detected for GFP-*At*FUT3, GFP-*At*FUT10.1, and GFP-*At*FUT10.2 with any of the activated sugar-nucleotide donors assayed. The only significant activity detected for GFP-*At*FUT7, GFP-*At*FUT8.1, and GFP-*At*FUT8.2, was for the hydrolysis of GDP-Fuc (Figure 4.2). While *At*FUT4 and *At*FUT6 also exhibit significant GDP-Fuc hydrolysis, *At*FUT1 does not. As such, the lack of significant GDP-Fuc hydrolysis detected for *At*FUT3, *At*FUT10.1, and *At*FUT10.2 does not definitively suggest that these proteins are inactive.

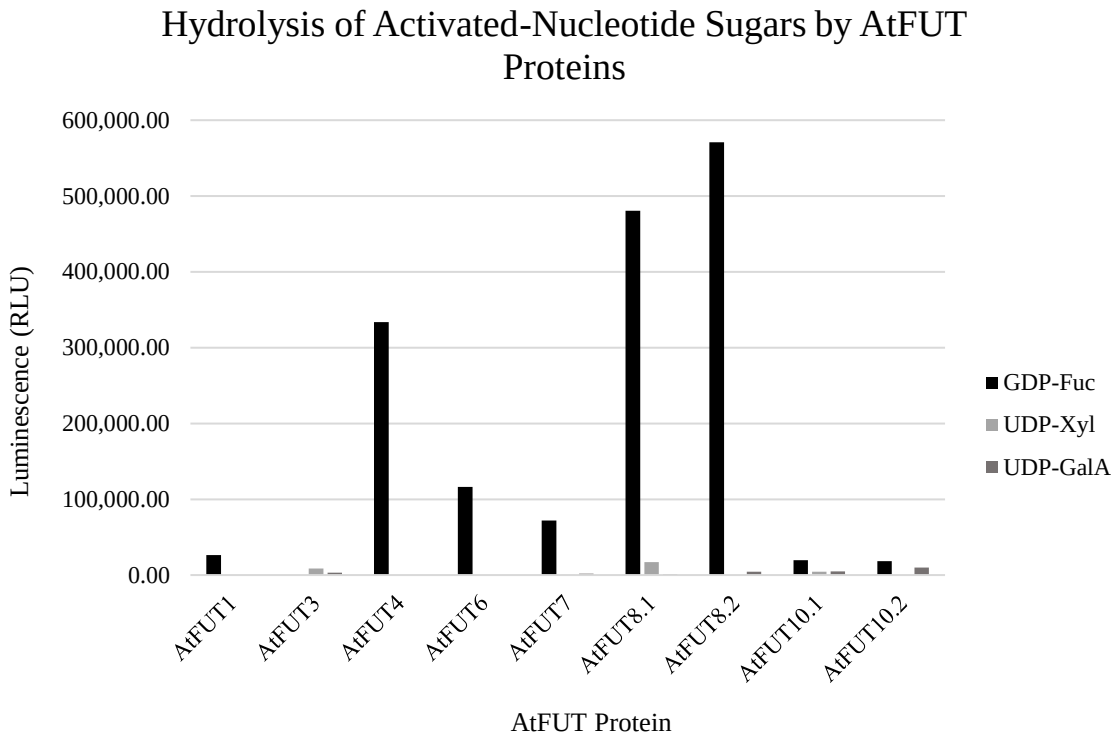

Figure 4.2. GDP and UDP-Glo hydrolysis data for remaining *At*FUT constructs. The remaining *At*FUT fusion-proteins were assayed for their abilities to hydrolize UDP-Xyl, UDP-GalA, and GDP-Fuc. GTs have previously been demonstrated to hydrolize their intended activated-nucleotide sugar donor in the absence of an acceptor. For all proteins the highest activity detected, in RLU, was for the hydrolysis of GDP-Fuc.

While we show here that the GFP-*At*FUT7, GFP-*At*FUT8.1, and GFP-*At*FUT8.2 proteins have detectable hydrolytic activity towards GDP-Fuc, all proteins (including *At*FUT3) were also assayed for transferase activities against over 100 synthetically synthesized oligosaccharides in a high-throughput microarray assay, in collaboration with Dr. Fabian Pfrengle (Max Plank Institute, Golm). In contrast to the data reported here, the only protein with detectable activity was GFP-*At*FUT7, which had activity with some degree of similarity to GFP-*At*FUT4 and GFP-*At*FUT6 (Figure 4.3). While GFP-*At*FUT7

recognized many of the same acceptors as GFP-*At*FUT4 and GFP-*At*FUT6, two acceptors with α-(1,5)-linked Ara, 55 and 81, that GFP-*At*FUT4 and GFP-*At*FUT6 recognized and fucosylated, are not fucosylated by GFP-*At*FUT7. This discrepancy may indicate that GFP-*At*FUT7 does not recognize α-(1,5)-linked Ara as well as both GFP-*At*FUT4 and GFP-*At*FUT6 do.

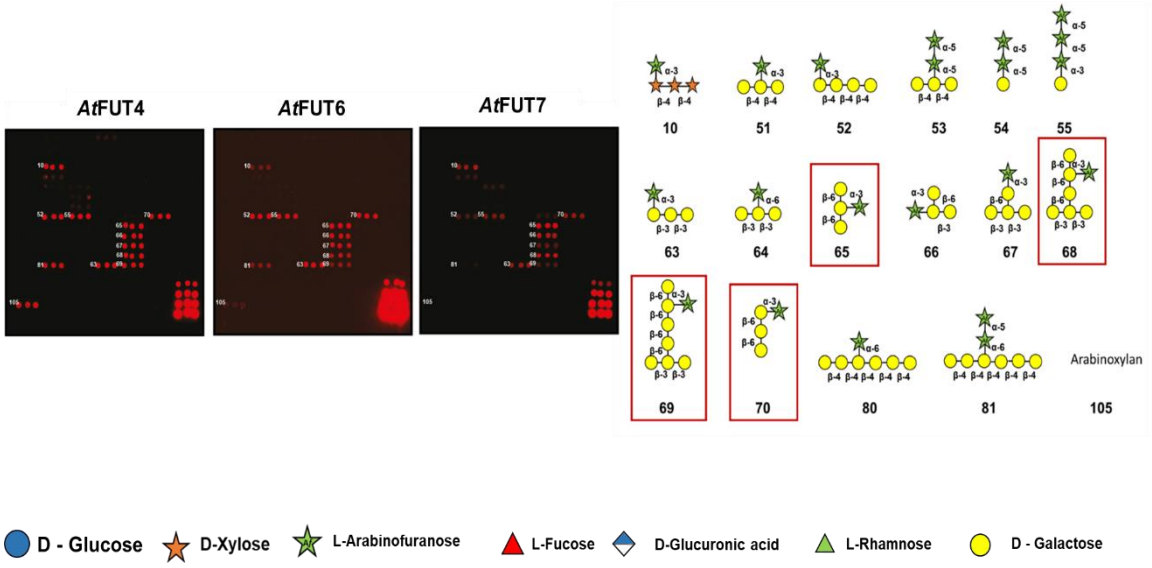

Figure 4.3. Microarray data for *At*FUT4, *At*FUT6 and *At*FUT7. Red spots designate the structures for which transferase activity was detected. The structures corresponding to the numbers listed on the microarray are found to the left. The structures surrounded by red boxes are those that were assayed with *At*FUT4 and *At*FUT6 using MALDI-TOF and GDP-Glo™. As evidenced, AtFUT7 has very similar acceptor specificity to *At*FUT4 and *At*FUT6. Spots found at the bottom right of the microarray are loading controls.

Interestingly, GFP-*At*FUT4, GFP-*At*FUT6, and GFP-*At*FUT7 are the three most highly expressed and successfully secreted proteins (Figure 4.1). The higher extent to which these proteins are expressed and secreted may indicate that these proteins are more easily made

by the HEK293 cells, which may also correlate with their tendency to exhibit more activity than the other proteins purified.

While we show that GFP-*At*FUT8.1 and GFP-*At*FUT8.2 had detectable activity for GDP-Fuc, they had no detectable activity in the microarray assay. These differences in detectable activity could be due to the structural differences between the oligosaccharides in the microarray assay and the fucosylated sidechains of the native structures on which Fuc is found. For example, the Fuc present on RG-I is located on an arabinogalactan (AG) sidechain. While the high-throughput microarray assay contains several AG oligosaccharides that could be RG-I-related, none are as structurally complex as the actual AG sidechain from RG-I. The same can be said for the fucosylated sidechains, A and B, of RG-II which are much more structurally complex than the oligosaccharides used in this assay. Furthermore, the time and unfavorable conditions the proteins experienced during their transport to Germany, in which they were shipped on ice and held up at customs for longer than expected, may also account for the lack of detectable activity in the microarray assay.

*At*FUT4 and *At*FUT6 Recombinant Proteins can be Made in Quantities Sufficient for Future Crystallography Studies

The GFP-*At*FUT4 and GFP-*At*FUT6 fusion-proteins were expressed in a 1 L culture of HEK293S cells, and the purified proteins were sent to the National Renewable Energy Lab (NREL, Golden CO) for crystallography trials. HEK293S cells were used in order to inhibit the formation of complex and hybrid *N*-glycans as these cells are deficient in the gene *GnT1*, whose product initiates the formation of complex and hybrid *N*-glycans that interfere with proper protein crystal formation. The 1 L cultures of the GFP-*At*FUT4 and GFP-

*At*FUT6 fusion-proteins were purified, incubated with His-GFP-TEV protease to remove their His8-sfGFP tag, and GFP-EndoF to truncate any *N*-glycans present to a single GlcNAc. Both His-GFP-TEV and GFP-EndoF were added in a 1:10 ratio relative to the fusion-proteins. The GFP-*At*FUT4 and GFP-*At*FUT6 that were digested with His-GFP-TEV and GFP-EndoF were successfully separated from their released tags (Figure 4.4).

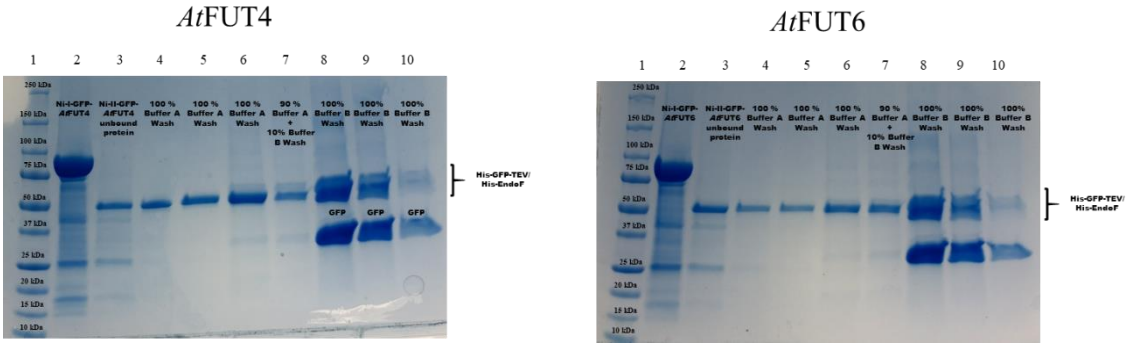

Figure 4.4. Small-scale His-GFP-TEV and GFP-EndoF digest of GFP-*At*FUT4 and GFP-*At*FUT6. *At*FUT4 and *At*FUT6 were incubated with TEV and EndoF in a 1:10 ratio at 4°C for a period of two days. Nickel-resin was then added to the proteins to separate the tags cleaved from GFP-*At*FUT4 and GFP-*At*FUT6, His-GFP-TEV and His-EndoF, and the tag-free proteins. Lane 1, ladder; lane 2, Ni-I purified GFP-*At*FUT4/GFP-*At*FUT6 protein; lane 3, tag-free Ni-II purified *At*FUT4/*At*FUT6 unbound protein; lane 4, 100% Buffer A wash of Nickel resin; lane 5, 100% Buffer A wash of Nickel resin; lane 6, 100% Buffer A wash of Nickel resin; lane 7, 90% Buffer A + 10% Buffer B wash of Nickel resin, lanes 8-10 100 % Buffer B was of Nickel resin to elute His-GFP-TEV, His-EndoF, uncleaved *At*FUT4/*At*FUT6, and the tags released from GFP-*At*FUT4/GFP-*At*FUT6.

The tag-free *At*FUT4 and *At*FUT6 proteins that were purified were sent to NREL where crystallography trials were unsuccessful. To aid in the formation of protein crystals, deletion constructs were made for GFP-*At*FUT4 and GFP-*At*FUT6 to remove a greater portion of the stem region that precedes the globular catalytic domain of these proteins.

The deletion constructs removed 20 amino acids and 33 amino acids from the original GFP-*At*FUT4 and GFP-*At*FUT6 constructs, respectively. Twenty ml HEK293 cell test cultures of GFP-*At*FUT4 and GFP-*At*FUT6 were done alongside their deletion counterpart for direct comparison of their fluorescence levels. The media from the GFP-*At*FUT4 and GFP-*At*FUT6 test cultures fluoresced at 334 and 159, while their deletion counterparts fluoresced at 82 and 103, respectively. The values for the GFP-*At*FUT4 and GFP-*At*FUT6 deletion constructs are marginally above the background fluorescence values of the media used for transfections. This suggests that the larger truncations of the deletion constructs are unfavorable and impede the proper production and secretion of these proteins in the HEK293 cells. The larger truncations of the deletion constructs leave only five amino acids before the first cysteine bond of the protein sequence as opposed to 25 in the original constructs. This may impede proper disulfide bond formation, and hence lead to less stable proteins than those produced from the original constructs, reducing their proper production and viability.

CONCLUSIONS

We show that, in addition to *At*FUT1, *At*FUT4, and *At*FUT6, additional GT37 FUTs can be successfully cloned and expressed in mammalian HEK293 cells. While *At*FUT2, *At*FUT5, and *At*FUT9 were not successfully cloned, *At*FUT3, *At*FUT7, *At*FUT8, and *At*FUT10 were cloned and successfully expressed to a level sufficient for downstream analyses. Future studies should aim to include *At*FUT2, *At*FUT5, and *At*FUT9 in these analysis through the use of gene synthesis The potential acceptor substrates for these enzymes remain unknown, and their activities as FUTs have only been postulated, but we can definitively show that some of them have hydrolytic activity only for their predicted

donor substrate, GDP-Fuc, suggesting that they too have FUT-specific activities. Additionally, as *At*FUT1 does not significantly hydrolyze GDP-Fuc, the lack of activity some of the proteins exhibited does not definitely suggest that they are inactive. While the lack of activity detected for GFP-*At*FUT8.1 and GFP-*At*FUT8.2 from a microarray assay contradicts the data we report here, this loss of activity could be due to the unfavorable conditions the proteins faced during transport to Germany, during which they were shipped only on ice and were held at customs for longer than expected. Future experiments to conclusively demonstrate if activity is present or not could entail the shipment of plasmid DNA to be expressed and purified from HEK293 cells in Germany, to increase the likelihood of obtaining still-active protein. Including oligosaccharides with greater complexity and similarity to the native fucosylated sidechains of RG-I and RG-II may also lead to the detection of activity for the enzymes that had detectable GDP-Fuc hydrolytic activity.

*At*FUT4 and *At*FUT6 express highly in both the HEK293 and HEK293S cell lines, and are expressed and secreted to a degree amenable for crystallography trials. Although initial crystallography trials were unsuccessful, proteins with larger deletions expressed poorly and as such would not be amenable for large-scale transfections. Shorter truncations of the original protein constructs could be made to possibly accommodate proper, stabilizing internal protein bond formation. Alternatively, as the original constructs produce functional, proteins to sufficient titer, crystallography trials could be repeated in collaboration with another lab. Overall, the findings reported here provide the first study into the activities of the *At*FUT3, *At*FUT7, *At*FUT8, and *At*FUT10 GT37 putative FUT proteins, as well as the large-scale production of the *At*FUT4 and *At*FUT6 proteins for

further structural studies. Continued efforts to elucidate the activities of these uncharacterized proteins may finally lead to the identification of the FUTs with specificity for RG-I and RG-II, while structural studies on *At*FUT4 and *At*FUT6 may lead to the definitive identification of the structural differences enabling the differential fucosylation of XyG and AGPs.

FUNDING

Work on fucosyltransferases in the authors' laboratories has been supported by the National Science Foundation Plant Genome Program (IOS-0923992) and the Center for Bioenergy Innovation (Oak Ridge National Laboratory), US Department of Energy (DOE) Bioenergy Research Center supported by the Office of Biological and Environmental Research in the DOE Office of Science. The authors also acknowledge the Division of Chemical Sciences, Geosciences, and Biosciences, Office of Basic Energy Sciences of the United States Department of Energy through grant DE-SC0008472 for funding studies of cell-type specific pectins in plant cell walls. This work was supported by the Chemical Sciences, Geosciences and Biosciences Division, Office of Basic Energy Sciences, U.S. Department of Energy grant (DE-SC0015662) to Parastoo Azadi at the Complex Carbohydrate Research Center and and NIH grants P01GM107012, P41GM103390, U01GM120408, R01GM130915 for protein expression.

CHAPTER 5

CONCLUSIONS

This dissertation provides an updated understanding of the activities and specificities of the *At*FUT4 and *At*FUT6 *A. thaliana* proteins, as well as the first reported studies on additional as-yet uncharacterized members of the GT37 FUT family from *A. thaliana*. I have also undertaken an overview of the activities and specificities of characterized plant FUTs to date, as well as the first large-scale analysis of the unusual phylogenetic relationships exhibited by plant FUTs (Chapter 2).

Cloning, expression, and purification of the *At*FUT4 and *At*FUT6 *A. thaliana* proteins in mammalian HEK293 cells demonstrates that this system allows for the successful production of functional enzymes in sufficient quantities amenable for down-stream studies. *At*FUT4 and *At*FUT6 produced in this manner maintain their previously established AGP-specificity. Contrary to previous findings, however, the work in this dissertation conclusively proves that *At*FUT4 and *At*FUT6 recognize the same oligosaccharides as acceptors and are not partially- redundant or non-redundant as had been previously suggested. The work in this dissertation shows that *At*FUT4 and *At*FUT6 are identical in their activities towards various AG- and non-AG-like oligosaccharides and demonstrates that the minimum acceptor structure that *At*FUT4 and *At*FUT6 recognize for fucosylation is an arabinose dimer. Additionally, the data reported here conclusively

demonstrates that *At*FUT4 and *At*FUT6, like *At*FUT1, catalyze the transfer of Fuc from GDP-Fuc onto these oligosaccharide acceptors in an α-(1,2)-linkage (Chapter 3).

This dissertation also provides the first reported cloning, expression, purification, and enzyme activity assays of several of the remaining GT37 FUTs from *A. thaliana*. The work reported here shows that some of remaining GT37 FUTs, like *At*FUT4 and *At*FUT6, exhibit activity specific for the hydrolysis of GDP-Fuc, but not other activated sugar-nucleotides. Not all of the GT37 FUTs assayed exhibited GDP-Fuc hydrolysis; *At*FUT1 exhibits low levels of GDP-Fuc hydrolysis. As such, a lack of hydrolytic activity towards GDP-Fuc cannot be used as an accurate determinant of activity for this gene family, but may suggest that the activities of the FUTs that do exhibit significant GDP-Fuc hydrolysis are more similar to *At*FUT4 and *At*FUT6, and that those that do not are more similar to the activity of *A*tFUT1. For example, *At*FUT7 which exhibits moderate GDP-Fuc hydrolysis was demonstrated to have an acceptor specificity similar to that of *At*FUT4 and *At*FUT6 from a microarray assay containing over 100 structurally diverse plant-derived oligosaccharides synthesized by a collaborating laboratory in Germany. None of the other GT37 FUTs that were assayed for the hydrolysis of GDP-Fuc exhibited any activity in the microarray assay, which may be due to the lack of sufficient structural diversity of the synthetic plant-derived oligosaccharides in comparison to the native fucosylated structures found in plants (Chapter 4).

Future activity assays with acceptor substrates more closely mimicking the structures of RG-I and RG-II, for example, should be conducted on the proteins that have already been successfully expressed. Additionally, it would be worthwhile to send plasmid DNA for transfection and expression in Germany, rather than sending purified protein overseas

to increase the chances that viable, active proteins are assayed. Additionally, future studies should aim to successfully create expression constructs for *At*FUT2, *At*FUT5, and *At*FUT9 to fully analyze all of the the *A. thaliana* GT37 FUTs. *At*FUT2, may be especially interesting to study as it does not group with the rest of the *AtFUT* genes, based on phylogenetic analyses (Chapter 2).

Future studies should also aim to successfully obtain crystal structures of the *At*FUT4 and *At*FUT6 proteins for detailed structural analyses. As demonstrated in this study, the fusion-protein versions of *At*FUT4 and *At*FUT6 can be efficiently produced in large-volumes and purified to amounts amenable for structural analyses. Obtaining crystal structures of *At*FUT4 and *At*FUT6 will provide invaluable insight into the structural differences that enable the differential fucosylation of XyG and AGPs. Additionally, detailed structural analyses may elucidate the propensity of *At*FUT4 and *At*FUT6 to hydrolyze GDP-Fuc to a much greater extent than *At*FUT1 does, a feature which already suggests significant differences in the structures of these enzymes. Differences in the rate of GDP-Fuc hydrolysis are also exhibited by the additional *At*FUT proteins that were assayed in this study. Detailed structural comparisons of *At*FUT1, *At*FUT4 and *At*FUT6 may enable the creation of better templates for the molecular modeling of the additional *A. thaliana* GT37 FUTs and may lead to better predictions of the possible acceptor substrates of these additional proteins.

REFERENCES

Atmodjo, M.A., Hao, Z., and Mohnen, D. 2013. Evolving Views of Pectin Biosynthesis. *Annu. Rev. Plant Biol* **64**: 747–779.

Bardor, M., Faveeuw, C., Fitchette, A.C., Gilbert, D., Galas, L., Trottein, F., Faye, L., and Lerouge, P. 2003. Immunoreactivity in mammals of two typical plant glyco-epitopes, core α(1,3)-fucose and core xylose. *Glycobiology* **13**: 427–434.

Bartetzko, M.P., and Pfrengle, F. 2019. Automated Glycan Assembly of Plant Oligosaccharides and Their Application in Cell-Wall Biology. *ChemBioChem* **20**: 877–885.

Bartetzko, M.P., Schuhmacher, F., Hahm, H.S., Seeberger, P.H., and Pfrengle, F. 2015. Automated Glycan Assembly of Oligosaccharides Related to Arabinogalactan Proteins. *Org. Lett*. **17**: 4344–4347.

Boisson, M., Gomord, V., Audran, C., Berger, N., Dubreucq, B., Granier, F., Lerouge, P., Faye, L., Caboche, M., and Lepiniec, L. 2001. *Arabidopsis glucosidase I* mutants reveal a critical role of *N*-glycan trimming in seed development. *EMBO J*. **20**: 1010–9.

Bondili, J.S., Castilho, A., Mach, L., Glössl, J., Steinkellner, H., Altmann, F., and Strasser, R. 2006. Molecular cloning and heterologous expression of β1,2-xylosyltransferase and core α1,3-fucosyltransferase from maize. *Phytochemistry* **67**: 2215–2224.

Bonin, C.P., Freshour, G., Hahn, M.G., Vanzin, G.F., Reiter, W.-D., and Hahn, M.G. 2003. The *GMD1* and *GMD2* genes of Arabidopsis encode isoforms of GDP-D-mannose 4,6-dehydratase with cell type-specific expression patterns. *Plant Physiol*. **132**: 883–92.

Bonin, C.P., Potter, I., Vanzin, G.F., and Reiter, W.D. 1997. The *MUR1* gene of *Arabidopsis thaliana* encodes an isoform of GDP-D-mannose-4,6-dehydratase, catalyzing the first step in the *de novo* synthesis of GDP-L-fucose. *Proc. Natl. Acad. Sci. U. S. A.* **94**: 2085–90.

Bonin, C.P., and Reiter, W.-D. 2000. A bifunctional epimerase-reductase acts downstream of the *MUR1* gene product and completes the *de novo* synthesis of GDP-L-fucose in *Arabidopsis*. *Plant J*. **21**: 445–454.

Both, P., Sobczak, L., Breton, C., Hann, S., Nöbauer, K., Paschinger, K., Kozmon, S., Mucha, J., and Wilson, I.B.H. 2011. Distantly related plant and nematode core α1,3-fucosyltransferases display similar trends in structure-function relationships. *Glycobiology* **21**: 1401–1415.

Cantarel, B.L., Coutinho, P.M., Rancurel, C., Bernard, T., Lombard, V., and Henrissat, B. 2009. The Carbohydrate-Active EnZymes database (CAZy): an expert resource for Glycogenomics. *Nucleic Acids Res*. **37**: 233–238.

Čapková, V., Fidlerová, A., Amstel, T. Van, Croes, A.F., Mata, C., Schrauwen, J.A.M., Wullems, G.J., and Tupý, J. 1997. Role of *N*-glycosylation of 66 and 69 kDa glycoproteins in wall formation during pollen tube growth *in vitro*. *Eur. J. Cell Biol*. **72**: 282–285.

Chou, Y.H., Pogorelko, G., Young, Z.T., and Zabotina, O.A. 2015. Protein-protein interactions among xyloglucan-synthesizing enzymes and formation of golgi-localized multiprotein complexes. *Plant Cell Physiol*. **56**: 255–267.

Chou, Y.H., Pogorelko, G., and Zabotina, O.A. 2012. Xyloglucan xylosyltransferases XXT1, XXT2, and XXT5 and the glucan synthase CSLC4 form Golgi-localized multiprotein complexes. *Plant Physiol*. **159**: 1355–1366.

Clough, S.J., and Bent, A.F. 1998. Floral dip: a simplified method for *Agrobacterium*-mediated transformation of *Arabidopsis thaliana*. *Plant J*. **16**: 735–743.

Cosgrove, D.J. 2014. Re-constructing our models of cellulose and primary cell wall assembly. *Curr. Opin. Plant Biol*. **22**: 122–131.

Coutinho, P.M., Deleury, E., Davies, G.J., and Henrissat, B. 2003. An Evolving Hierarchical Family Classification for Glycosyltransferases. *J. Mol. Biol*. **328**: 307–317.

Darvill, A.G., Albersheim, P., McNeil, M., Lau, J.M., York, W.S., Stevenson, T.T., Thomas, J., Doares, S., Gollin, D.J., and Chelf, P. 1985. Structure and function of plant cell wall polysaccharides. *J. Cell Sci. Suppl*. **2**: 203–17.

Faïk, A., Bar-Peled, M., DeRocher, A.E., Zeng, W., Perrin, R.M., Wilkerson, C., Raikhel, N. V, and Keegstra, K. 2000. Biochemical characterization and molecular cloning of an α-1,2-fucosyltransferase that catalyzes the last step of cell wall xyloglucan biosynthesis in pea. *J. Biol. Chem*. **275**: 15082–15089.

Faïk, A., Chileshe, C., Sterling, J., and Maclachlan, G. 1997. Xyloglucan galactosyl- and fucosyltransferase activities from pea epicotyl microsomes. *Plant Physiol*. **114**: 245–254.

Farkas, V., and Maclachlan, G. 1988. Fucosylation of exogenous xyloglucans by pea microsomal membranes. *Arch. Biochem. Biophys*. **264**: 48–53.

Feingold, D. S., and Avigad, G. 1980. Sugar nucleotide trans- formations in plants. In: P. K. Stumpf, and E. E. Conn (Eds.), *The Biochemistry of Plants: A Comprehensive Treatise*, Vol. 3, Academic Press, New York, pp. 101–170.

Fry, S.C., McNeil, M., Grant Reid, J.S., Voragen, A.G.J., Mort, A.J., Maclachlan, G.A., Kato, Y., Selvendran, R.R., Lorences, E.P., Albersheim, P., et al. 1993. An unambiguous nomenclature for xyloglucan-derived oligosaccharides. *Physiol. Plant*. **89**: 1–3.

Goldsmith, M.H.M. 1977. The Polar Transport of Auxin. *Annu. Rev. Plant Physiol*. **28**: 439–478.

Hallgren, P., Lundblad, A., and Svensson, S. 1975. A new type of carbohydrate protein linkage in a glycopeptide from normal human urine. *J. Biol. Chem*. **250**: 5312–5314.

Hansen, S.F., Harholt, J., Oikawa, A., and Scheller, H. V. 2012. Plant Glycosyltransferases Beyond CAZy: A Perspective on DUF Families. *Front. Plant Sci*. **3**: 1–10.

Harmoko, R., Yoo, J. Y., Ko, K. S., Ramasamy, N. K., Hwang, B. Y., Lee, E. J., Kim, H. S., Lee, K. J., Oh, D.-B., Kim, D.-Y., Lee, S., Li, Y., Lee, S. Y., and Lee, K. O. 2016. *N*-glycan containing a core α1,3-fucose residue is required for basipetal auxin transport and gravitropic response in rice (*Oryza sativa*). *New Phytol*. **212**: 108–122.

Heiss, C., Klutts, J.S., Wang, Z., Doering, T.L., and Azadi, P. 2009. The structure of *Cryptococcus neoformans* galactoxylomannan contains *β*-D-glucuronic acid. *Carbohydr. Res.* **344**: 915.

Imayoshi, I., and Kageyama, R. 2011. The role of notch signaling in adult neurogenesis. *Mol. Neurobiol*. **44**: 7–12.

Jefferson, R.A., Kavanagh, T.A., and Bevan, M.W. 1987. GUS fusions: *β*-glucuronidase as a sensitive and versatile gene fusion marker in higher plants. *EMBO J.* **6**: 3901–3907.

Joly, C., Léonard, R., Maftah, A., and Riou-Khamlichi, C. 2002. α4-Fucosyltransferase is regulated during flower development: Increases in activity are targeted to pollen maturation and pollen tube elongation. *J. Exp. Bot*. **53**: 1429–1436.

Knoch, E., Dilokpimol, A., and Geshi, N. 2014. Arabinogalactan proteins: Focus on carbohydrate active enzymes. *Front. Plant Sci.* **5**: 198.

Leiter, H., Mucha, J., Staudacher, E., Grimm, R., Glössl, J., and Altmann, F. 1999. Purification, cDNA cloning, and expression of GDP-L-Fuc:Asn-linked GlcNAc α1,3-fucosyltransferase from mung beans. *J. Biol. Chem*. **274**: 21830–21839.

Léonard, R., Lhernould, S., Carlué, M., Fleurat, P., Maftah, A., and Costa, G. 2005. Biochemical characterization of *Silene alba* α4-fucosyltransferase and Lewis^a products. *Glycoconj. J*. **22**: 71–78.

Liang, Y., Basu, D., Pattathil, S., Xu, W.-L., Venetos, A., Martin, S.L., Faik, A., Hahn, M.G., and Showalter, A.M. 2013. Biochemical and physiological characterization of *fut4* and *fut6* mutants defective in arabinogalactan-protein fucosylation in *Arabidopsis*. *J. Exp. Bot*. **64**: 5537–51.

Liepman, A.H., Wightman, R., Geshi, N., Turner, S.R., and Scheller, H.V. 2010. Arabidopsis - A powerful model system for plant cell wall research. *Plant J*. **61**: 1107–1121.

Liu, L., Paulitz, J., and Pauly, M. 2015. The presence of fucogalactoxyloglucan and its synthesis in rice indicates conserved functional importance in plants. *Plant Physiol*. **168**: 549–60.

Lombard, V., Golaconda Ramulu, H., Drula, E., Coutinho, P.M., and Henrissat, B. 2014. The carbohydrate-active enzymes database (CAZy) in 2013. *Nucleic Acids Res*. **42**: D490–D495.

Lukowitz, W., Nickle, T.C., Meinke, D.W., Last, R.L., Conklin, P.L., and Somerville, C.R. 2001. *Arabidopsis cyt1* mutants are deficient in a mannose-1-phosphate guanylyltransferase and point to a requirement of *N*-linked glycosylation for cellulose biosynthesis. *Proc. Natl. Acad. Sci. U. S. A.* **98**: 2262–2267.

Lund, C.H., Bromley, J.R., Stenbæk, A., Rasmussen, R.E., Scheller, H. V., and Sakuragi, Y. 2015. A reversible *Renilla* luciferase protein complementation assay for rapid identification of protein-protein interactions reveals the existence of an interaction network involved in xyloglucan biosynthesis in the plant Golgi apparatus. *J. Exp. Bot*. **66**: 85–97.

Luo, Y., Nita-Lazar, A., and Haltiwanger, R.S. 2006. Two distinct pathways for *O*-fucosylation of epidermal growth factor-like or thrombospondin type 1 repeats. *J. Biol. Chem*. **281**: 9385–9392.

Martinez-Duncker, I., Mollicone, R., Candelier, J.-J., Breton, C., and Oriol, R. 2003. A new superfamily of protein-*O*-fucosyltransferases, α2-fucosyltransferases, and α6-fucosyltransferases: phylogeny and identification of conserved peptide motifs. *Glycobiology* **13**: 1C – 5.

Meents, M.J., Watanabe, Y., and Samuels, A.L. 2018. The cell biology of secondary cell wall biosynthesis. *Ann. Bot*. **121**: 1107–1125.

Meng, L., Forouhar, F., Thieker, D., Gao, Z., Ramiah, A., Moniz, H., Xiang, Y., Seetharaman, J., Milaninia, S., Su, M., Bridger, R., Veillon, L., Azadi, P., Kornhaber, G., Wells, L.,

Montelione, G.T., Woods, R.J., Tong, L., Moremen, K.W. 2013. Enzymatic basis for *N*-glycan sialylation: *Structure of rat α2,6-sialyltransferase (ST6GAL1) reveals conserved and unique features for glycan sialylation*. *J. Biol. Chem.* **288**: 34680–34698.

Misawa, H., Tsumuraya, Y., Kaneko, Y., and Hashimoto, Y. 1996. α-L-Fucosyltransferases from Radish Primary Roots. *Plant Physiol*. **110**: 665–673.

Mohnen, D. 2008. Pectin structure and biosynthesis. *Curr. Opin. Plant Biol*. **11**: 266–277.

Moremen, K.W., Ramiah, A., Stuart, M., Steel, J., Meng, L., Forouhar, F., Moniz, H.A., Gahlay, G., Gao, Z., Chapla, D., Wang, S., Yang, J.-Y., Prabhakar, P.K., Johnson, R., Rosa, M. D., Geisler, C., Nairn, A.V., Seetharaman, J., Wu, S.-C., Tong, L., Gilbert, H. J., Labaer, J., Jarvis, D. L. 2017. Expression system for structural and functional studies of human glycosylation enzymes. *Nat. Chem. Biol*. **14**: 156–162.

Ndeh, D., Rogowski, A., Cartmell, A., Luis, A. S., Basl?e, A., Gray, J., Venditto, I., Briggs, J., Zhang, X., Labourel, A., Terrapon, N., Buffetto, F., Nepogodiev, S., Xiao, Y., Field, R. A., Zhu, Y., O'Neill, M. A., Urbanowicz, B. R., York, W. S., Davies, G. J., Abbott, D. W., Ralet, M.-C., Martens, E. C., Henrissat, B., and Gilbert, H. J. 2017. Complex pectin metabolism by gut bacteria reveals novel catalytic functions. *Nature* **544**:65–70.

Neumetzler, L., Humphrey, T., Lumba, S., Snyder, S., Yeats, T.H., Usadel, B., Vasilevski, A., Patel, J., Rose, J.K.C., Persson, S., and Bonetta, D. 2012. The *FRIABLE1* Gene Product Affects Cell Adhesion in Arabidopsis. *PLoS One* **7**: e42914.

O'Neill, M.A., Eberhard, S., Albersheim, P., and Darvill, A.G. 2001. Requirement of borate cross-linking of cell wall rhamnogalacturonan II for *Arabidopsis* growth. *Science* **294**: 846–849.

Okada, T., Ihara, H., Ito, R., and Ikeda, Y. 2017. Molecular cloning and functional expression of Lewis type α1,3/α1,4-fucosyltransferase cDNAs from *Mangifera indica* L. *Phytochemistry* **144**: 98–105.

Okajima, T., and Irvine, K.D. 2002. Regulation of Notch signaling by *O*-linked fucose. *Cell* **111**: 893–904.

Palma, A.S., Vila-Verde, C., Pires, A.S., Fevereiro, P.S., and Costa, J. 2001. A novel plant α4-fucosyltransferase (*Vaccinium myrtillus* L.) synthesises the Lewis^a adhesion determinant. *FEBS Lett.* **499**: 235–238.

Pauly, M., Albersheim, P., and Darvill, A. 2001. Effects of the *mur1* mutation on xyloglucans produced by suspension-cultured *Arabidopsis thaliana* cells. *Planta* **214**:67–74.

Pauly, M., and Keegstra, K. 2016. Biosynthesis of the Plant Cell Wall Matrix Polysaccharide Xyloglucan. *Annu. Rev. Plant Biol*. **67**: 235–259.

Peña, M.J., Kong, Y., York, W.S., and O'Neill, M.A. 2012. A Galacturonic Acid-Containing Xyloglucan Is Involved in *Arabidopsis* Root Hair Tip Growth. *Plant Cell* **24**: 4511–4524.

Perrin, R.M., DeRocher, A.E., Bar-Peled, M., Zeng, W., Norambuena, L., Orellana, A., Raikhel, N. V, and Keegstra, K. 1999. Xyloglucan fucosyltransferase, an enzyme involved in plant cell wall biosynthesis. *Science* **284**: 1976–1979.

Puhlmann, J., Bucheli, E., Swain, M.J., Dunning, N., Albersheim, P., Darvill, A.G., and Hahn, M.G. 1994. Generation of monoclonal antibodies against plant cell-wall polysaccharides. I. Characterization of a monoclonal antibody to a terminal alpha-(1→2)-linked fucosyl-containing epitope. *Plant Physiol*. **104**: 699–710.

Ralph, J., Lundquist, K., Brunow, G., Lu, F., Kim, H., Schatz, P.F., Marita, J.M., Hatfield, R.D., Ralph, S.A., Christensen, J.H., Boerjan, W. 2004. Lignins: Natural polymers from oxidative coupling of 4-hydroxyphenyl- propanoids. *Phytochem. Rev*. **3**: 29–60.

Reiter, W.-D., Chapple, C., and Somerville, C.R. 1997. Mutants of *Arabidopsis thaliana* with altered cell wall polysaccharide composition. *Plant J*. **12**: 335–345.

Reiter, W.-D., Chapple, C.C.S., and Somerville, C.R. 1993. Altered growth and cell walls in a fucose-deficient mutant of Arabidopsis. *Science* **261**: 1032–1035.

Reiter, W.-D., and Vanzin, G.F. 2001. Molecular genetics of nucleotide sugar interconversion pathways in plants. *Plant Mol. Biol*. **47**: 95–113.

Reuhs, B.L., Glenn, J., Stephens, S.B., Kim, J.S., Christie, D.B., Glushka, J.G., Zablackis, E., Albersheim, P., Darvill, A.G., and O'Neill, M.A. 2004. L-Galactose replaces L-fucose in the pectic polysaccharide rhamnogalacturonan II synthesized by the L-fucose-deficient *mur1 Arabidopsi*s mutant. *Planta* **219**: 147–157.

Ridley, B.L., O'Neill, M.A., and Mohnen, D. 2001. Pectins: Structure, biosynthesis, and oligogalacturonide-related signaling. *Phytochemistry* **57**: 929–967.

Roberts, L.M., Mellor, R.B., and Lord, J.M. 1980. Glycoprotein fucosyl transferase in the endoplasmic reticulum of castor bean endosperm cells. *FEBS Lett*. **113**: 90–94.

Rocha, J., Cicéron, F., Sanctis, D. de, Lelimousin, M., Chazalet, V., Lerouxel, O., and Breton, C. 2016. Structure of *Arabidopsis thaliana* FUT1 reveals a variant of the GT-B class fold and provides insight into xyloglucan fucosylation. *Plant Cell* **28**: 2352–2364.

Ruprecht, C., Bartetzko, M.P., Senf, D., Dallabernadina, P., Boos, I., Andersen, M.C.F., Kotake, T., Knox, J.P., Hahn, M.G., Clausen, M.H., et al. 2017. A synthetic glycan microarray enables epitope mapping of plant cell wall glycan-directed antibodies. *Plant Physiol*. **175**: 1094–1104.

Sarria, R., Wagner, T.A., O'Neill, M.A., Faik, A., Wilkerson, C.G., Keegstra, K., and Raikhel, N. V 2001. Characterization of a family of Arabidopsis genes related to xyloglucan Fucosyltransferase1. *Plant Physiol*. **127**: 1595–606.

Schaewen, A. von, Sturm, A., O'Neill, J., and Chrispeels, M.J. 1993. Isolation of a mutant *Arabidopsis* plant that lacks *N*-acetyl Glucosaminyl Transferase I and is unable to synthesize Golgi-modified complex *N*-linked glycans. *Plant Physiol*. **102**: 1109–18.

Schneider, M., Al-Shareffi, E., and Haltiwanger, R.S. 2017. Biological functions of fucose in mammals. *Glycobiology* **27**: 601–618.

Seifert, G.J., and Roberts, K. 2007. The Biology of Arabinogalactan Proteins. *Annu. Rev. Plant Biol* **58**: 137–61.

Sheikh, M.O., Halmo, S.M., Patel, S., Middleton, D., Takeuchi, H., Schafer, C.M., West, C.M., Haltiwanger, R.S., Avci, F.Y., Moremen, K.W., Wells. 2017. Rapid screening of sugar-nucleotide donor specificities of putative glycosyltransferases. *Glycobiology* **27**: 206–212.

Shi, S., and Stanley, P. 2003. Protein *O*-fucosyltransferase 1 is an essential component of Notch signaling pathways. *Proc. Natl. Acad. Sci*. **100**: 5234–5239.

Showalter, A.M., and Basu, D. 2016. Extensin and Arabinogalactan-Protein Biosynthesis: Glycosyltransferases, Research Challenges, and Biosensors. *Front. Plant Sci*. **7**: 1–9.

Sim, J.S., Kesawat, M.S., Kumar, M., Kim, S.Y., Mani, V., Subramanian, P., Park, S., Lee, C.M., Kim, S.R., and Hahn, B.S. 2018. Lack of the α1,3-fucosyltransferase gene (*OsfucT*) affects anther development and pollen viability in rice. *Int. J. Mol. Sci*. **19**: 1225–1247.

Smith, D.K., Harper, J.F., and Wallace, I.S. 2018a. A potential role for protein *O*-fucosylation during pollen-pistil interactions. *Plant Signal. Behav*. **13**: e1467687.

Smith, D.K., Jones, D.M., Lau, J.B.R., Cruz, E.R., Brown, E., Harper, J.F., and Wallace, I.S. 2018b. A putative protein *O*-fucosyltransferase facilitates pollen tube penetration through the stigma–style interface. *Plant Physiol*. **176**: 2804–2818.

Smith, P. S., Peña, M. J., York, W. S., and Urbanowicz, B. R. (2019) Analytical Techniques for the Characterization of Domain of Unknown Function 579 Family Members and Their Roles in the Synthesis of Methylated Plant Cell Wall Epitopes (in review *SLAS Technol*.).

Soto, M.J., Urbanowicz, B.R., and Hahn, M.G. 2019. Plant Fucosyltransferases and the Emerging Biological Importance of Fucosylated Plant Structures. *CRC. Crit. Rev. Plant Sci*. **38**: 327 – 338.

Staudacher, E., Altmann, F., Wilson, I.B.H., and März, L. 1999. Fucose in *N*-glycans: From plant to man. *Biochimica et Biophysica Acta* **1473**: 216–236.

Staudacher, E., Dalik, T., Wawra, P., Altmann, F., and März, L. 1995. Functional purification and characterization of a GDP-fucose: *β-N*-acetylglucosamine (Fuc to Asn linked GlcNAc) α1,3-fucosyltransferase from mung beans. *Glycoconj. J*. **12**: 780–786.

Strasser, R., Altmann, F., Mach, L., Glössl, J., and Steinkellner, H. 2004. Generation of *Arabidopsis thaliana* plants with complex *N*-glycans lacking β1,2-linked xylose and core α1,3-linked fucose. *FEBS Lett*. **561**: 132–136.

Takenaka, Y., Kato, K., Ogawa-Ohnishi, M., Tsuruhama, K., Kajiura, H., Yagyu, K., Takeda, A., Takeda, Y., Kunieda, T., Hara-Nishimura, I., et al. 2018. Pectin RG-I rhamnosyltransferases represent a novel plant-specific glycosyltransferase family. *Nat. Plants* **4**: 669–676.

Tan, L., Showalter, A.M., Egelund, J., Hernandez-Sanchez, A., Doblin, M.S., and Bacic, A. 2012. Arabinogalactan-proteins and the research challenges for these enigmatic plant cell surface proteoglycans. *Front. Plant Sci*. **3**: 140.

Temple, H., Mortimer, J.C., Tryfona, T., Yu, X., Lopez-Hernandez, F., Sorieul, M., Anders, N., and Dupree, P. 2019. Two members of the DUF579 family are responsible for arabinogalactan methylation in Arabidopsis. *Plant Direct* **3**: 1-4.

Tryfona, T., Liang, H.C., Kotake, T., Tsumuraya, Y., Stephens, E., and Dupree, P. 2012. Structural characterization of Arabidopsis leaf arabinogalactan polysaccharides. *Plant Physiol*. **160**: 653–666.

Tryfona, T., Theys, T.E., Wagner, T., Stott, K., Keegstra, K., and Dupree, P. 2014. Characterization of FUT4 and FUT6 α-(1→2)-fucosyltransferases reveals that absence of root arabinogalactan fucosylation increases arabidopsis root growth salt sensitivity. *PLoS One* **9**: 1–13.

Tuomivaara, S.T., Yaoi, K., O'neill, M.A., and York, W.S. 2015. Generation and structural validation of a library of diverse xyloglucan-derived oligosaccharides, including an update on xyloglucan nomenclature. *Carbohydr. Res.* **402**: 56–66.

Urbanowicz, B.R., Bharadwaj, V.S., Alahuhta, M., Peña, M.J., Lunin, V. V., Bomble, Y.J., Wang, S., Yang, J.Y., Tuomivaara, S.T., Himmel, M.E., Moremen, K. W., York, W. S., and Crowley, M. F. 2017. Structural, mutagenic and *in silico* studies of xyloglucan fucosylation in *Arabidopsis thaliana* suggest a water-mediated mechanism. *Plant J.* **91**: 931–949.

Vanzin, G.F., Madson, M., Carpita, N.C., Raikhel, N. V, Keegstra, K., and Reiter, W.-D. 2002. The *mur2* mutant of *Arabidopsis thaliana* lacks fucosylated xyloglucan because of a lesion in fucosyltransferase *At*FUT1. *Proc. Natl. Acad. Sci. U. S. A.* **99**: 3340–5.

Verger, S., Chabout, S., Gineau, E., and Mouille, G. 2016. Cell adhesion in plants is under the control of putative *O*-fucosyltransferases. *Development* **143**: 2536–2540.

von Schaewen, A., Sturm, A., O'Neill, J., and Chrispeels, M. J. 1993. Isolation of a mutant Arabidopsis plant that lacks *N*-acetyl Glucosaminyl Transferase I and is unable to synthesize Golgi-modified complex *N*-linked glycans. *Plant Physiol.* **102**: 1109–1118.

Wang, Y., Shao, L., Shi, S., Harris, R.J., Spellman, M.W., Stanley, P., and Haltiwanger, R.S. 2001. Modification of epidermal growth factor-like repeats with *O*-fucose: Molecular cloning and expression of a novel GDP-fucose protein *O*-fucosyltransferase. *J. Biol. Chem.* **276**: 40338–40345.

Wen, F., Celoy, R.M., Nguyen, T., Zeng, W., Keegstra, K., Immerzeel, P., Pauly, M., and Hawes, M.C. 2008. Inducible expression of *Pisum sativum* xyloglucan fucosyltransferase in the

pea root cap meristem, and effects of antisense mRNA expression on root cap cell wall structural integrity. *Plant Cell Rep*. **27**: 1125–1135.

Willats, W.G.T., Mccartney, L., Mackie, W., and Knox, J.P. 2001a. Pectin: Cell biology and prospects for functional analysis. *Plant Mol. Biol*. **47**: 9–27.

Wilson, I.B.H. 2001. Identification of a cDNA encoding a plant Lewis-type α1,4-fucosyltransferase. *Glycoconj. J*. **18**: 439–447.

Wilson, I.B.H., Rendić, D., Freilinger, A., Dumić, J., Altmann, F., Mucha, J., Müller, S., and Hauser, M.-T. 2001. Cloning and expression of cDNAs encoding *α*1,3-fucosyltransferase homologues from *Arabidopsis thaliana*. *Biochim. Biophys. Acta*. **1527**: 88–96.

Wu, Y., Williams, M., Bernard, S., Driouich, A., Showalter, A.M., and Faik, A. 2010. Functional identification of two nonredundant *Arabidopsis* α(1,2)fucosyltransferases specific to arabinogalactan proteins. *J. Biol. Chem*. **285**: 13638–45.

Yong, W., Link, B., O'Malley, R., Tewari, J., Hunter, C.T., Lu, C.A., Li, X., Bleecker, A.B., Koch, K.E., McCann, M.C., McCarty, Donald R., Patterson, S. E., Reiter, W.-D., Staiger, C., Thomas, S. R., Vermerris, W., Carpita, N.C. 2005. Genomics of plant cell wall biogenesis. *Planta* **221**: 747–751.

Zentella, R., Sui, N., Barnhill, B., Hsieh, W.P., Hu, J., Shabanowitz, J., Boyce, M., Olszewski, N.E., Zhou, P., Hunt, D.F., and Sun, T-P. 2017. The *Arabidopsis O*-fucosyltransferase SPINDLY activates nuclear growth repressor DELLA. *Nat. Chem. Biol*. **13**: 479–485.